A Constant Power, Load Independent Microwave Source

J.W. Gerber

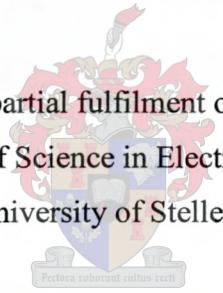

Thesis presented in partial fulfilment of the requirements for the
degree of Master of Science in Electronic Engineering at the
University of Stellenbosch

Supervisor: Prof. J.B. de Swardt

December 2002

Declaration

I, the undersigned, hereby declare that the work contained in this thesis is my own original work and that I have not previously in its entirety or in part submitted it at any university for a degree.

J.W Gerber

Summary

In the past few years, a need for consulting on microwave heating has surfaced. Since most specialised microwave components are imported, this adds a hefty price tag in developing the infrastructure for such consultation. This thesis looks at the design of low cost alternatives for use in the laboratory.

A microwave source output with variable output power is often required for consultation. The calculation of product costs may also be simplified if the available microwave power is constant despite load changes.

The magnetron as a load was first investigated and a high voltage SMPS was then designed to control the output of the magnetron according to operator / consulting requirements. To ensure adequate feedback of system output and load matching, a dual directional coupler has been designed and implemented.

Since the amount of microwave power required has a direct impact on the initial capital expenditure, costs need to be kept low by optimising the system. An impedance matching unit was designed to match the magnetron with the load, saving energy and reducing system costs. Through automation, the system will strive for the optimum load condition without operator intervention.

Opsomming

Die afgelope paar jaar het 'n behoefte ontstaan aan konsultasiewerk op die gebied van mikrogolfverhitting. Aangesien gespesialiseerde komponente meestal ingevoer word, bemoeilik die koste daarvan die ontwikkeling van die nodige infrastruktuur vir konsultasie. Hierdie tesis kyk na die ontwerp van goedkoper alternatiewe vir laboratoriumgebruik.

'n Mikrogolf bron met 'n verstelbare kraglewering is dikwels nodig tydens konsultasiewerk. Produk kosteberekinge kan ook vereenvoudig word indien die mikrogolf kraglewering konstant bly, ongeag produk veranderinge.

Die magnetron as GS las is eers ondersoek waarna 'n hoogspanning geskakeldekragbron ontwerp is om die uittree van die magnetron te verstel volgens operateur- / konsultasievereistes. 'n Dubbele direksionele koppelaar is ontwerp en by die laboratorium opstelling gevoeg om voldoende terugvoer van die kraglewering en impedansie aanpassing te verseker.

Die hoeveelheid mikrogolf drywing wat benodig word, het 'n direkte impak op die aanvanklike kapitale uitgawe vir die stelsel. 'n Optimale stelsel is dus noodsaaklik om kostes te bespaar. 'n Impedansie-aanpassingsnetwerk is ontwerp om die magnetron en las by mekaar aan te pas om sodoende energie en kostes te bespaar. Deur outomatisering streef die stelsel na optimale werkverrigting sonder enige ingryping deur die operateur.

Acknowledgments

Thanks to each one that did not give up hope, especially my parents who endured with me. For every friend that said, "Keep the faith," "Keep the strength" and all your prayers. To my Saviour and Lord, for the privilege and grace to tackle and complete this thesis.

Contents

List of Tables

List of Figures

List of Principal Symbols and Abbreviations

~	– Approximately
$\propto$	– Directly proportional to
EMI	– Electromagnetic Interference
ε_r	– The dielectric constant of a material
FA-TX	– Filament Transformer
HF	– High-frequency
HV	– High-voltage
IGBT	– Integrated Bipolar Transistor
PC	– Personal Computer
P_f	– Forward Power, power that is travelling towards the load
Pr	– Reflected Power, power that is reflected from or travelling away from the load
RF	– Radio Frequency
SMPS	– Switch-mode power supply
$\tan\delta_e$	– The loss tangent of a material
VRT	– Variable ratio transformer
ZVS	– Zero Voltage Switching
ZVS-CV	– Zero Voltage Switching, Clamped Voltage
ZVT	– Zero Voltage Transition
ZCS	– Zero Current Switching

Chapter 1 Introduction

1.1 Introduction

Nowadays microwave heating is used on a growing diversity of products. The range of "ovens" – rather cavities – that are used is also multiplying, ranging from standard household ovens to single mode circular cavities to radiated conveyor feed systems in industry. Even plasma systems!

For consultation in industry, it is necessary to demonstrate and test equipment, techniques and products without having too much of the set-up costs that this diversity would imply.

The diversity in specifications when evaluating a specific product / procedure, can be illustrated through some examples:
Constant product temperature: When reactivating spent granules of activated carbon, a substance used in extracting gold from ore pulp in the mining industry, the carbon needs to be kept at a constant temperature for 10-15minutes. What makes this difficult is the fact that the carbon has an exothermic reaction with oxygen – it starts to burn! After the reactivation, the granules also need to be cooled at a certain rate to minimise waist from granule crumbling.

Drying: When manufacturing chipboard (used in making cupboards), the glue for the chips is mixed according to the moisture content of the specific batch of chips. Conventional drying used to determine the moisture content can take up to 24 hours. By making a calculated guess after a few hours, manufactures add the glue, but add some extra as a safety measure – a sub-optimum process. Using microwave drying, a small sample can be fully dried within an hour and the manufacturer can calculate the exact amount of glue to be used.

Meat thawing / tempering: Frozen meat is heated from –20°C to –5°C for further processing in industry. The heating needs to be slow to guarantee an even temperature distribution in the product. The typical processing time for 30kg of meat is 5-8minutes.

Brick drying: A conveyer system is used where the bricks are first dried at a low power level until their critical moisture content level is reached. After this point, more power can be applied. If the high power is applied too soon, the bricks will crack.

Other applications include the pasteurisation of drinks, the post baking of biscuits and the sintering of ceramics.

The requirements for a test set-up used in consultation would include:

Efficiency - Efficiency is closely linked to running and set-up costs.

Adaptability - Different power levels that might be required.

- Different types of magnetrons that need to be tested / used.

Real time data - The captured data gives the user / client more accurate knowledge on the cost, efficiency and overall viability of a product or procedure. Results would be quantitative rather than approximate.

All of these requirements are directly or indirectly linked to the amount of microwave energy that is absorbed by the load. From this need, a system was designed and built to supply constant microwave power to a load. The system would also be able to keep a load at an approximately constant temperature since the temperature is affected by the power. By *constant* microwave power it is implied that the power would be at the level the user specifies and this reference level may vary with time. For a constant reference, the power would be controlled to stay constant even though the load may vary.

1.2 System overview

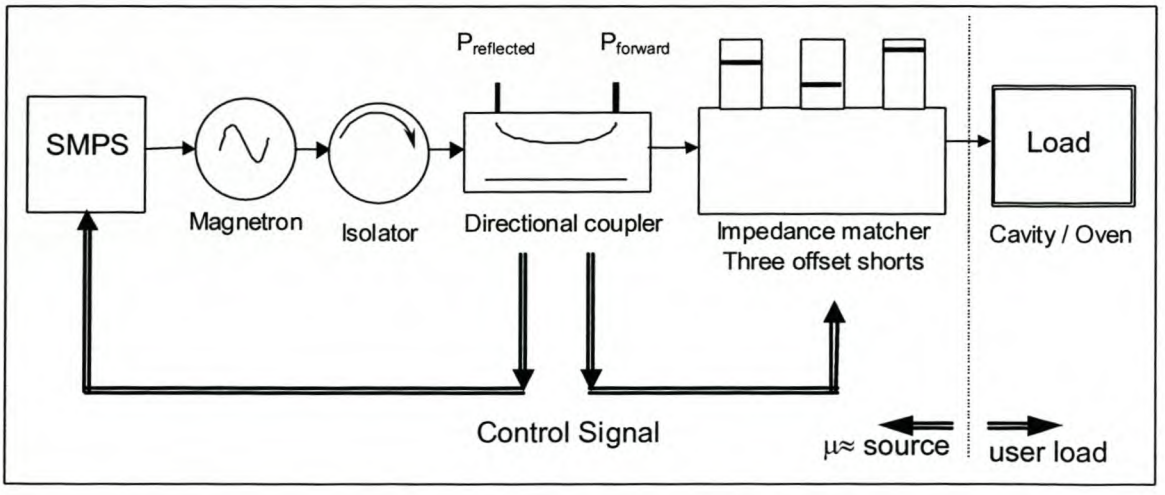

Figure 1.1 System overview

The power level applied to the load could be varied by reflecting / deflecting more or less power before it reaches the load. This is not ideal, as the reflected power would be wasted, creating an inefficient system. A more elegant approach is required.

In this system, microwave power variation is accomplished by changing the DC supply voltage / current to the magnetron (*Figure 1.1*). A DC-to-DC switch-mode power supply (SMPS) is used as a variable supply with a reference output supplied by the user. Chapter 2 looks at the ins and outs of a magnetron and the different supplies used in industry. Chapter 3 gives a short overview on the different SMPS topologies that can be used and then details the design of this system's supply.

Variable power only solves half of the problem. It is also necessary for the load to effectively absorb the transmitted power. This requires the magnetron and load to be (impedance) matched. This is the point of maximum power transfer where the load impedance (Z_{load}) equals the complex conjugate of the internal impedance of the magnetron ($Z_{magnetron}$). By using an impedance matching unit, the impedance that magnetron is subjected to, is changed to $Z_{magnetron}'$ and simultaneously that of the load to Z_{load}'. Three variable offset shorts were used to implement the matching unit and control was implemented to the electro-mechanical unit via serial command from a personal computer (PC). Chapter 4 covers the matching unit, including the theoretical analysis, mechanical and electrical construction. Chapter 6 gives more information on the control of the system and the matching strategy that was implemented.

It is necessary to provide the user or client with quantitative measurements. This includes amongst others, the amount of power delivered to the load and the efficiency of the system. A dual directional coupler splits the radio frequency (RF) wave into its forward and reflected travelling parts. By measuring these, it is possible to determine the power absorbed by the load ($P_{forward} - P_{reflected}$ power) and the efficiency of the matching unit. The control also uses these as feedback to change the matching unit and / or the power delivered by the magnetron according to the goal function / requirements of the product. Chapter 5 describes the design and implementation of a dual directional coupler.

Chapter 7 concludes by evaluating the system according to a few practical situations / goal functions. A few "not so practical" examples also show the type of extremes to which the system can be subjected too and what knowledge can be gained from some of these situations. In conclusion, Chapter 8 gives the overall performance of the system and recommends any improvements that can be made.

For photographs of the different components and the test system, refer to Appendix C.

Chapter 2 Magnetron Supplies

Before looking at the supplies that are used and could be used for a magnetron, it is important to first look at the DC characteristics of the magnetron itself. That is, the magnetron as a load.

2.1 Load Characteristics of a Magnetron

The magnetron has a voltage to current non-linearity similar to that of a diode. A simple DC model is given in *Figure 2.1*. From this model, one can generate the familiar V-I load curves of *Figure 2.2*.

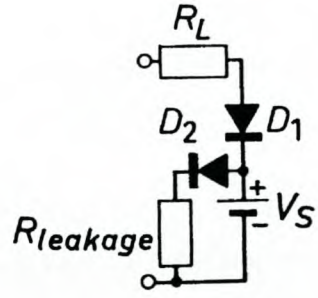

Figure 2.1 A DC model of a magnetron [1]

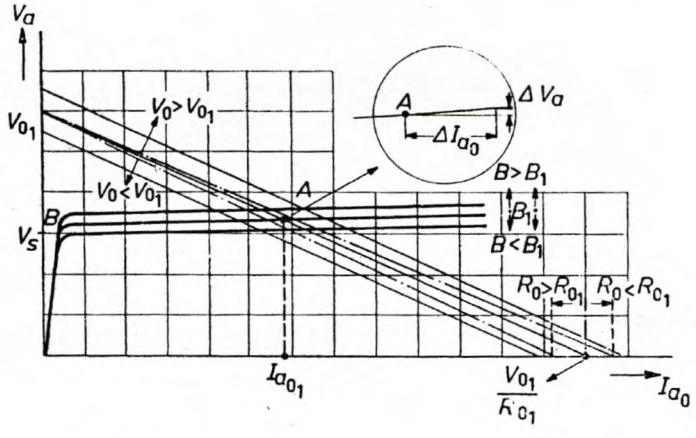

Figure 2.2 V-I DC input characteristics of a magnetron [1]

The magnetron conducts almost no current until a certain voltage is reached – Vs, the π-mode voltage. For a standard 800W magnetron, the π-mode voltage is approximately 3900V. Below this voltage, the DC loading is only 0 to 20mA. This gives a dynamic resistance of $^{\partial V}/_{\partial I} \sim 195k\Omega$. After this point, a small increase in input voltage gives a large increase in input current. A dynamic resistance of 50 to 100Ω is typical.

These curves (performance charts) do not stay constant and are only valid for certain load conditions. One way of changing the curve is by changing the magnetic flux density under which the magnetron operates. This gives the vertically displaced lines of *Figure 2.2*. The change in flux density alters the output power for a certain DC voltage, but also changes the efficiency of the magnetron, depending on the biasing point – *Figure 2.3*.

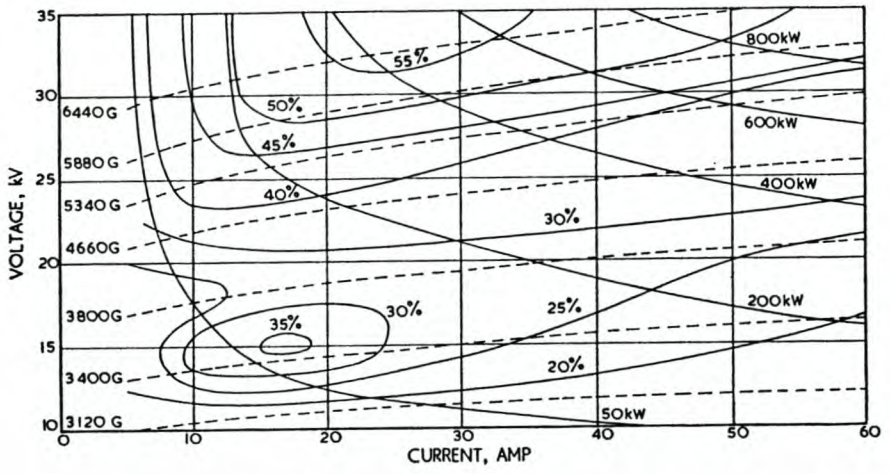

Figure 2.3 More detailed V-I curves, efficiency[%] vs. flux density[G] [2]

As one can see from *Figure 2.2*, it is possible to keep either V or I constant, change the flux and thereby change the output power of the magnetron. This is often used in high power magnetrons to control the output power. For standard commercial magnetrons, a solid magnet is used, giving rise to a constant magnetic flux.

The load curves can also change in a less controllable manner: The curve can change with time as the anode ages. This will lead to lower emissions, but might also lead to a lower "running" voltage, i.e. the magnetron operates at 3900V compared to the 4100V of a new magnetron for the same output power. The operating temperature also changes the V-I curve with insufficient cooling dramatically reducing the output power / efficiency.

The magnetron has a transfer function from input to output and vice versa of 0.5-1.5dB. Therefore, whatever happens on the RF side also happens on the input - that is, the output from the DC supply. One of the more severe load changes is arcing in the waveguide, thereby effectively shorting the magnetron supply. Load pulling can also occur where changes in the load reflection coefficient (RF side) "pull" the working frequency of the magnetron. The characteristics of the RF load may be different at this changed frequency, having a secondary

effect on the magnetron and supply. It also has the effect of pulling the (DC) biasing point of the magnetron supply [3].

If this pulling is too severe (the VSWR reaches 4 or above, *Figure 2.4*), the magnetron will start moding [3]. A magnetron is designed to oscillate in "π" mode and is therefore optimal in this mode. During moding, oscillation moves to the "π-1" mode, which is at a different frequency. The magnetron consumes more power and is less efficient in this mode. With a constant DC current supply, this mode will be sustained, but with a normal un-smoothed supply, the magnetron should drop out of moding as the input voltage (rectified sine wave) drops to zero. The cooling equipment is inadequate to handle the large increase in dissipated power, resulting in overheating and structural meltdown, for example imagine 800W + 300W dissipated in a 40x80x80mm volume! Meredith [4] gives a detailed description on how moding occurs and what actually happens during moding.

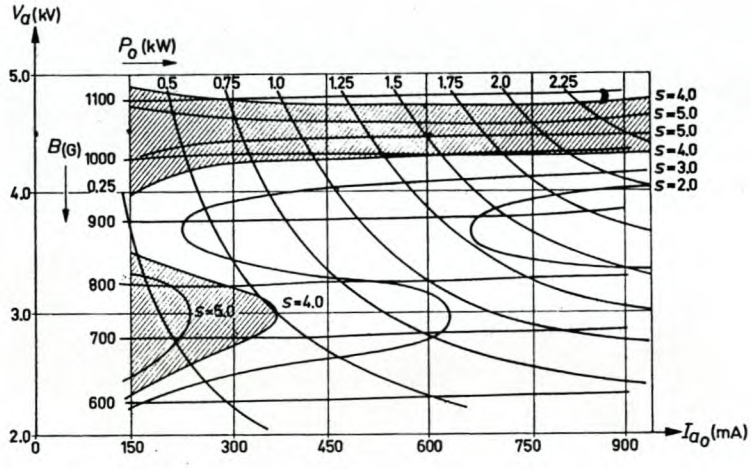

Figure 2.4 "Safe Operating Area" in VSWR vs. Load Lines [1]

Datasheets as the ones in *Figure 2.2* to *Figure 2.4* are available, giving the power supply designer better "preparation" when starting out. More data is also available for the RF side, contained in a "Rieke" diagram as in *Figure 2.5*. This is a Smith chart with usually only the VSWR < 3 part drawn.

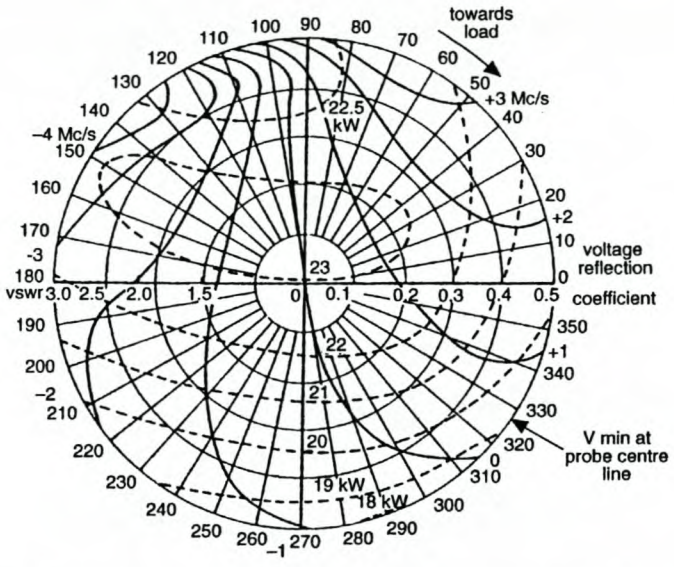

Figure 2.5 Rieke Diagram of a magnetron [4]

Unfortunately these datasheets are scarce and for many magnetrons not even available. What one can keep in mind though, is the maximum "allowable" VSWR before the probability of moding becomes certain. This value is by default chosen as 3 or 4, but is actually a function of the peak to average value of the anode current as one can see from *Figure 2.6.*

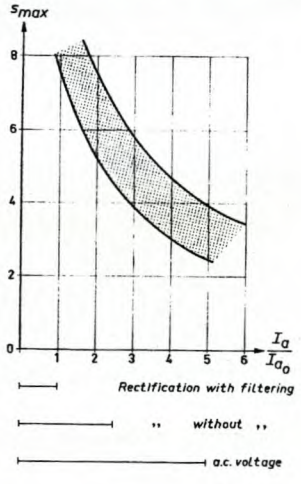

Figure 2.6 The ratio peak to average current versus the allowable output VSWR [4]

The effect of using half wave doubling (maximum VSWR of 3), to using full wave rectification (maximum VSWR of 6) or a smoothed DC supply (maximum VSWR of 8 or more), can be compared.

In most set-ups, a circulator or an isolator is used on the RF side to give the magnetron a matched load. Not only does the isolator keep the magnetron cooler by preventing reflected

power from reaching the magnetron, it also provides the magnetron with a load with a VSWR close to unity. The possibility of moding from a load mismatch is therefore greatly reduced.

There is another small, but important influence. The filament of the magnetron cathode is heated to assist the emissions from the magnetron. The filament uses a 50Hz, 3.3V, 12A supply (typical commercial magnetron), which is just an extra winding or two on the high-voltage (HV) transformer in commercial ovens. At switch-on, the filament pre-heats the cathode and during operation maintains a good temperature for electron emissions. The 50Hz of the filament supply influences the working point of the magnetron and if more precise voltage or current control is expected, the control of the supply should cater for this effect. Note that it is also possible to operate the magnetron with the filament switched off, once the magnetron has been ignited. The input voltage to the magnetron should be increased by 100V / 200V for the same output power. The higher voltage increases back bombardment - the effect of "unused" electrons plunging back to the cathode, causing it to self-heat. Refer to paragraph 7.2 for measured results on the effect the filament has on the magnetron supply.

2.2 The Ideal Power Supply

The magnetron is not an "ideal" load. The non-linearity of the DC loading makes it very sensitive to changes in the mains supply. The added possibility of arcing / shorting of the output, also adds to the designer's problems.

An ideal supply would cater for these requirements, overcome or at least stabilize some of the shortfalls of the loading and lend control to the user.

The ideal supply can be described as follows [5]:

1. A constant-current anode supply, such that the anode current cannot rise above the set level even under short-circuit fault conditions.
2. Control of anode current from a current source, maintaining constant magnetic field to the magnetron.
3. Rapid response of anode current to a control signal from a servo system deriving its reference signal either from a set (and programmable) anode current or power output, with an option for additional control from process parameters such as temperature, throughput etc.

4. A minimum level of stored energy in the system. During fault conditions this stored energy would either discharge through the magnetron or back into the supply.
5. Small size and weight.
6. Low cost.
7. Minimum inherent generation of interference signals, making it relatively easy to screen and filter to meet international standards.
8. An ability to modulate the applied anode current to spread the frequency-spectrum of the magnetron output. This is a desirable feature for multimode oven operation and also for reducing interference to other services operating at the same frequency.

To these one can add high efficiency (90% and above) as well as a low ratio of anode ripple current to average current (*Figure 2.6*). The lower ripple would be in contrast to 8 (above), but would allow a higher load mismatch before moding. This would also narrow the band of output frequencies from the magnetron for use with single mode cavities.

2.3 Standard Fixed Magnetron Supplies

A few standard power supply topologies are used in general. These differ in the level of control, the complexity of the circuitry, safety features, cost as well as application ranges, be that high or low power, commercial or industrial use. At 2.45GHz, commercial units deliver approximately 1kW of RF power whereas industrial units deliver up to 6kW of RF power.

2.3.1 Full Bridge Rectifier Supply

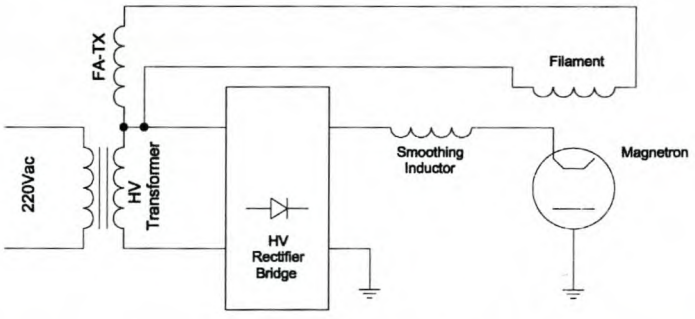

Figure 2.7 The Full Bridge Supply

Though this supply is not used on its own / in this basic format, it still supplies an overview on how a magnetron supply is constructed.

A HV transformer steps-up the voltage from the AC line (single phase 220V or three phase 380V for higher power supplies.) The output voltage can be anything from 3.5kV up to 17kV and higher. The output of the transformer is rectified through a full bridge rectifier and is often filtered by a smoothing inductor or a high-voltage capacitor on the output. The first option is preferred, as high-voltage capacitors are far more expensive and bulky than inductors with a high isolation to ground.

The negative rail of the smoothed DC is connected to the cathode of the magnetron with the positive rail connected to ground / the casing of the magnetron. The anode of the magnetron is constructed as the outside of the casing and is therefore also connected to ground. Some magnetrons have the polarity swapped, but this is the exception.

There is a separate supply to the magnetron (often an extra winding on the same HV transformer). This is the filament transformer (FA-TX) or filament supply. The filament heats the cathode to assist electron emissions, the same as one would find in old valve tubes. The supply can be AC as it only supplies a heating element and is a low voltage (3-12V), high current (10A up to 120A) supply.

2.3.2 Half-Wave Voltage Doubler Supply

Its ruggedness, simple construction and a low component count are some of the main attractions to this supply. Mass production also lowered pricing on both the supply and the domestic size magnetron, making it the supply used in most domestic ovens.

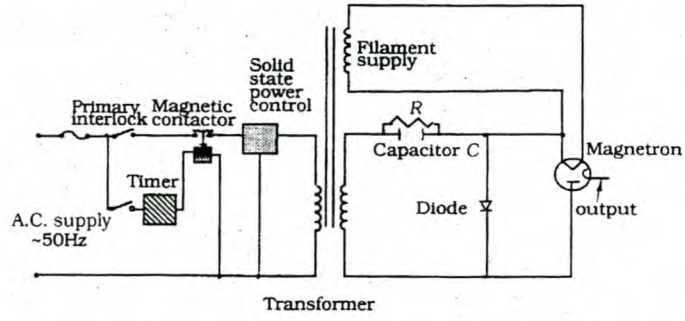

Figure 2.8 The Half-wave Voltage Doubler Supply [6]

The supply functions as follows: During the positive half cycle of the 50Hz line voltage, the diode conducts the current and capacitor C charges to V_{sec}. V_{sec} is the voltage on the

secondary side of the high-voltage transformer and is in the order of 2000V. During the negative half cycle, the diode is reverse biased and the negative voltage adds in series with the stored voltage in the capacitor to give an anode voltage of $2xV_{sec}$, hence the term "voltage doubler" supply. As the anode voltage reaches the π-mode voltage, current starts to flow through the magnetron and microwave power is emitted. This topology has the advantage that the voltage ratings of the output diode and capacitor is only half the magnetron supply voltage, or V_{sec}, compared to 2x V_{sec} for the full bridge rectifier.

A filament transformer / winding is added in series with the anode voltage to pre-heat the cathode and improve emissions.

The transformer used in this supply is usually built undersize. This is motivated by the cost saving for commercial units, but there is also a stabilising effect. The transformer would saturate more easily which would cause extra heating. As long as cooling is efficient, this is no problem. The saturation will limit the maximum output current, as the output voltage would stop rising with an increase in current as it reaches saturation. Since the *core* is saturated, the FA-TX would also saturate, lowering the filament voltage, cooling down the cathode and also lowering emissions.

Safety measures include a thermal switch for overheating of the magnetron and usually some mechanical form of overload protection. This is only a small help as internal meltdown from an arc could occur before the increase in heat would trigger the switch. A bleeder resistor (R) is used to discharge the capacitor when the oven is off for the safety of an operator repairing the supply.

Power control in this supply is limited to duty cycle control. This means that the average power is controlled with reference to a timer - *Figure 2.8*. For a set level, say 20% of P_{max}, the magnetron is on for 20% of the time and off for 80% of the time. That is:

$$P_{avg} = P_{\max} \times \frac{\Delta t}{T}$$

"T" or the total averaging time is approximately 30s for domestic ovens. It takes approximately 3s for a magnetron to switch on from cold (at first switch-on) and 0.5s from hot (during a heating cycle). This "time lag" limits the dynamics of a possible control loop as well as the minimum output power. "Δt" has a minimum of approximately 2x 0.5s = 1s. The

fact that 100% power would be delivered during the "on" cycle is also undesirable when the product being heated has a high thermal heating to microwave power ratio. That is: during a short high power interval, the product might overheat with hot spots developing or thermal runaway. During a longer, constant low / medium power interval, overheating has a lesser chance of occurring. Heat conduction in the product lowers the occurrence of hot spots. Localised overheating is usually not that much of a problem with domestic products but needs consideration with industrial applications such as the baking of ceramics or the reactivation of activated carbon.

2.3.3 Saturated Transformer Supply

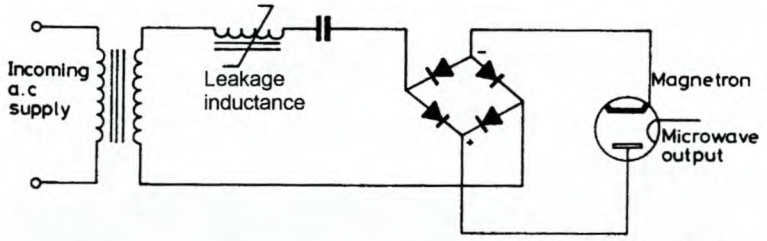

Figure 2.9 The Saturated Transformer Supply [16]

The saturated transformer supply adds some stabilising into the default supply. A transformer is designed to saturate effectively creating a leakage inductance, *Figure 2.9.* The leakage inductance is combined with a series or parallel capacitor to resonate at 10% above the line frequency – i.e. 55Hz.

As the load current rises, the inductance value falls, resulting in an increase in the resonant frequency [4]. The resonant curve therefore also shifts higher, resulting in a drop in the load current. *Figure 2.10* illustrates this effect.

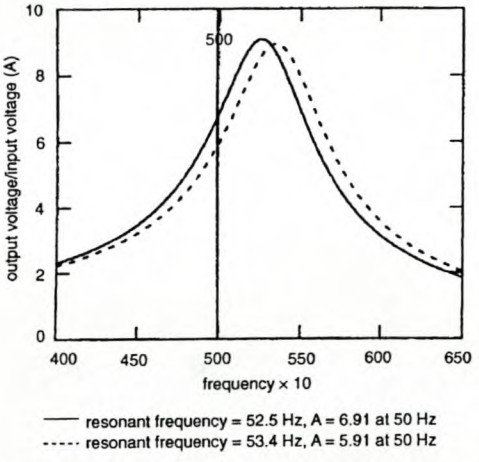

Figure 2.10 Resonant characteristics of the saturated transformer [4]

This stabilisation damps any changes in the input voltage with a ±10% change in the input voltage resulting in only a ±0.5% change in the anode current. The drawback is the sensitivity towards the line frequency, with a 1% change in frequency resulting in a 9% change in anode current. Electricity suppliers do not always guarantee their line frequency to below this variation.

2.4 Variable Supplies

Although the first topologies are quite usable, they lack the possibility of power control. Except for power averaging, these supplies do not have a means of adapting from one power requirement to another or to a specific heating profile. This necessitates a variable supply.

2.4.1 Adjustable Transformer Supply

This supply works just like the full bridge supply, except for the output voltage from the HV transformer, which is adjustable. In its simplest form, a variable-ratio transformer (VRT) is added in front of the HV transformer as in *Figure 2.11*

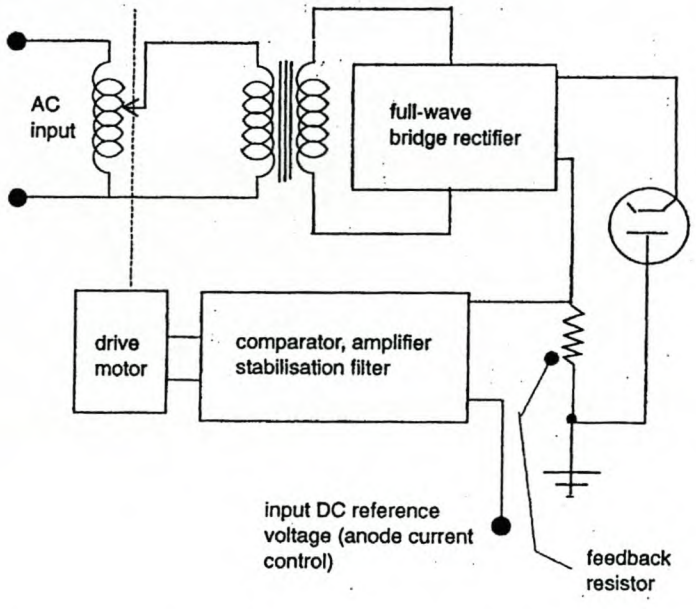

Figure 2.11 Variable-ratio-transformer anode-current controller [4]

A servomotor adjusts the VRT, changing the input voltage to the HV transformer until the required anode current is reached.

The minimum output voltage from the VRT transformer is about 20% less than the magnetron π-mode voltage as there is no need to adjust the voltage lower – the magnetron is already off. The power rating of the VRT would be the same as that of the HV transformer.

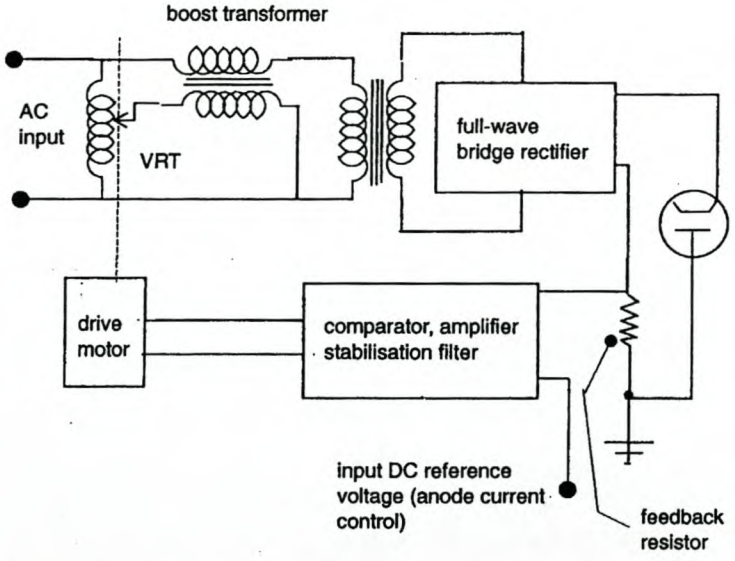

Figure 2.12 Modified VRT supply with a reduced rating on the VRT [4]

It is possible to use an extra transformer to boost the primary voltage as shown in *Figure 2.12*. The standard HV transformer would once again output a voltage approx. 20% below the π-mode voltage. With the boost transformer and the VRT, the input to the HV transformer is boosted to the required output voltage level. In this topology, the VRT has a far lower power rating since only the "extra" voltage / power is transformed to the HV transformer. The boost transformer needs to conduct the rated current.

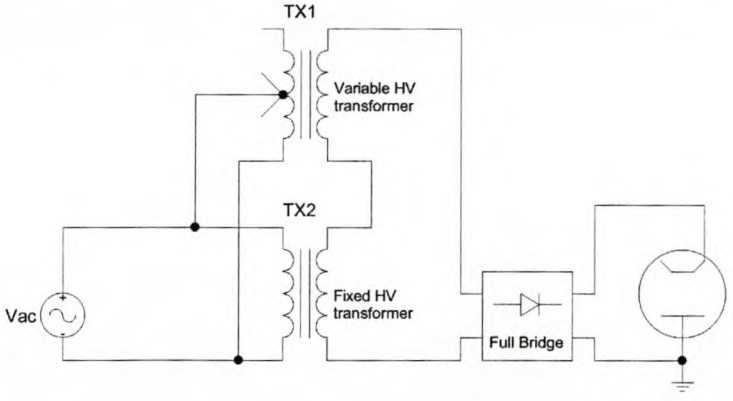

Figure 2.13 Modified VRT supply with a "piggy-back" transformer

An alternative to the above set-up would be a fixed HV transformer at 20% below π-mode and an extra "HV" transformer stacked on top – *Figure 2.13.* Changing the ratio of the second transformer will vary the output voltage as required. Care should be taken to confirm that the isolation of the second transformer to earth is sufficient, as the operating output is the sum of the two voltages.

2.4.2 Variable Magnetic Field Supply

As mentioned in Chapter 2.1, the V-I curves of a magnetron can be changed by changing the magnetic flux density applied to the magnetron. By controlling the magnetic flux, we are able to change the anode current and thereby change the output power of the magnetron.

A specific type of magnetron is used for this topology. The magnetron has a fixed magnet to supply the magnetic flux plus an electromagnet to change the applied flux. The magnetron is powered by a basic supply while the electromagnet is powered from a variable supply. Since the power rating of the electromagnet is far lower than that of the magnetron (< 1%), a simple thyristor controller and feedback loop can be used to vary the flux.

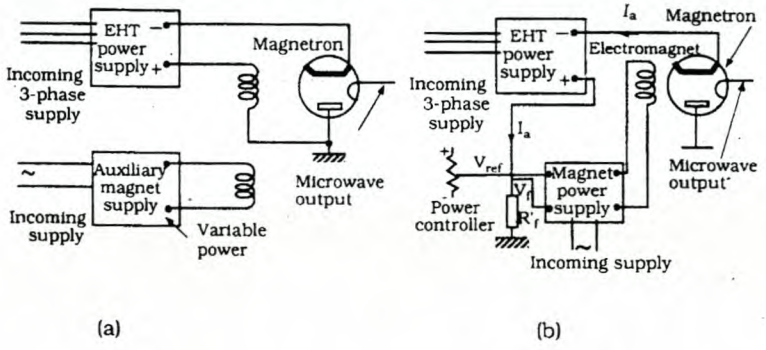

Figure 2.14 Series excited electromagnet (a), separately excited electromagnet (b) [4], [13]

Two different topologies can be used for exciting the electromagnet [16]. In the first, series excitation, the electromagnet is in series with the anode - *Figure 2.14(a).* As the current to the anode changes because of variations in the DC voltage, the magnetic flux also changes and compensates for the variation. The disadvantage of the series excitation is the required auxiliary winding to provide magnetic flux at start-up. Any rapid change in the anode current (under fault conditions) would also induce a high voltage across the terminals of the winding and extra protection is required. The output power of the magnetron can only be changed indirectly by varying the anode current.

An alternative is the separately excited electromagnet - *Figure 2.14(b)*. This time a completely separate supply drives and controls the electromagnet. A sensing resistor (R_f) feeds back the anode current through a loop stabilising filter after which it is compared to a reference / control value. The comparator output controls the firing angle of a thyristor set and thereby changes the DC voltage applied to the electromagnet. The magnetic flux varies according to this applied voltage.

There is an unwanted time delay in the supply, the first contributor being the self-inductance of the electromagnet (in the order of tenths of milliseconds). The second is from the construction of the magnetron itself. A copper ring is usually used to help prevent the moding effect [3], but a change in flux will induce a current in the ring that will in turn oppose the change in flux. This gives a further delay of a few milliseconds before the flux settles. These delays will limit the maximum bandwidth of a control loop.

Electromagnet control is only available on higher power magnetrons (>6kW). For lower power magnetrons the designer will have to resort to the topologies that change the anode current / voltage directly.

2.4.3 Thyristor Controlled Supply

Figure 2.15 shows the basic thyristor supply with current feedback from a resistor. The controller changes the firing angle - the time it takes before the thyristors conduct current - of a thyristor pair. By changing the firing angle, the average voltage to the HV transformer is changed and therefore also the voltage to the magnetron. A smoothing choke is used after the rectifier to filter the ripple from the HV supply.

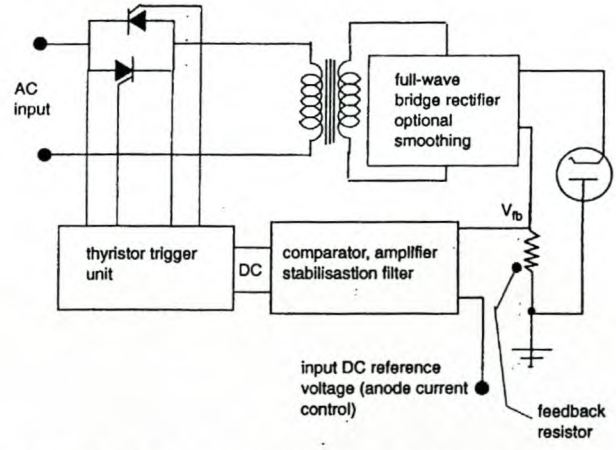

Figure 2.15 Phase-controlled, thyristor power supply [4]

Graphically the line voltage changes as follows: (a) The AC voltage into the system is sent through the thyristor pair. (b) As the phase angle (alpha) is stretched more and more, less of the sine wave "reaches" the HV transformer. After the transformer, the output is put through (c) a full bridge rectifier and finally filtered with (d) a smoothing choke and / or a capacitor filter. *Figure 2.16* shows how the voltage changes as it passes through the system, with a step-up in voltage (the transformer) before the rectification and filtering. Only the switch-on time of thyristors can be controlled. Switch-off occurs at the zero transient of the current, because of the physical characteristics of a thyristor. [7]

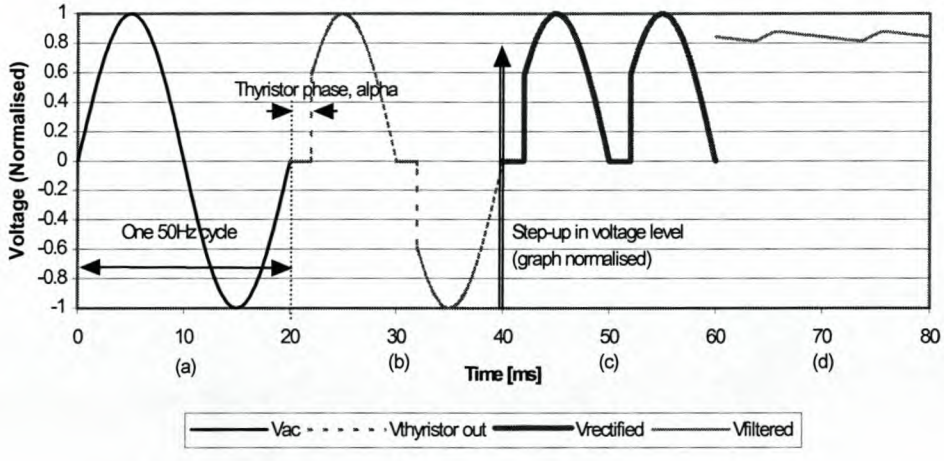

Figure 2.16 Voltage Shapes in a Thyristor Supply

Because the input is no longer sinusoidal, the design of the transformer has to cater for a relatively high RMS line current. The voltage rating of the thyristors should also be considered carefully, because of the inductance of the transformer. Since the magnetron is "off" until the π-mode voltage is reached, the HV transformer is only an inductor that loads the thyristors with a lagging phase. This may lead to unstable switching as the current through the thyristors will not pass through zero at the same time as the voltage and the use of a snubber circuit would be advised. A similar effect would occur as the voltage drops below the π-mode threshold at the roll off of the 50Hz. The current to the magnetron would drop to almost zero, but the transformer would still like to maintain the current flow, inducing a reverse voltage across the magnetron and the thyristors.

The thyristor supply gives an effective duty cycle control with a T_{total} of 10ms – from the rectified 50Hz line frequency. A vast improvement from that of a timer controlled duty cycle. Control speed and bandwidth is still limited by the large transformer inductance and the optional filtering inductor. The sensing and feedback enable the use of safety mechanisms to

protect the supply against over current and over heating of the magnetron or supply. The response time is once again a maximum of 10ms – the maximum time before the next zero crossing of the thyristor current. This compares well to the 30ms or more that it would take a mechanical switch to open.

2.4.4 Switch-Mode Power Supply

With thyristors, the 50Hz line can be switched "on" on demand, but not "off". Switch-off has to "wait" for a zero transient of the current. Modern power electronics are available to switch the supply "on" *and* "off" on demand and at high frequencies. This makes it possible to increase the line frequency seen by the HV transformer substantially.

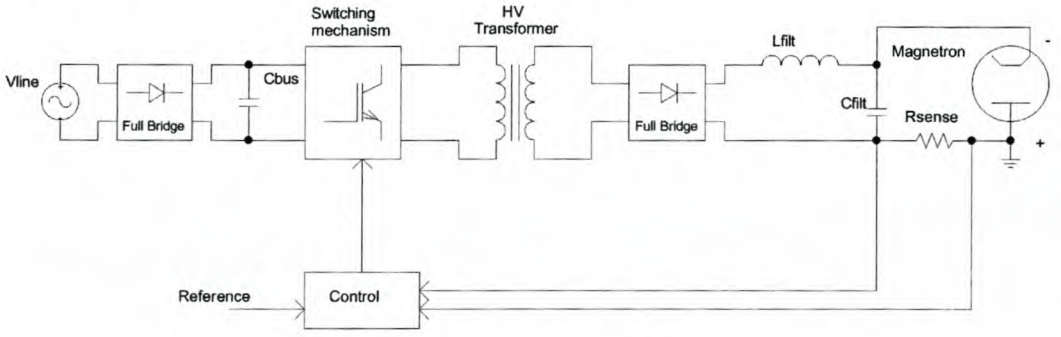

Figure 2.17 A basic magnetron SMPS – FA-TX not shown

From *Figure 2.17*, a SMPS will rectify and filter the 50Hz line voltage before it reaches the switching components. Silicone components (IGBT's, FET's, GTO's…) switch the rectified voltage on and off to form a high-frequency square wave, which is then scaled up to the correct voltage using a high-voltage, high-frequency transformer. Finally the high-voltage output is rectified and filtered before connection to the magnetron. A resistor is used for feedback to control the switching of the active devices in a similar fashion as the thyristor supply. The filament supply can be supplied separately off the 50Hz supply or from a separate step-down transformer connected to the main high-frequency transformer. This would require high current, high-frequency diodes and therefore the former is preferred.

The higher switching frequency implies:

(a) A high-frequency transformer can be used. These transformers use a ferrite core and are far less bulky and lighter than a low frequency transformer. The number of required turns for effective power transfer from primary to secondary is also substantially lower, simplifying the manufacturing.

(b) The control loop can have a much higher bandwidth resulting in faster, more accurate control.

(c) Protection circuitry can switch off the supply in a few microseconds instead of milliseconds.

Another advantage is the lower amount of output filtering required for a smooth DC supply. The output filter no longer needs to reject harmonics of 50Hz, but harmonics of 20kHz and higher. The required inductor (and capacitor) values would be lower and the physical size smaller at these higher frequencies. The main advantage besides the size and weight reduction, is the dramatic reduction in stored energy on the load side of the supply. Less stored energy means less damage during fault conditions and therefore less down time on a plant. Refer to Appendix A for more information on the stored energy in the system and a comparison of the amount of stored energy in the different topologies.

Chapter overview

In this chapter we considered the magnetron as a load and the effect its non-linearity and low input / output transfer function would have on a supply. The ideal power supply was sketched as well as the most commonly used magnetron supplies. These are the full bridge rectified, the half-wave voltage doubler and the saturated transformer supplies. We also investigated the variable supplies namely the adjustable transformer, the variable magnetic field, thyristor controlled and switch-mode supplies. The SMPS is considered to be the closest to the ideal supply and will be discussed further in Chapter 3.

Chapter 3 SMPS Design

As a basic goal, a magnetron SMPS should control the output to the magnetron more accurately and faster than conventional supplies. Other reasons and goals can also be put forward when starting with a design. This chapter describes the requirements for a magnetron SMPS, gives a brief overview of the construction and functioning of the supply and then highlights some of the design considerations.

The following primary requisites were chosen in the laboratory application of a SMPS as a magnetron supply:

a) Light weight. With a standard 50Hz, 1.2kW supply weighing in at approximately 22kg, this requisite receives primary status after only moving the supply a few times.
b) Output power adjustability. The basic use of the SMPS would be to give an adjustable output voltage / current which in turns gives an adjustable magnetron output power according to the user requirements.
c) Magnetron adaptability. The supply should be able to adjust for different types of magnetrons. Each type would have a different I-V-P curve, a different I_{max} and a different π-mode voltage. Requiring a different supply for every type of magnetron in the laboratory would be very cumbersome and require a lot of reshuffling of equipment. For the "standard" household magnetrons ranging from 600W to 1.2kW, I_{max} can vary between 250mA and 600mA and the corresponding operating voltages between 3500V and 4600V, determined by the π-mode voltage.
d) Safety mechanisms and fault detection. These include over-current and short-circuit protection and detecting overheating and damage to switching devices.

Secondary requisites would include:

e) A low amount of stored energy.
f) Low output ripple (HV-DC).
g) The magnetron output power should be directly proportional to the control voltage. When using a thyristor supply, the output voltage is a function of the sine waveform and $V_{control}$. The magnetron output power has the further diode-like non-linear relationship to the output voltage, making it far from directly proportional to $V_{control}$. If a D/A converter supplies the reference voltage, only a small portion of its range would control the power, making small steps in the power level difficult.

3.1 Switching Topologies

There are quite a few topologies available for switch-mode power supplies. Since our interest is only in the application for magnetron HV supplies, we can narrow down the range of topologies.

3.1.1 Half Bridge DC-DC Converter

The half bridge converter uses two switching devices for conversion, hence the name.

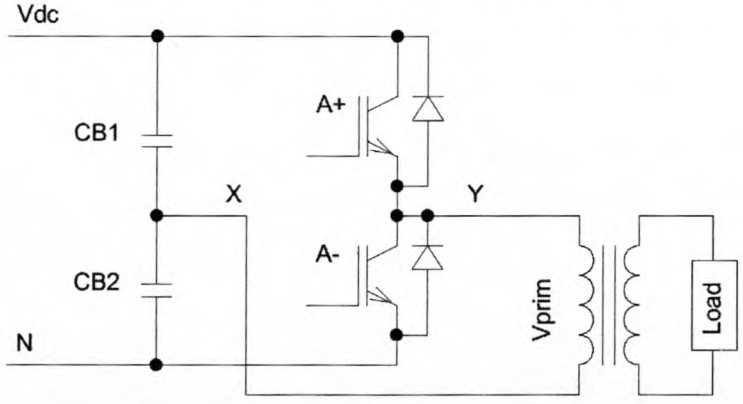

Figure 3.1 Half bridge converter construction [14]

Billings [14] gives an overview of the functioning of the half bridge converter. The main considerations for our application are the following:

Advantages of the half bridge supply: The split bus capacitor circuit (CB_1 and CB_2) has the advantage that any imbalance in the switches / transferred energy per half cycle will be absorbed by the capacitors. This curbs the problem of staircase saturation of the transformer core, associated with some topologies.

Disadvantages: The input voltage to the step-up transformer is only $\pm {}^{Vdc}/_{2}$, which requires a high primary current for higher power applications. Because of the difficulty in constructing a high-frequency, high-current winding, the half bridge is only used for supplies up to 500W [14]. Paragraph 3.2.3 explains some of the problems associated with high current ratings in high frequency switching as far as skin and proximity effects are concerned.

3.1.2 Full Bridge DC-DC Converter

Similar to the half bridge converter, the full bridge uses a stacked pair of switches, this time two stacks or phase arms – *Figure 3.2.*

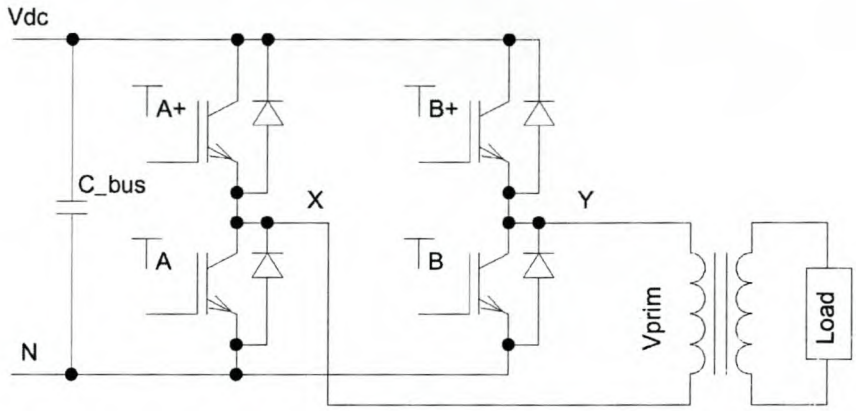

Figure 3.2 Full bridge converter [14]

By switching on either T_{A+} and T_{B-} or T_{A-} and T_{B+}, a voltage of $\pm V_{dc}$ is switched across the primary of the transformer. If switches T_{A-} and T_{B-} or T_{A+} and T_{B+} were active, the primary voltage would be zero. The maximum duty cycle has to be limited to prevent two switches in the same phase arm from being switched on simultaneously and shorting the supply.

The full bridge can be used in a few different switching strategies depending on the application of the converter. Amongst others are:

1. Pulse width modulation (PWM) with bipolar or unipolar voltage switching for DC motor drives. [7]
2. Pulse width modulation (PWM) with bipolar or unipolar voltage switching for DC-to-AC inverters. [7]
3. Voltage cancellation or phase shifted switching specifically for high intermediate frequency conversion with isolating transformer supplies. This is the switching strategy of interest for the magnetron supply [7], [14].

In phase-shifted control, switches T_{A+}, T_{A-} and T_{B+}, T_{B-} are treated as two switch pairs. All the switches function at a 50% duty cycle - slightly less with the dead time (td) to prevent shorting – while the switches in a pair are out of synchronisation with each other. By changing the phase difference between the two pairs, the average output voltage is varied. Refer to *Figure 3.3*.

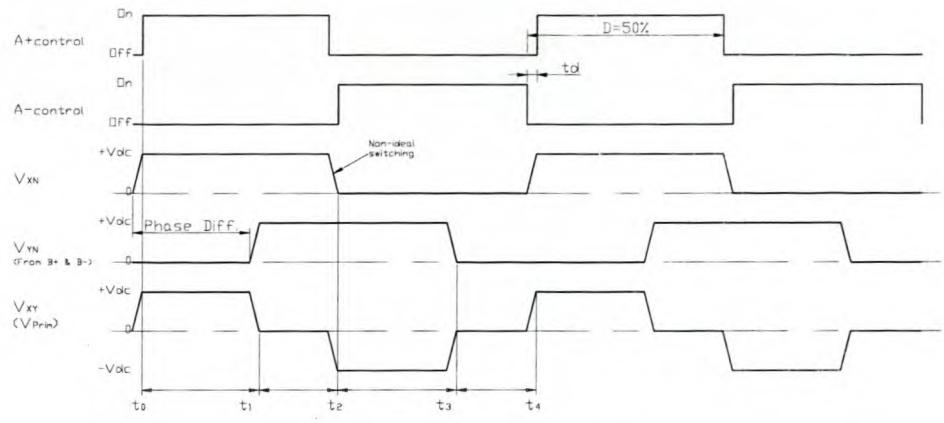

Figure 3.3 Phase shifted switching

At time t_0, switch T_{A+} switches on, T_{A-} is off, T_{B+} is off and T_{B-} is on. Therefore node *X* (*Figure 3.2*) is at $+V_{dc}$ with respect to node *N*. Since T_{B-} is on, node *Y* is at 0V and V_{prim} (V_X-V_Y) of the transformer equals $+V_{dc}$. Just before time t_1, switch T_{B-} starts to switch off. At t_1, switch T_{B+} switches on, T_{B-} is off and node *Y* goes to +Vdc. The voltage across the transformer changes to 0V since both nodes are at the same potential. Just before t_2, switch T_{A+} starts to switch off. At t_2, switch T_{A-} switches on, T_{A+} is off and node *X* goes to 0V. The voltage across the transformer changes to $-V_{dc}$ since V_X-V_Y = 0 - $+V_{dc}$ = $-V_{dc}$. Just before t_3, switch T_{B+} starts to switch off. At t_3, T_{B-} switches on and V_{prim} returns to zero. Just before time t_4, switch T_{A-} starts to switch off. From t_4 onward, the sequence repeats itself. In this manner, voltages of $\pm V_{dc}$ or 0V with a zero average value and varying duty cycle are generated across the primary winding.

Since the primary voltage is $\pm V_{dc}$, the full bridge can transfer twice the amount of power as a half bridge for the same amount of primary current. A DC blocking capacitor might be required in series with the transformer if the two switching pairs and their parasitic elements are not balanced / equal. The imbalance and subsequent transformer saturation can be eliminated through careful design and layout.

The full bridge design is used in this thesis for its higher power capabilities, but also because of the higher input voltage to the transformer. This lowers the required number of secondary windings for a HV output.

3.1.3 Resonant Switching

Developing technologies explore the use of the full bridge further. Higher switching frequencies are possible with newer technologies, but a limiting factor is the losses during switching and the consequent heating of the device. In an ideal switch, switch-on / -off would occur with no transients, but with physical components, it takes time for the switches to switch off - *Figure 3.4*. During this time, the product of the switch voltage and current is not at its minimum as during steady-state operation and more power would be dissipated in the switch. The amount of power is the same for every switching cycle, hence the higher the number of switches per second (switching frequency), the higher the average amount of power dissipated. Another limiting factor is the high level of EMI generated by hard switching devices that are carrying high currents or voltages.

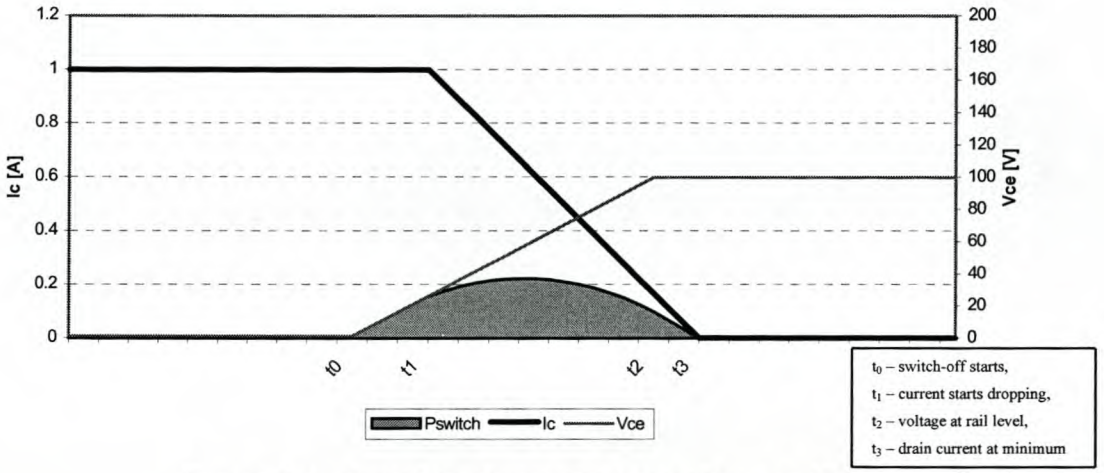

Figure 3.4 Switching Losses in Active Devices [7]

Resonant converters try to minimise the losses by changing the switch state when the minimum amount of losses would occur. Either a current or voltage remains zero during switching thereby lowering the effective power loss. The term "resonant" is deduced from the apparent L-C resonance that is utilized to force / shape the current or voltage into a desired state.

There are two main resonance categories:

1. "Load" resonance. Here the load itself is part of the resonant circuit and the current through the load is at zero when switching occurs [7], [15], [19]. The current and voltage waveforms are also more sinusoidal, improving the EMI levels. Unfortunately the peak levels are much higher than the equivalent square wave topology, which is counterproductive for EMI levels.

2. "Switch" resonance. This time the current through the switch itself or the voltage across it is (almost) zero [7], [17], [18]. Terminologies that are often used are zero voltage switching (ZVS), zero voltage transition (ZVT), zero current switching (ZCS) and zero voltage switching, clamped voltage (ZVS-CV) – an improvement to ZVS. These topologies are simpler to implement than the load resonance as they only revolve around a single switch at a time. The improvement in efficiency might not be as much, but the peak levels in the waveforms are not as high as with load resonance, once again improving the EMI levels.

Some designers are sceptical about the viability and real improvements of resonant switching, especially load resonant switching [15]. The cost saving made in improving efficiency is often lost in the higher level of complexity of the design. The complexity also hinders production streamlining with the variance in component values and layout parasitics requiring the retuning of the circuit. EMI levels are not always lower and a wide range of load conditions is not always tolerated.

Because of the complexity of the load resonant converter, the simpler full bridge phase-shifted topology is used. The phase shifted topology can be improved to a ZVS-CV topology if a higher efficiency is required, as the topology is very similar [17], [18].

3.2 Design Overview

The following technical specifications were used in the design of the SMPS:

a) Drive a magnetron with a power rating of 850W to 1.25kW. This requires approx. 2.2kW input power.
b) A HV output between 3.5kV and 4.6kV average.
c) $I_{DC,avg}$ adjustable from ~0mA to 500mA.
d) Use the average output DC current as control / feedback. This requirement stems from the fact that $Pout_{rf} \propto I_{DC,avg}$ (approx.).
e) Low output voltage ripple.
f) High switching frequency. A switching frequency of 50kHz was selected, as this would give a control loop bandwidth of approx. 5kHz. As this is three decades higher than the line frequency, filtering components would be significantly smaller resulting in lower stored energy.

g) Use a 0-10V reference input voltage to adjust the magnetron from 0 to Imax and therefore Pmax. Imax should be adjustable for use with different magnetrons.

h) Use a standard 220VAC, single-phase input supply.

i) Any other requirements as detailed for an ideal supply (2.2) should also be taken into consideration.

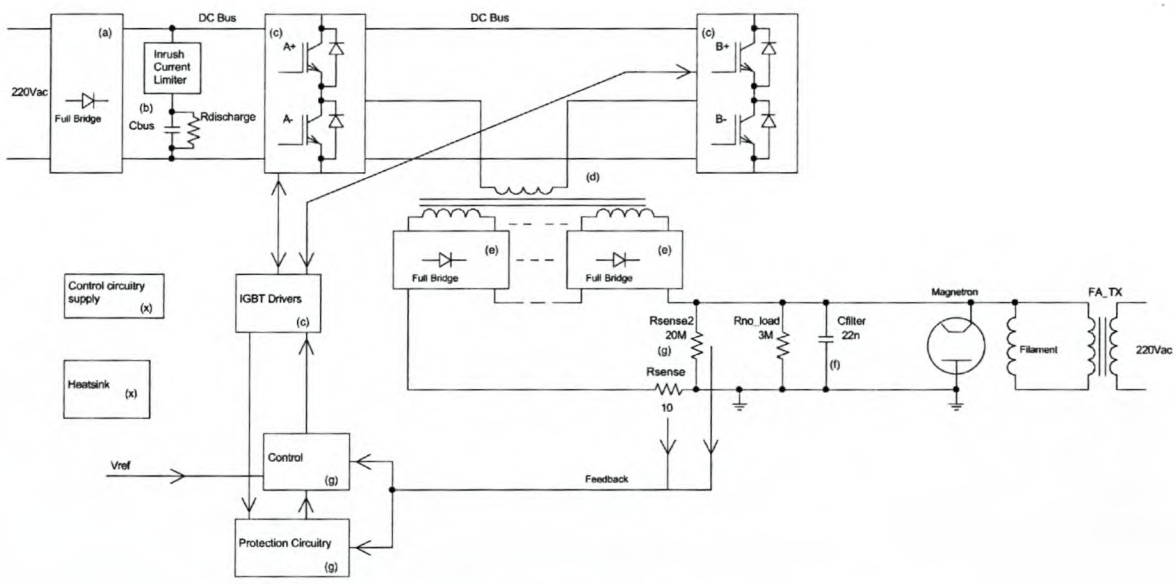

Figure 3.5 SMPS Overview

From these specifications, a SMPS was constructed as shown in *Figure 3.5*. The supply consists of the following:

a) A full bridge rectifier to convert the 220VAC to DC.

b) A DC bus capacitor for smoothing the rectified AC. An inrush current limiter is also included to limit the high inrush current into the capacitor at switch-on. This high current pulse would otherwise strain the diode bridge and shorten its mean time between failures / life cycle. A resistor is also added in parallel with the capacitor to discharge the capacitor when the supply has been switched off.

c) Two phase arms with IGBT switches (the "full bridge") and their corresponding switch drivers.

d) A high-frequency (HF), HV transformer to step-up the voltage level.

e) HF, HV rectifiers.

f) Output filter.

g) The control circuitry. This includes the sensing resistors for feedback, the loop stabilising filter, switch drive control and fault protection logic. It also compares the output current with the reference supplied from the user.

x) Weaved in-between are the necessary isolation components, control power supply and cooling apertures – that is the heat sink and cooling fan. At an efficiency of 90%, 220W of heat is still generated in the supply requiring care in designing the cooling of the unit.

The design of some of these components will be further analysed.

3.2.1 IGBT selection

The switching devices are selected according to their rated voltage and current, usually with a 100% margin on the voltage because of inductive overshoots. In a high frequency switching application, the maximum allowable switching frequency is also a factor and is usually limited by the total losses in the device as mentioned in 3.1.3.

Harris semiconductor [20], suggests the following in selecting the maximum operating frequency of an IGBT: The minimum of -

$$f_{\max_1} = \frac{0.05}{td(off)_i + td(on)_i},$$

where td(off) and td(on) is the switching time of the device.

And $$f_{\max_2} = \frac{P_D - P_C}{E_{on} + E_{off}},$$

where P_D is the absolute maximum power dissipated in the device, P_C is the conducted losses and E_{on} and E_{off} is the energy required to switch the device on and off respectively.

$$P_D = \frac{T_{j_{\max}} - T_{casing}}{R_{\theta_{JC}}},$$

and

$$P_C = V_{CE}.I_{CE}.D,$$

where D is the duty cycle per switch – 50%.

If the casing can be kept at ~50°C, the rest of the calculations can be done from the datasheets of the device. The final choice was an IGBT from Harris, the HGTG20N60B3D. This is a 40A, 600V device with a high-speed anti-parallel diode included in the package. The calculations for this device are:

$$f_{\max_1} = \frac{0.05}{275ns + 20ns} \sim 169.5kHz$$

$$P_D = \frac{150°C - 50°C}{0.76} = 131W,$$

$$I_{CE} = \frac{P_{out}}{V_{DC}.\eta} = \frac{2200W}{311V_{(rectified)} \times 0.9_{(efficiency)}} \sim 7.86A \Rightarrow 12A \text{ for extra safety margin,}$$

$$P_C = 2V \times 12A \times 0.5 = 12W,$$

Therefore:

$$f_{\max_2} = \frac{131 - 12}{250\mu J + 500\mu J} \sim 158kHz$$

This is well clear of the required 50kHz. The anti-parallel diode can handle 30A and has a t_{rr}=45ns, far less than the switch-off time of the IGBT and consequently having no effect on the switching of the IGBT.

Four Motorola IGBT drivers (MC33153) are used to drive the IGBT's, as they have the necessary device de-saturation detection and drive current. The drivers were also designed for use with opto-couplers, which are required for isolation between the control and power circuitry.

3.2.2 Output Rectifier

The output from the HF, HV transformer is in the region of $5200V_p$ ($4600V_{avg}$ at a maximum duty cycle of 90%, 500mA). With a preferred margin of 100% on the voltage rating, the output rectifier has to rectify 10kV at 50kHz!

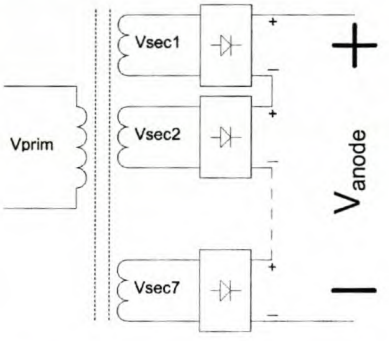

Figure 3.6 HV transformer, split and stacked secondary windings

Since no rectifiers are available in this category, the secondary of the transformer is split into seven sections, each with its own rectifier bridge - *Figure 3.6*. The MUR1100E from Motorola is used to construct each diode bridge. It can handle 1A forward current with a t_{rr} of 100ns and can withstand a reverse voltage of up to 1000V. This gives a safety margin of

35%. The total power dissipation per diode is also low, only 0.5W per diode. This gives a 25°C temperature rise above ambient in the diode.

3.2.3 High-Frequency, HV Transformer

The HF, HV transformer steps-up the voltage from the full bridge to the required output level. The following are the electrical specifications for the transformer:

Output Power ~ 2.2kW

Vprim ~ $311V_p$

Vsek ~ $4600V_{rms} = 5111V_p$ at a maximum duty cycle of 90%

F_{switch} = 50kHz, square wave.

With a $5kV_p$ output voltage, isolation in the transformer is a definite consideration. Primary-to-secondary and secondary-to-secondary isolation is improved by using glass fibre discs between the windings on the coil former - *Figure 3.7*. Layers of glass fibre tape on the centre of coil former and on the sides improve the isolation to ground. Since the secondary winding is split into 7 stages (3.2.2), the stage that is connected to the anode of the magnetron (and ground) is also the one next to the primary winding, lowering the required isolation between primary and secondary.

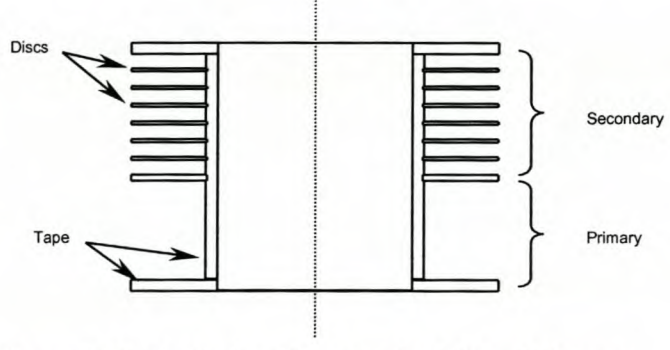

Figure 3.7 Isolating discs on the HV coil former

Siemens / Matsushita – now Epcos – supplies a software utility that predicts the power capability of their ferrite cores, given the operating frequency, topology and fill factor of the transformer. The software is based on equations that are commonly available in literature in the design of transformers ([7], [14], [15]) and simplifies the selection of an appropriate core substantially.

The software uses the following design equation:

$$P_{trans} = C.f.\Delta B.S.f_{Cu}.A_N.A_e$$

C is determined by the topology used for the design (push-pull, single-ended or flyback), f is the switching frequency, ΔB is the sweep in flux density, S is the current density in the windings, f_{Cu} is the copper fill factor, A_N is the winding window size and A_e is the effective area of the core.

In a practical design, the availability and cost of a specific core is also part of the selection criteria. Even though an ETD59-N67 core would have been the preferred selection, a PM62-N27 core was selected, as the first was not readily available. The compromise is a higher operating temperature and smaller copper window. In hindsight, a more suitable core with a lower operating temperature could have been selected. A larger copper area would also help in lowering copper losses because of the proximity effect on the windings. As per example, calculations will be done for the ETD59-N67 core.

For the ETD59-N67 core (from the Epcos software):

Ptrans = 2292W at a temperature rise of 40°C,

$\Delta B = 294\text{mT} \Rightarrow \hat{B} = 147\text{mT}$,

S or $J_{rms} = 3.9\text{A/mm}^2$,

f_{Cu} or $k_{Cu} = 0.3$. This low value is to allow for litz wire on the primary and the extra isolation discs on the secondary windings,

$A_e = 368\text{mm}^2$, $A_N = 365\text{mm}^2$, $l_N = 106.1\text{mm}$ (the avg. winding length), weight = 260g/set.

At 147mT, the specific power dissipation for N67 is ~30mW/g $\Rightarrow$ 7.87W core losses or a 20°C temperature rise.

Calculate the minimum number of windings for the primary:

$$\hat{V}_{pri} = N_{pri}.A_N.\omega.\hat{B} \Rightarrow N_{pri} = \frac{311V}{365.10^{-6}mm^2.2\pi.5.10^4 Hz.147mT} = 18.4 \approx 19 windings \ldots [7]$$

And the corresponding number of secondary windings:

$$N_{sec} = \frac{V_{sec}}{V_{prim}}.N_{prim} = \frac{5111}{311}.19 = 312.2 \sim 45/secondary \ldots$$ 7 secondary windings

The available copper area per primary winding is:

$$A_{Cu,prim} = \frac{k_{Cu}.A_N}{2N_{pri}} = \frac{0.3 \times 365mm^2}{2 \times 19} = 2.88mm^2$$

And per secondary winding:

$$A_{Cu,sec} = \frac{k_{Cu}.A_N}{2N_{sec}} = \frac{0.3 \times 365mm^2}{2 \times 315} = 0.17mm^2$$

It is not only the available space that influences the conductor size / construction, but also the skin and proximity effects.

The skin effect is the effect of current tending to flow on the outer part of a conductor, because of eddy currents that are induced inside the conductor. With an increase in frequency, the "depth" to which current will flow in a conductor, decreases. The depth at which the current density has decreased by $^1/_e$, is called the skin depth of the conductor and is a function of the conductivity and the frequency of the AC current. If a conductor is up to twice as thick as the skin depth, the skin depth has no major effect on current flow through the conductor. If the skin effect yields a too high current density, multiple isolated copper strings can be used to share the current. The diameter of each individual string is used for skin depth calculations. If these strings are combined and weaved, it is called Litz wire.

The proximity effect is the effect current in nearby conductors has on the current in a specific conductor. The effect increases with the number of layers used to construct a transformer primary / secondary. Because of the proximity effect, the conductor thickness might have to be lowered more than required for a satisfactory skin depth. Billings [14] gives a few standard graphs on the required thickness for a certain number of layers versus switching frequency. Another solution is to interleave the primary and secondary windings [7], [15]. Because of the isolation requirements, this is not an option.

The switching frequency of this supply is 50kHz, but it is a square wave supply implying current flow at higher harmonics. Pressman [15] suggests using the first three harmonics in calculating an average skin depth for a conductor conducting a 50% duty cycle square wave. The reasoning is that most of the power would be in these three harmonics. This average skin depth is then used to calculate the separate string diameters. The full bridge, phase shifted supply applies a symmetric waveform to the transformer, eliminating even harmonics. The duty cycle is also between 38% and 45% (close to 50%) during standard operation, making the assumption of lower high order harmonics possible.

The average skin depth for the first three odd harmonics are:

$$\delta = \sqrt{\frac{2}{\omega\mu\sigma}} = \sqrt{\frac{2}{2\pi f.\mu_r\mu_0\sigma_{Cu}}} = \sqrt{\frac{2}{2\pi f.1.\mu_0 \times 4.5.10^7}} \approx \frac{75}{\sqrt{f}}[mm] \ldots [7], [14]$$

$\delta_{50kHz} = 0.33mm$, $\delta_{150kHz} = 0.19mm$,

$\delta_{250kHz} = 0.15mm$,

$\delta_{avg} = 0.22mm$, therefore a conductor diameter of up to 0.44mm is acceptable.

For the primary winding:

$A_{winding} = 2.88mm^2$, $A_{string} = 0.152mm^2$ (0.44mm conductor) $\Rightarrow$ 19 strings.

Since the 19 windings on the primary would probable require 5 layers of windings, we would have to lower the conductor diameter down to 0.35mm or even lower for the proximity effect.

$A_{string}=0.096mm^2$ (0.35mm conductor) $\Rightarrow$ 30 strings,

For the secondary windings:

$A_{winding}=0.17mm^2$, $A_{string}=0.096mm^2$ (0.35mm diameter) $\Rightarrow$ 2 strings.

Since the current in the secondary windings is far lower than the primary winding, a single, thicker string can be used. A single string would improve the fill factor (f_{Cu}) and this gives us the freedom to increase the wire thickness. Although the copper losses could be slightly higher, the increase in diameter should compensate for the "unused" copper inside the wire and thereby lower the losses. The reduction in the complexity of the construction is also a great improvement.

$A_{string}=0.196mm^2$ (0.5mm diameter) $\Rightarrow$ 1 string.

Note: it is also possible to use thin sheets of copper to construct the windings. The same rules apply as far as skin depth and proximity effects are concerned, but the fill factor is up to twice as good as with Litz wire, allowing more space for copper or isolating material.

3.2.4 Output Filter

Output filtering is required to minimise the voltage ripple on the output of the supply. Simple capacitive filtering, a smoothing inductor or both can be used. The main concern in selecting components is the correct voltage rating on the capacitor and sufficient isolation to ground on the inductor.

A high-voltage series capacitor string is used to do the necessary filtering for this supply and its value is calculated using a standard hold up time equation. Standard filter equations can

also be used to calculate the required rejection of the switching frequency. Good rejection of high-frequency harmonics is only possible if low effective series resistance (ESR) capacitors are used. PCB layout should also minimise the effective series inductance (ESL) of the filter, except if it is part of the filter design.

For a 1% drop in the output voltage in 1μs (the dead time between switches on the supply), 10nF of capacitance is required. With almost 55% safety margin on the voltage rating, eight 1000V, 220nF low ESR Wima capacitors are used in series to filter the output. This gives an effective capacitance of 27.5nF, almost three times more than required at full load, but useful at lower output levels when the dead time would be longer.

A high-impedance, high-voltage resistor can be placed in parallel with each capacitor to facilitate voltage sharing on the string.

3.2.5 Controller

Since a full bridge, phase shifted topology was chosen, the necessary control IC had to be found. The UC3875 from Unitrode is such a device.

Some of the features of the IC and also the motivation for its selection are:

- Soft-start capability. The output would slowly be ramped up to the set value at start-up or during temporary fault conditions (over-current). A start-up time of 2 seconds was set through component selection.
- Variable switch-on delays. This feature ensures that two switches in the same phase arm would not be switched on at the same time resulting in a short circuit of the supply. A delay / dead time of ~ 700ns was selected – almost three times longer than the switch off time of the IGBT's.
- Adjustable frequency of oscillation. The frequency was set to the specified 50kHz.
- Wide band integrated operational amplifier. At high switching frequencies, the control circuit should be equipped to navigate fast changes in the supply. The UC3875 has a 7MHz input bandwidth.
- Sufficient IGBT drive current. Although the Unitrode can supply sufficient drive current to the IGBT's, separate drivers were used, as IGBT de-saturation sensing is not included in the chip structure.

3.2.6 Stability Analysis and Control

3.2.6.1 Controller Transfer Function

With reference to Mohan [7], the transfer function of the supply can be determined by recognising the different steady states of the supply. There are three defined states:

- Current is conducted in one direction through the transformer.
- Current is conducted in the opposite direction through the transformer.
- No current flow in the transformer, be that from either bottom or top switches in the bridge being on at the same time.

By analysing each state and acquiring the state variable description, the transfer function for the converter can be found. The result is the same as for a forward converter:

$$T_{pl}(s) = T_p(s).T_m(s) = \frac{\tilde{v}_o}{\tilde{v}_c} = 17.V_d.\frac{1+sr_CC}{LC\left(s^2 + s\left[\frac{1}{C.Z_{load}} + \frac{r_C + r_L}{L}\right] + \frac{1}{LC}\right)}.T_m$$

where T_p is the transfer function of the converter,

T_m is the transfer function of the controller IC – 0.33,

17 is the transformer winding ratio,

V_d is the bus voltage – 311V,

L is the leakage inductance of the transformer – 4.9mH, extracted by determining the equivalent circuit for the transformer according to the procedure in Sen [21],

r_L is the series resistance of the transformer windings – 1743Ω,

C is the effective capacitance of the filter capacitors – 27.5nF,

r_C is the resistance of the filter capacitors – 0.4Ω,

Z_{load} is the effective resistance of the magnetron – ~20kΩ.

Furthermore, we wish to control the average output *current*. Therefore:

$$\frac{\tilde{i}_o}{\tilde{v}_c} = \frac{\tilde{v}_o}{\tilde{v}_c}.\frac{\tilde{i}_o}{\tilde{v}_o} \text{ where } \frac{\tilde{i}_o}{\tilde{v}_o} \text{ is the gradient of the magnetron I-V curve during operation.}$$

From the I-V curves:

$$\frac{\tilde{i}_o}{\tilde{v}_o} = \frac{0.4A - 0.1A}{4500V - 4120V} = \frac{1}{1267} \text{ for a 1250W magnetron,}$$

$$\frac{\tilde{i}_o}{\tilde{v}_o} = \frac{0.138A - 0.014A}{4074V - 3960V} = \frac{1}{917} \text{ for an 850W magnetron.}$$

For voltages lower than the π-mode voltage, the slope is unpredictable and can be as low as:

$$\frac{\tilde{i}_o}{\tilde{v}_o} = \frac{0.014A}{3960V} = \frac{1}{275k}$$

The loop controller should be tested for stability in this extreme value range. Note: certain magnetrons might have a negative slope in some areas, which can lead to instability.

Finally there is the current sensing resistor, adding another constant to the transfer function:

$$\frac{\tilde{i}_o}{\tilde{v}_c} = T_p.T_m.\frac{1}{917}.10$$

3.2.6.2 Loop Filter

The aim of the loop filter is to limit the control bandwidth to approximately five times lower than the switching frequency, provide enough stability to the system (i.e. a 60° phase margin) and minimise the steady state error (i.e. a high DC gain).

From *Figure 3.9*, the bandwidth of the converter (T_{pl}) is ~ 49kHz with an 850W magnetron. With a 1250W magnetron, this lowers to ~ 38kHz. The DC gain of the system is ~ 26dB and the gain at 8kHz, our target loop bandwidth, is 17dB.

A "boost" topology is often used for the loop filter to increase the phase margin [7]. Unfortunately, this topology does not work as efficiently in reducing the loop bandwidth – something we wish to do here. The pole at zero hertz (of the boost filter) is moved to change the cut-off frequency and the rest of the circuit is calculated.

Since the magnetron is almost open circuit below the π-mode voltage, the feedback loop would be broken. To help stabilise the supply, a 3MΩ resistance is added in parallel with the magnetron. Under normal operation, this resistance has an insignificant influence on the dynamics of the supply and during an "open circuit" condition it helps to close the loop.

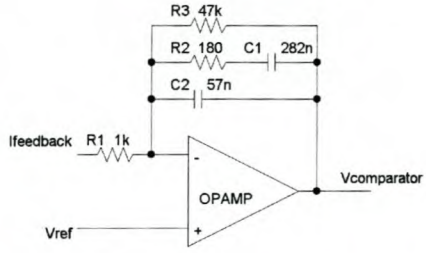

Figure 3.8 Loop Filter

Figure 3.8 shows the final loop filter with the system response depicted in *Figure 3.9*.

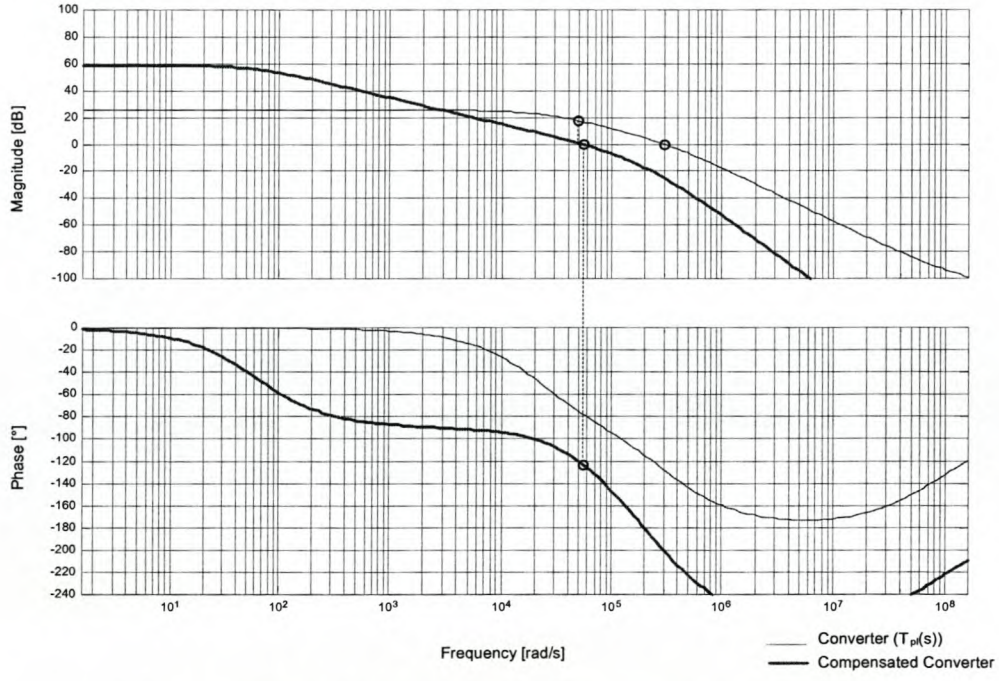

Figure 3.9 Bode Plot of the Transfer Function of the Converter

For the different magnetrons, the results are as shown in Table 3-1. Even though the performance is not good on the slope of the 850W magnetron and an "open circuit" load, our only concern here is stability – which is achieved.

Table 3-1 SMPS Stability with Magnetron Changes

Load	Phase Margin [°]	Bandwidth [Hz]	DC Gain [dB]
850W	59	8400	59
1250W	67	6300	56
850W (initial slope 1/275k)	110	27	9.5
3MΩ	NA	NA	-11

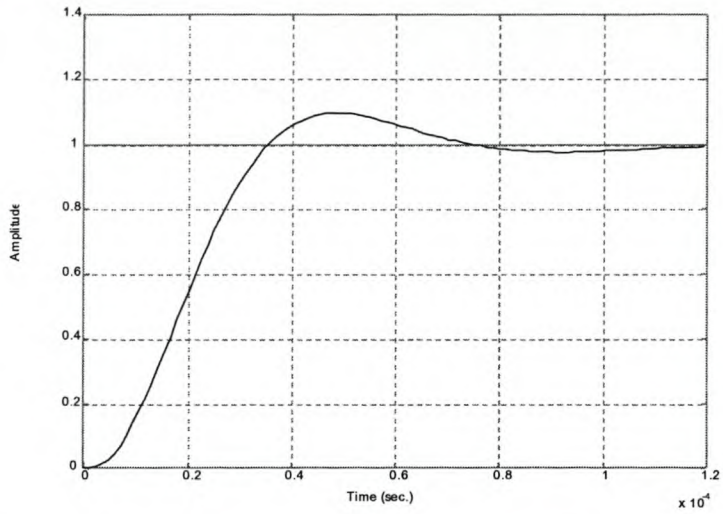

Figure 3.10 Step Response, Simulated – 850W Magnetron

Figure 3.10 shows the simulated step response of the supply with an 850W magnetron. This is a very fast response (0.1ms settling time) and raised a concern that signal noise on the user reference voltage might be transferred to the magnetron. A low pass filter is added to the *reference* voltage to prevent unnecessary fluctuations from line noise. The final reference voltage step response gives a 20% (2V) to 40% (4V) step within 4ms - *Figure 3.11*. This is more than adequate for the control from the user.

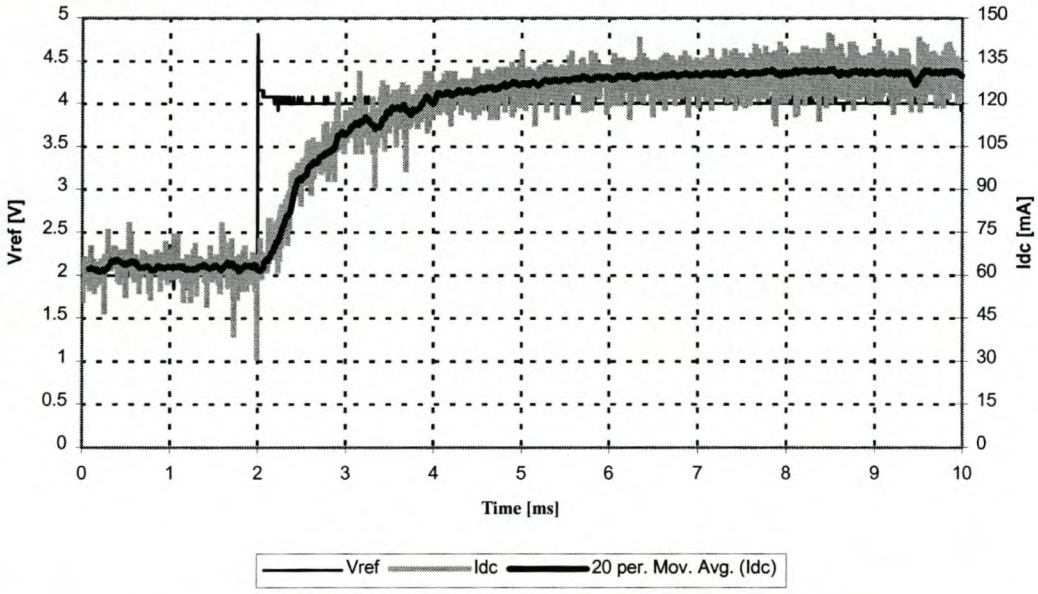

Figure 3.11 Step response - 63mA (255W_{DC}) to 132mA (535W_{DC}), 850W magnetron

3.3 Results

Firstly, let's evaluate the supply requisites initially put forward:

- A light weight supply. The SMPS plus external FA-TX weighs 6.2kg - 5.5kg excluding the FA-TX. This is three times lower than the 1250W, 50Hz supply and less than half of an 850W thyristor supply (20.6kg).
- Adjustable output power. Even though the full power range could not be tested because of noise susceptibility and the availability of a 1250W magnetron, the supply was tested from ~8W_{RF} to 520W_{RF} output power with an 850W magnetron. The DC power delivered to the magnetron at 520W_{RF} is 1020W at a power supply efficiency of 89%. Refer to paragraph 7.5 for more detail on the adjustability and efficiency of the supply.
- Magnetron adaptability. Although the control voltage is fixed on a 0-10V / 0-100% scale, the 100% set point can be adjusted from 180mA to 530mA by using a variable resistor. In a similar manner the over-current protection circuit can be adjusted to limit the average output current below a specified value in the same range. An output voltage of up to 4700$V_{DC,avg}$ can be supplied therefore any magnetron falling within this range of current and voltage can be accommodated. The only extra requirement is the FA-TX for the specific magnetron.
- Safety mechanisms included in the supply are two over-temperature inputs, one for the SMPS and one for the magnetron. The average of the output current is also fed back to control logic, which will trigger a soft start of the supply if the average rises too far above the set point. Short circuit protection is also included in the design.
- The supply stores a very small amount of energy that would be discharged to the magnetron during a fault condition. The total amount of energy in the inductance of the transformer and the filter capacitors is only 0.227J. Refer to Appendix A for a comparison of the amount of stored energy to other supplies.

While measuring the output ripple of the supply, a few interesting effects were noticed. The FA-TX seems to have quite an effect on the magnetron characteristics and therefore a secondary effect on the loading of the SMPS. Though this effect was expected, the magnitude and form thereof was not. The ripple on the supply is twice as high when the transformer is on compared to when it is switched off. *Figure 3.12* displays the ripple on the output current

at different output levels with the effect of the transformer clearly visible. From the waveform, it looks like the filament itself has an effect on the dynamic response of the magnetron. With the FA-TX on, the output has a 14% peak ripple. After switching the transformer off, the ripple drops to 8.5% peak.

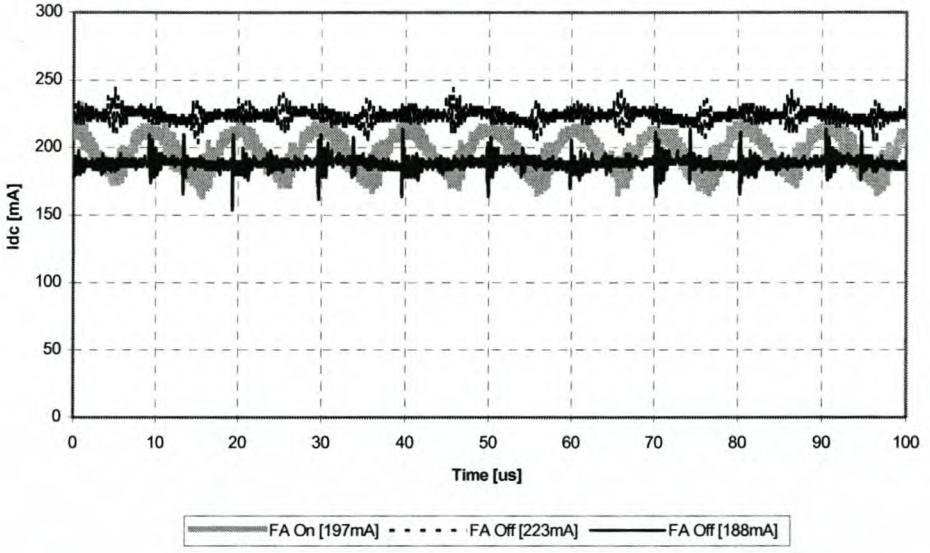

Figure 3.12 I_{DC} ripple - Effect of the FA-TX on the output current ripple

Evaluating the output voltage ripple (*Figure 3.13(a)*), the 50Hz from the FA-TX is clearly visible. When switching the FA-TX off, the DC cathode voltage rises by ~150V (*Figure 7.3*) to maintain the output power by self-heating / back-bombardment. If this was a similar effect, the frequency of the oscillation would be 100Hz since the filament heats on the positive and the negative parts of the sine wave. Alternatively the 50Hz is from some magnetising effect from the filament adding in / out of phase with the permanent magnet on the magnetron. *Figure 3.13(b)* also shows a zoomed-in version of the output ripple voltage. This higher frequency "oscillation" is also of an undetermined origin. For the exact reason for both of these oscillations, one would have to investigate the dynamics and construction of a magnetron further. This is beyond the scope of this thesis and most existing literature, as an exact model - predicting both DC and RF characteristics of a magnetron - is not available yet. With the FA-TX on, the output ripple is 1% peak and this lowers to 0.7% peak when it is switched off. *Figure 7.3* and *Figure 7.4* display some of the effects the FA-TX has on the magnetron.

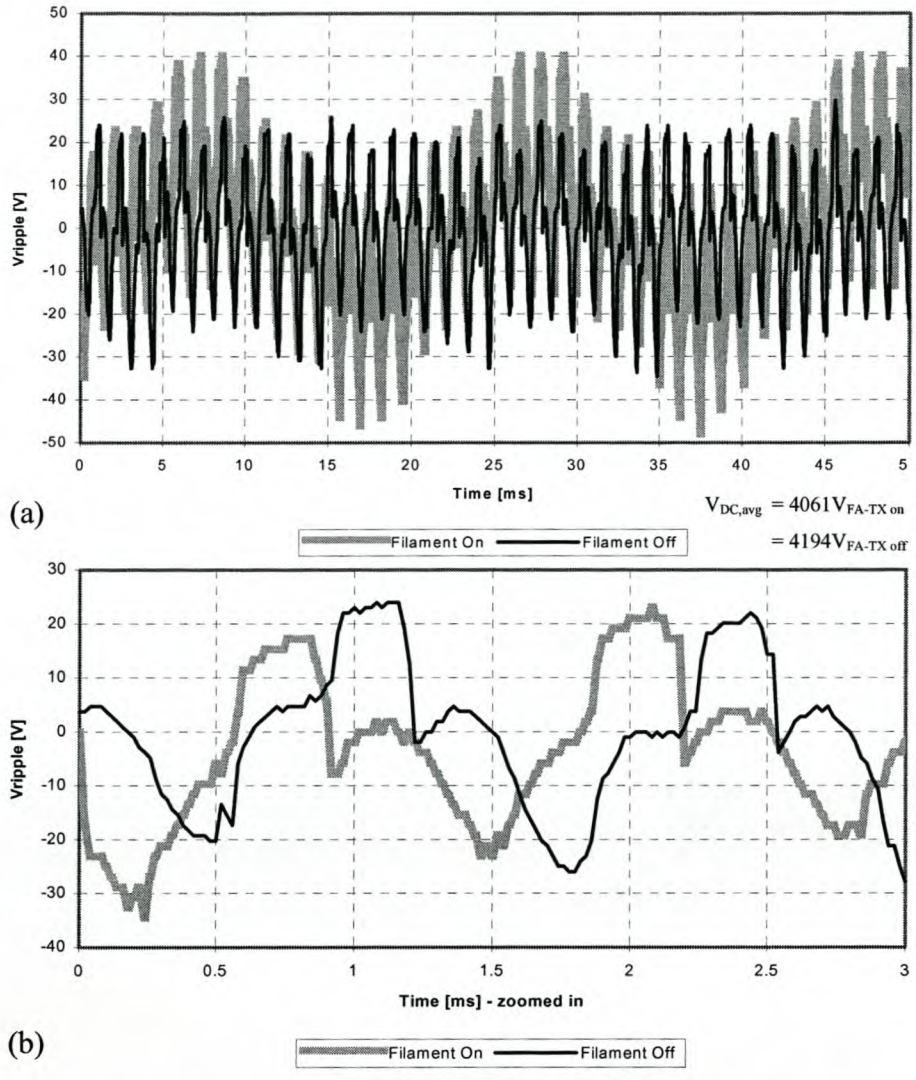

Figure 3.13 V_{DC} ripple - Effect of the FA-TX on the output voltage ripple

During the initial design of the SMPS control loop, an error was made in *not* using the dynamic impedance of the magnetron and the supply started to oscillate at medium power levels. Although this is not a scientific method, it proves the accuracy of the combined SMPS and magnetron dynamic models when the frequency of oscillation is compared to the corrected model. The model predicted an oscillation / instability at 35kHz and an oscillation was measured at 28kHz, only a tenth of a decade error in predicting the frequency.

As a final evaluation of the SMPS, it is compared to a commercial magnetron SMPS from Richardson Electronics - Table 3-2. Except for the limited output power from the magnetron (due to noise susceptibility and incorrect transformer selection), the supply compares very favourably to the commercial unit. Its main strengths lie in the capability to adapt to different

magnetrons, fast response time and the ability to supply a "magnetron friendly" output down to very low power levels (1% of P_{max}).

Table 3-2 SMPS Comparitive Performance

	P_{out}(max)	I_{out}(max)	V_{out}(max)	Output Voltage Ripple	Magnetron Range	Command Response Time	Minimum RF Output Power (Magnetron size)
SMPS	1.1kW	260mA (Limited by supply's power)	4700V	≤1%	Any supply within Current and Voltage range	4ms	1% (850W)
SM445 (Richardson Electronics)	1.8kW	450mA	4600V	<4%	Supplies similar to 2M137 (Usually within 5% of Vmax)	10-40ms	10% (1250W)

Chapter Overview

We started this chapter by highlighting the general requirements for a magnetron SMPS in laboratory applications. This is then translated into technical specifications for our design. A brief overview of some of the available SMPS switching topologies took us to the specifics of the design, especially focussing on, amongst others, the design of the HF transformer and the control loop for the SMPS. Some of the results in evaluating the supply were listed and the supply satisfies most of the original requirements. The rest of the results, most of them system orientated, will be covered in Chapter 7.

Chapter 4 Impedance Matching Unit

An impedance matching unit is one of the essential components in a microwave set-up. It helps the user optimise power transfer to the load, thereby increasing system efficiency and lowering the running costs. Without the matcher, reflected power from a mismatch would simply be dumped into the water load of the circulator.

The unit enables the user to change from a conveyor set-up for heating liquids to a small closed unit drying wood and then to a custom chamber for heating small quantities of carbon. Each time a satisfactory efficiency can be achieved by simply matching the magnetron to the load. If the load is sufficiently matched to the magnetron, one might also use the system without a circulator. The magnetron requires a load matching with a VSWR < 4, but preferable < 1.2.

4.1 Unit Requirements

For practical reasons, the following requirements can be highlighted for a matching unit:

1. The unit should be simple to use.
2. RF leakage should be below international safety limits.
3. The bandwidth should cover the range of frequencies of a magnetron.
4. The ability to match a wide range of impedances.
5. High power capability.
6. Acceptable matching / position repeatability.

To these one can add:

7. Light weight – especially with WR340 and larger waveguide systems.
8. The unit should not require a long set-up time – this complements (1).
9. Accessibility / controllability by a PC with the option of automated matching.

Matching would be required at the start of a test sequence to match the magnetron with the load, but also at a later stage as the loads' characteristics change, as is the case when drying a product.

4.2 Theory

Three "elements" are used in a distributed matching structure to give the user sufficient freedom to cover the Smith chart. "Coverage" refers to the range of impedances that can be matched. Depicted on a Smith chart, it indicates an area - *Figure 4.4.*

4.2.1 Capacitive Post Elements

This structure uses three capacitive stubs inside the waveguide for matching. Adjustable screws are often used to realize these elements - *Figure 4.1(a).*

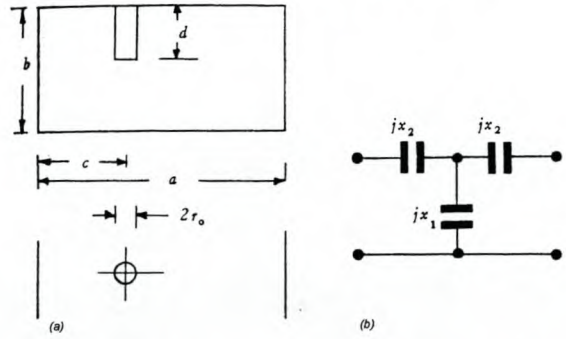

Figure 4.1 The capacitive post (a) and its equivalent circuit (b) [11]

Each post adds a shunt and two series capacitive elements (*Figure 4.1(b)*) to the waveguide line-up. The equivalent components can be calculated using the diameter ($2r_0$), height (d) and spacing from the sidewall (c). Using a centred post, simplifies the calculations. Alison [11] gives some equation to calculate the equivalent impedances, as well as graphs to indicate the effect of mechanical tolerance on the placing and dimensions of a stub. Since a manually adjustable unit was available on hand, this was first inspected. The unit utilizes posts / stubs.

Each stub consists of a copper stub that is lowered into the waveguide, using a screw feed on top - *Figure 4.2.* The feed also has a rotation counter as a reference to the displacement.

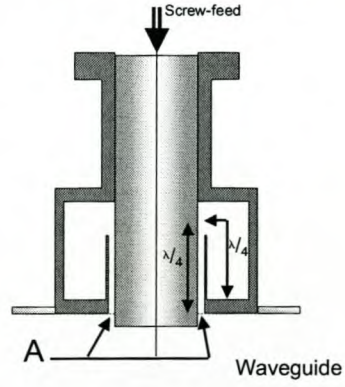

Figure 4.2 Centre stub construction

An ideal electrical contact is not always possible at the entrance through the waveguide wall - point "A" in *Figure 4.2* - since free movement of the stub is required for tuning. Leaving a gap around the post would act as a "coaxial" pick-up and RF would radiate from the waveguide, creating a dangerous environment. This problem is overcome by using a quarter wave short topology to create a virtual short at the waveguide edge.

This topology was not implemented for the following reasons:

- The mechanical structure was beyond our in-house manufacturing capabilities.
- The capacitive post has a limited power handling capability. By lowering the post, the distance between the two walls are lower and arcing at higher power levels are more likely.
- The limited power handling also determines the maximum post length, thereby limiting the possible coverage of the matcher.

4.2.2 Shunt Offset Short Elements

An alternative topology would be to use offset short matching elements - *Figure 4.3*. From Collin [8], two shunt offset shorts spaced a distance "*d*" apart, can match any load – except for a certain region determined by the spacing "*d*" - *Figure 4.4*. By using a third stub, any admittance within this region is first transformed outside the "no-match" area. The remaining two stubs can then match the transformed impedance.

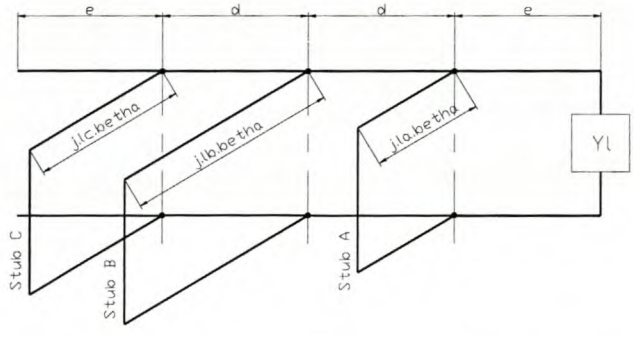

Figure 4.3 Three stubs - graphical representation [8]

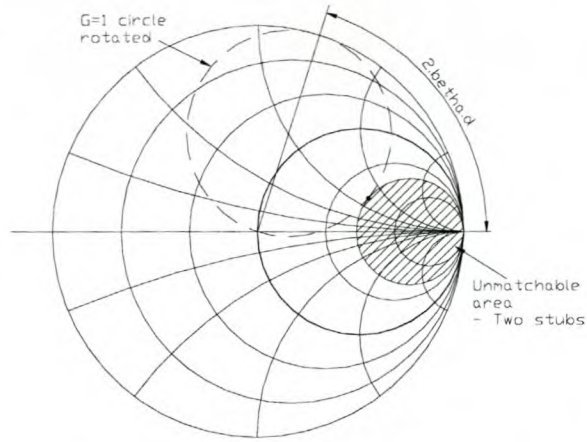

Figure 4.4 Graphical coverage of 2 stubs [8]

A spacing d of $\sim \lambda/8$ or $3\lambda/8$ is preferred, as this gives the lowest frequency sensitivity to the stub / offset position.

To realize a variable shunt offset short in a waveguide, a T-section is constructed. The T-junction is on the narrow wall, as a junction to the broad wall would imply a series element, Harvey [2]. An aluminium block is moved up and down inside the T-piece to vary the offset distance. The three arms / T-sections are spaced evenly. More detail on the mechanical construction is available in paragraph 4.4.

4.3 Simulation

Since the arms are spaced within a wavelength of each other at 2.4GHz and each one is almost as wide as it is spaced from the next arm, they interact with each other. It would not be possible to simulate one arm in a finite element package and then extrapolate the effect of the full structure. To simulate the full structure would also consume too many resources (CPU time), especially with the total number of offset possibilities.

Matlab was used to simulate a "scaled down" version of the matching unit. The waveguide and offset shorts were treated as standard transmission lines that are cascaded. Neither the effect of the stubs on each other, nor the fact that the width of a T-piece is in the order of a wavelength, was considered. Only the phase distortion associated with waveguides is included.

This simulation is only used as an exercise to determine the possible coverage and is not meant to be an *exact* representation.

Since the magnetron prefers to see a matched load, the simulation is to determine what type of load can be matched. The s-parameters of each section (*Figure 4.5*) are first calculated. By transforming the different s-parameter sets to T-parameters, the cascaded T-parameters can be calculated and once again be transformed to s-parameters. Finally the input impedance can be calculated, with a matched load on the output.

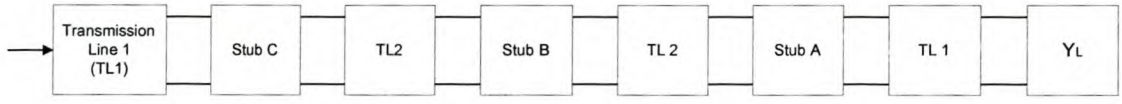

Figure 4.5 Subsections in the simulation of the matching unit

Mathematically this would be:

The s-parameters of a length l of a transmission line:

$$s = \begin{bmatrix} 0 & e^{jl\beta} \\ e^{jl\beta} & 0 \end{bmatrix}, \text{ where } \beta = \frac{2\pi}{\lambda_g} \text{ and } \lambda_g \text{ is the cut-off wavelength of the waveguide}$$

The input reflection coefficient of the offset short can be calculated using:

$$\Gamma_{in} = s_{11} + \frac{s_{12}s_{21}\Gamma_L}{1 - s_{22}\Gamma_L}, \text{ with } \Gamma_L = -1, \text{ a shorted termination.}$$

The effective admittance of each stub is then calculated. The admittance is used since the offset shorts are in shunt with the main waveguide.

$$y = \frac{Z_o}{Z} \text{ where } \frac{Z}{Z_o} = \frac{\Gamma_{in} - 1}{\Gamma_{in} + 1} \text{ and } y \text{ is the normalized admittance}$$

Using Medley [9], the shunt equivalent of the T-piece / offset short is calculated:

$$S_y = \begin{bmatrix} \frac{-y}{2+y} & \frac{2}{2+y} \\ \frac{2}{2+y} & \frac{-y}{2+y} \end{bmatrix}$$

The S to T and inverse transformations (Frickey [10]) are used to calculate the cascaded effect of the stubs and waveguide sections. With a matched load, the input impedance of the structure equals S_{11}.

Figure 4.9 shows the correlation between the simulated and measured results. The total coverage was also measured and found to be excellent - *Figure 4.8*. The figure shows the effect of moving each stub approximately 63mm outward in ~2mm steps.

4.4 Mechanical Construction

An aluminium block is moved inside the waveguide to act as a short – *Figure 4.6*. Graphite powder assists the movement of the block and also improves the electrical contact to the wall.

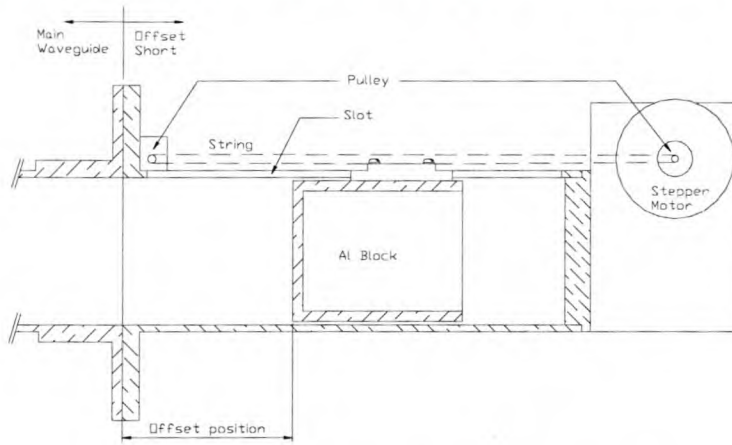

Figure 4.6 Side-view of offset short

Movement is achieved by using a stepper motor and a thin nylon string wrapped around a smooth post / pulley. The string is attached to the Al-block with a small "saddle" that moves inside a slot in the wall. To ease movement, the block was also hollowed out to make it lighter. As with the capacitive stub, RF leakage is an important consideration. The width of the slot was kept as narrow as possible. The construction and position of the saddle are also such that there is no direct path for the RF from the inside to the outside of the waveguide. The saddle is shorted to the waveguide through the aluminium block.

The advantage of a stepper motor is the known step size. If a servo or other type of motor had been used, some form of position / displacement feedback would be required. The stepper motor would give a step in degrees of rotation that translates into a distance of linear movement, according to the axes diameter of the motor.

The choice of the string is motivated by the high strength to thickness ratio of nylon. The bending radius is also small, making the possible post / pulley size small. If the string is thick, the effective radius of the axes is larger and the pulling strength of the motor lower. The pulling strength / force of the motor is calculated as: $Force(F) = \frac{MotorTorque(T)}{EffectivePulleyRadius(r)}$ where the maximum torque is a fixed value for a specific motor and the radius determined by the axes diameter and string thickness. If F is too

low, the motor might not move the Al-block, the block might slip or the motor might overheat.

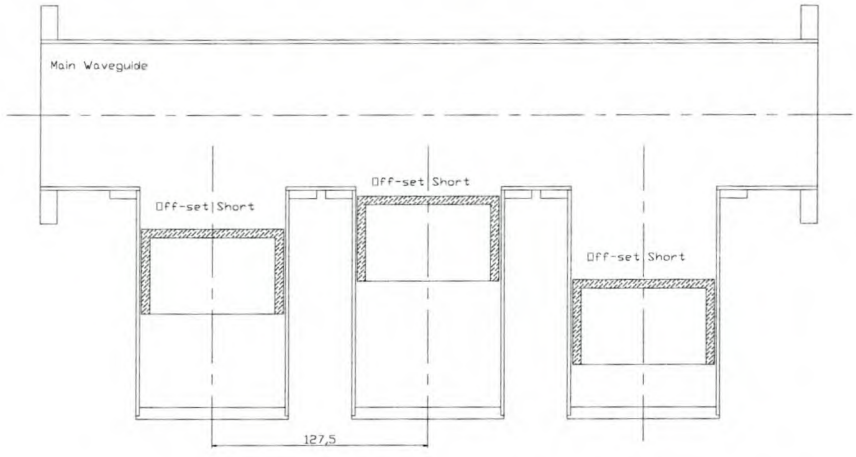

Figure 4.7 Matching unit – broad side view

The three stubs where evenly spaced at ~127.5mm - *Figure 4.7.*

4.5 Electrical Construction

The driving circuit of the three stepping motors is based on some examples from Jones [12]. A micro-controller handles the interface to a PC through serial communications and coordinates the different mechanisms on board. Appendix B.2 details the final schematic diagram and interface.

The following is implemented on the electronic controller board:

- A manual / PC control option – a PC is not required to use the matcher; it can be set through manual command.
- A default switch-on position – all offsets are moved to zero offset / "home" at switch-on.
- Limit switches and indicators – these prevent possible overrun resulting in damage to the motor or mechanics.
- Manual command includes "step up", "step down" and "home" commands for each motor.
- PC control receives a single serial byte that designates the following:
  (Appendix B.1 lists the finer detail)
  - Number of the motor that is addressed – 1, 2 or 3
  - Command – move up or down

- Number of consecutive steps to take – up to 31 steps or ~10mm of movement. If zero (0) steps are specified, the command is interpreted as a "home" command, that is: move until the minimum offset limit is triggered.

Only one motor can be addressed at a time, but since response is quick, this is no drawback.

After the command is sent through, the micro-controller replies with one byte, indicating:

- Command successfully completed.
- Command not completed since the minimum / maximum limit was reached while executing the command. A number of "n" steps of the command were not taken.
- Command error as: (a) the previous command is not yet completed,
  (b) the command received specifies upward / downward movement and the maximum / minimum limit had already been reached during a previous command.

The matching unit can now be controlled from any software capable of driving a serial port on a PC.

4.6 Results

To test the accuracy and coverage, the matching unit is connected to a matched load and the remaining port is connected to a network analyser.

A Pascal program controls the network analyser, downloads s_{11} from the network analyser and steps the motors through the different positions. Each short can be offset by up to 73mm and one motor step gives a movement of ~ 0.33mm. A short can move 31 steps or 10.2mm in 0.5s in a single command.

To get a good idea of the coverage, each short was moved from 0mm to ~63mm in increments of ~2.3mm or 7 motor steps. *Figure 4.8* shows the coverage of the unit. The slightly lower coverage in *(a)* is because of the greater wavelength at 2.42GHz. This becomes even more apparent at lower frequencies, but that is not a concern since the magnetron only works in a limited frequency band. The coverage would be slightly better if the full range of 73mm is used.

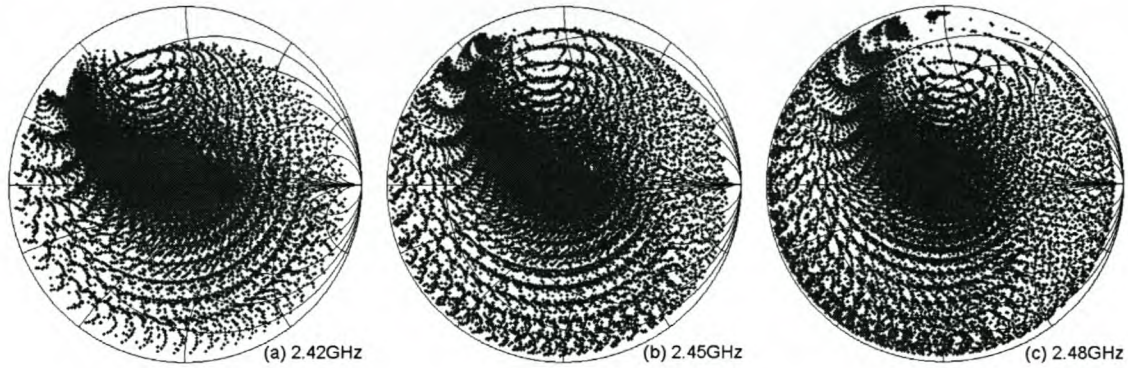

Figure 4.8 Impedance coverage

Figure 4.9 shows the measured and simulated results for each short. The figure shows only one short moved at a time, from zero to 63mm, while the other two remained at zero offset. As one can see, the stubs are not at the optimum spacing for a low frequency sensitivity and a spacing of slightly less - $5\lambda/8 \sim 105mm$ - (if possible) or more - $7\lambda/8 \sim 148mm$ - would have been better than the current design.

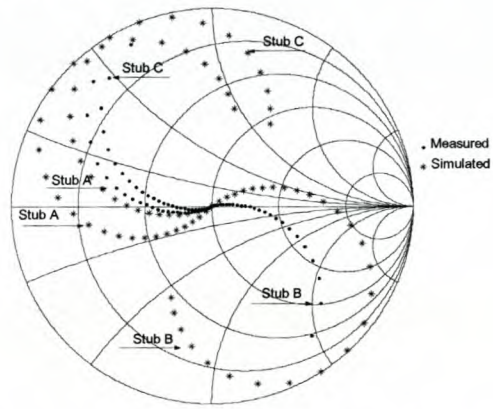

Figure 4.9 Single stubs – measured and simulated results

Comparing the simulation to the measured results, the measured phase spacing between the shorts is close to the predicted values. The "outward" movement per arm tend to be far less than the simulation. The simulated points are also spaced well apart whereas the measured values show almost no contribution at low offset values, with increased effect at higher offset values. This can be expected since the simulation considers the short to be a lumped element at a specific point in the waveguide, while the structure distributes the short over the width of the waveguide wall or ~86mm.

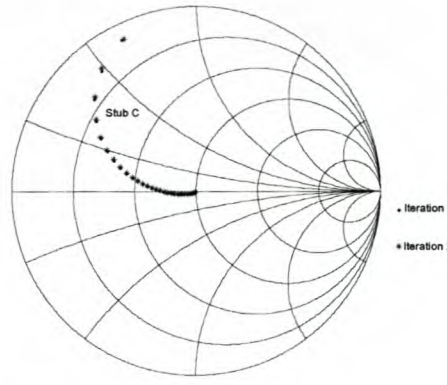

Figure 4.10 Stub position repeatability

Figure 4.10 shows the repeatability of displacement for a single stub over two runs. During system measurements (Chapter 7), an error of ~6.4 to 8.9% or 2mm was measured between the position of the short and the expected offset according to the number of steps taken. This is attributed to the nylon string sometimes slipping on the pulley of the stepper motor. The slipping should not be a problem in most practical measurements, but a "home" command as reference should be considered if a long step sequence is used.

As far as safety is concerned, the maximum leakage from any point on the structure was measured as 3mW/cm^2 @ 280W RF. That is 8.5mW/cm^2 for a standard 800W magnetron. This is measured *at* the slot in the waveguide. The maximum allowable level for long-term exposure is 10mW/cm^2 for 8 hours according to USA standards. The unit would therefore be within this limit, especially since the radiation would be attenuated at $1/r^2$ away from the slot.

More results on actual matching problems are listed in Chapter 7.

Chapter Overview

This chapter described how an impedance matching unit was constructed. The basic mechanical construction and electronic / software interfaces are discussed and the unit's performance was measured. According to these results, the unit complies with all the requirements set for a matching unit. These requirements are: ease of use, low RF leakage, sufficient bandwidth coverage, sufficient impedance coverage, high power capability (by design), position repeatability and controllability via a PC. With the aluminium construction, it even satisfies 5.1 (7) – a light weight construction.

Chapter 5 Dual Directional Coupler

In most set-ups, we wish to maximise the RF power transmitted from the magnetron to the load by using an impedance matching network. To determine how well the match between the magnetron and load is, a dual directional coupler is used.

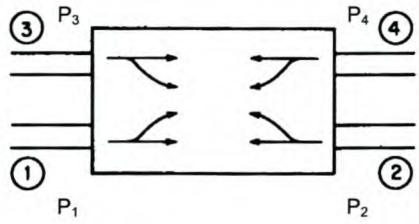

Figure 5.1 Dual directional coupler. Arrows indicate the flow of power [8]

The coupler splits off a small, known portion of the power from the main RF forward travelling path (P_1 to P_2) to a separate port (P_4). Refer to *Figure 5.1.* In the same manner a small, but equal portion of the reverse travelling or reflected power (P_2 to P_1) is split off to another port (P_3). These power levels are usually measured using detector diodes that return a voltage according to the amount of RF power detected. The reflection coefficient of the load can be calculated as: $\Gamma_L = \sqrt{\frac{|P_3|}{|P_4|}}$

5.1 Directional Coupler Topologies in Waveguides

All the topologies consist of the following basic principle: energy is coupled from one or more apertures inside one waveguide to another waveguide. The forward power is constructively, and the reflected power destructively added to produce the directivity of the coupler from either the physical distance between a number of slots / holes or the position and orientation of slots / holes in the waveguide. In single hole applications, the combination of the magnetic currents and electric fields determine whether the "split off" is directionally constructed in the second waveguide or not. The amount of coupling is determined by the size of the aperture(s).

The single hole or Bethe-hole coupler (*Figure 5.2(a)*) uses two waveguides that cross at an angle. A hole is placed in the broad side of the guides, in the centre of the wall. As the magnetic field is circularly polarised at the transverse plane, either clockwise or anti-clockwise depending on the direction of propagation of the wave, it couples a circular

polarised field into the second guide, through the hole. This field then excites a unidirectional propagation in the second waveguide, giving rise to the directivity. Directivity can also be achieved by placing the coupling hole off centre or by making the hole elliptical in shape [8]. The coupling coefficient is not that sensitive to frequency, but the directivity is, making this a narrow band device. The bandwidth can be improved by using two coupling holes diagonally across the waveguide, spaced at $\lambda/4$ (*Figure 5.2(b)*) or a small cruciform (*Figure 5.2(c)*) for coupling.

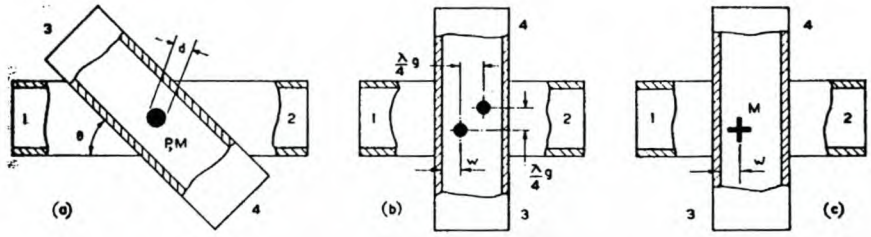

Figure 5.2 Single (a) and twin coupling holes (b), twin slot or cruciform coupling (c) [2]

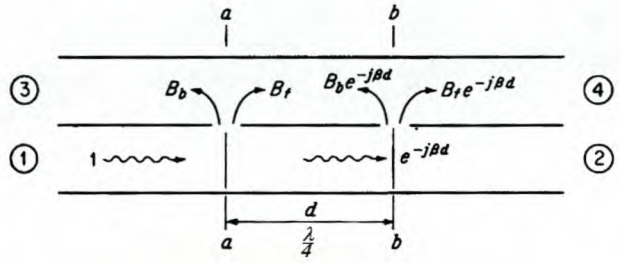

Figure 5.3 Two hole / slot directional coupler[8]

Another way of implementing a directional coupler, is by using an array of identical holes / slots in the broad side wall between the waveguides at a spacing of $\lambda/4$.

By looking at a two hole example (*Figure 5.3*), a small portion of the incoming wave is split off to the second wave guide. Since this portion is very small, the main power level is approximately the same size and an equal amount is split off at the second slot. The forward travelling waves will add in phase in the second waveguide, but the backward travelling waves will cancel. This is because the second backward travelling wave ($B_b e^{-j\beta d}$) would have travelled 180° (90° going forward + 90° coming back) by the time it reaches the first slot and would therefore be the inverse of the wave travelling backwards from the first slot ($B_b e^{-j\beta d}$, d=0), consequently resulting in cancellation. Once again the coupling is not very frequency sensitive, but since the spacing of the slots are related to the phase difference and therefore the

wavelength, the directivity is. A solution is to use more than 2 holes / slots to improve the bandwidth of the coupler, [2].

5.2 Coupler Design

With all the directional couplers mentioned above, the unidirectional wave is still travelling in a waveguide. To measure the amount of forward / reverse power, one still requires a waveguide to coaxial transition to connect the coupler to a power meter / detector diode. It would be far simpler (and physically smaller) if the second wave-"path" had been a coaxial cable. If care is taken to match the transitions / coupling apertures where the wave travels from one medium to another, a hybrid coupler could function with satisfactory results.

5.2.1 Theory

The main objective would be to design the coupling ports to have the same amount of coupling, be matched from the waveguide to the 50Ω of the coaxial line and to have the coupling ports 90° or $\lambda/4$ apart.

A quarter wavelength (90°) can be calculated in both mediums:

Waveguide: $$\frac{\lambda_g}{4} = \frac{\lambda}{4\sqrt{1-\left(\frac{\lambda}{\lambda_0}\right)^2}}, \qquad (a)$$

Coaxial conductor: $$\frac{\lambda_c}{4} = \frac{\lambda}{4\sqrt{\varepsilon_r}}, \qquad (b)$$

where λ_0 is the cut-off wavelength of the waveguide, equal to $2a$ (twice its width),

λ is the free space wavelength of the centre frequency and is smaller than λ_0, and

ε_r is the relative permeability of the dielectric used in the coaxial conductor and is greater than, or equal to 1.

Therefore λ_g is unequal to λ_c since $\lambda_g > \lambda$ and $\lambda_c \leq \lambda$. A quarter wavelength in the coax is shorter than in the waveguide and it would be impossible to connect the two coupling points with the coax! We can make the length of the coax 270° to reach the second port. The only difference would be that the forward and reverse ports on the coupler would swap as indicated in *Figure 5.4*.

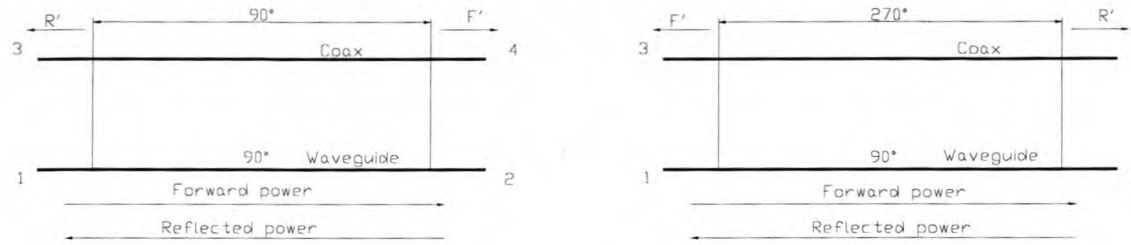

Figure 5.4 Forward and reverse ports with 90° and 270° coax length

5.2.2 Waveguide section

The waveguide with two coupling holes was simulated using a finite element software package. The output of a magnetron is usually 2.45-2.46GHz ±10MHz, but it varies up to ±50MHz if load pulling and the variation in the supply voltage / current is added. The spacing was optimised for a centre frequency of 2.45GHz, roughly the centre of the output spectrum, with a coupling of –50dB. This would give a maximum of 10mW into a detector diode with a magnetron of 1kW output power. A standard WR340 waveguide was used for the simulation. Two N-type connectors were used to couple the incident wave from the waveguide.

From *(a)*, the spacing between the two connectors is calculated as:

$$\frac{\lambda_g}{4} = \frac{c/f}{4\sqrt{1-\left(\frac{c/f}{2a}\right)^2}} = \frac{c/2.45e+9}{4\sqrt{1-\left(\frac{c/2.45e+9}{2\times 86e-3}\right)^2}} = 43.529mm, \lambda = \frac{c}{f}$$

where c is the speed of light in a vacuum.

A spacing of 43.5mm was tested during simulation. A phase difference of 89.97° to 90.04° was found from the simulation. *Figure 5.8* shows the simulated phase values.

Since there was no indication on how much coupling could be expected, the simulation started with an N-type connector flush to the waveguide. Both the centre pin and the Teflon piece were flush with the inside wall. The simulation predicted a coupling of ~ -38.3dB. Through iterative simulation, the flush section was moved away from the waveguide to lower the coupling and the centre pin was extended to improve the matching of the transition. *Figure 5.5* gives the dimensions that were used in the design. Note that this gave a coupling slightly higher than required. The coupling became more sensitive to the displacement as the pin was

moved away from the waveguide wall and the final "tuning" was left until the physical structure was assembled.

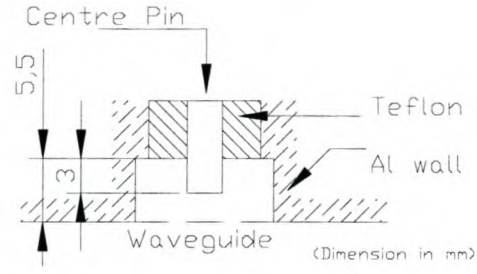

Figure 5.5 Waveguide to coaxial transition

The full waveguide structure as depicted in *Figure 5.6* was simulated and the results are shown in *Figure 5.7* and *Figure 5.8*. The measured results, $S_{1,3}$, $S_{1,4}$ and $P_{3,4}$ are also shown.

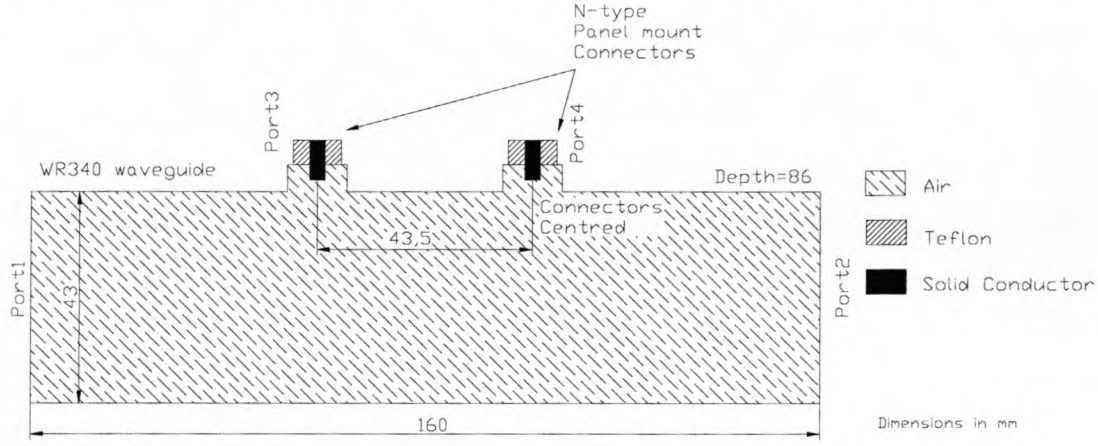

Figure 5.6 Waveguide structure

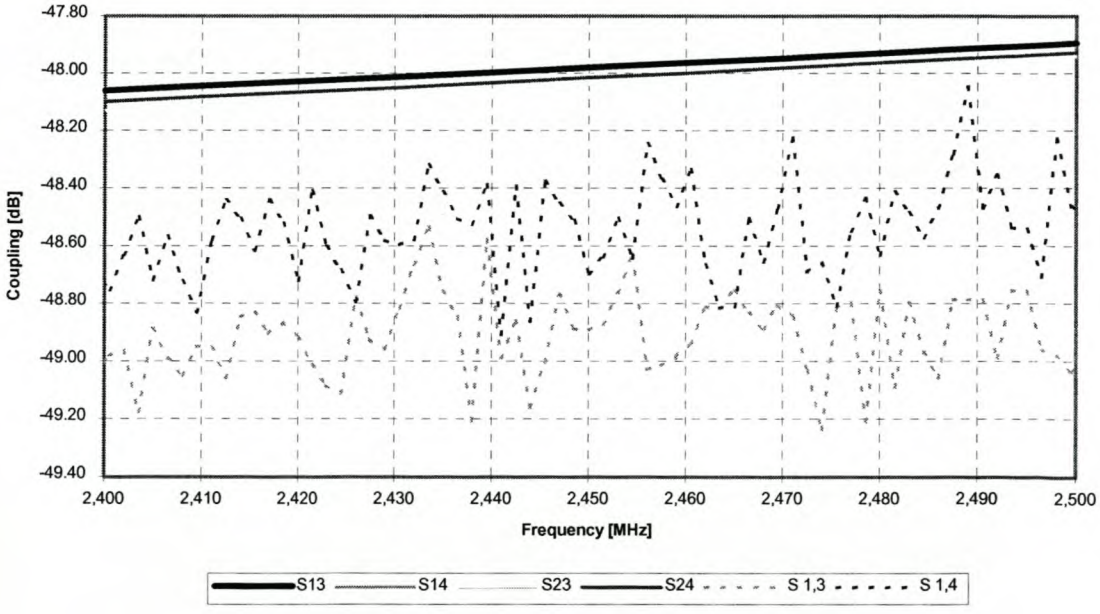

Figure 5.7 Coupling to the 2 ports – simulated and measured

The great variation / ripple in the measured results can be contributed to the very low power levels measured as well as the accuracy of the WR340 transitions and standards that were used – S_{11} ≥-30dB for the transitions.

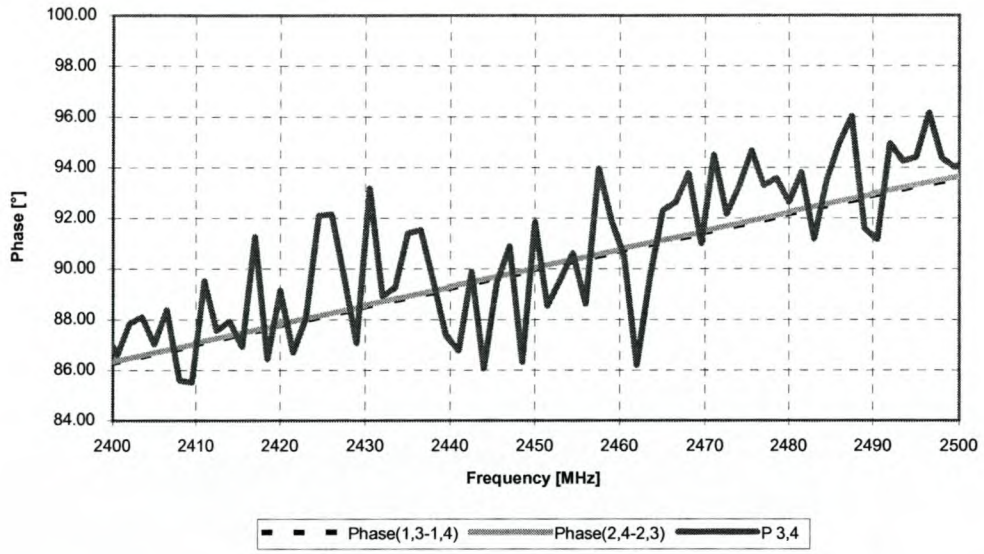

Figure 5.8 Phase difference between the ports – simulated and measured

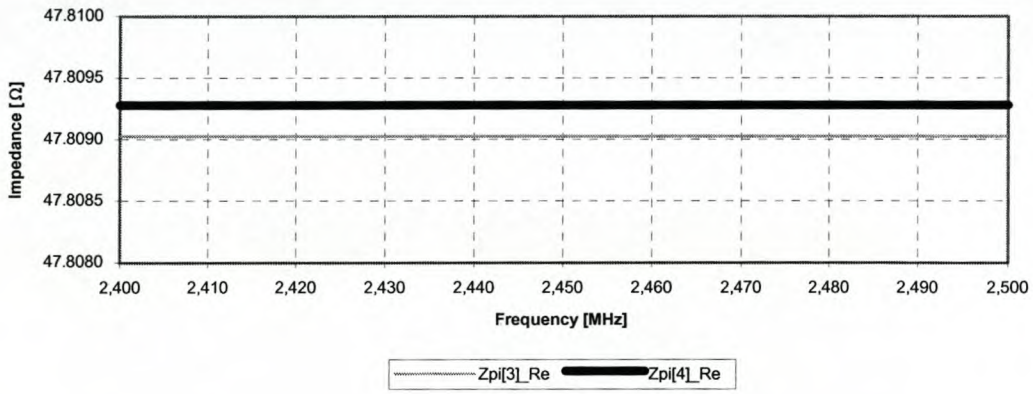

Figure 5.9 Simulated impedance of the two coupling ports

The impedance (Zpi) of the two coupling ports was also extracted from the simulation. From *Figure 5.9* the impedance is ~ 48Ω, which is close to the 50Ω of the coaxial line. The coaxial structure should therefore not be adversely affected by the coupling ports.

There is a slight difference in the coupling (0.07dB max.) and phase (0.08° max.) between the ports in the simulation. Since the structure is symmetric, this difference should not occur. It is possible that the meshing in the simulation was not symmetric and this would give rise to the slight difference.

The measured coupling also differs from the simulated value by approx. 0.6dB while the phase difference between the two ports is close to the expected value. The coupling error can be contributed to a slight difference between the offset of the N-type connectors from the waveguide wall and that of the simulation. Most of the WR340 waveguides that are available are also not perfectly "flat". They tend to bow in the centre by up to 2mm from both sides on the broad side. The difference in coupling between the two ports (~0.2dB) can be contributed to something as small as the aluminium burring on the edge of the coupling holes. All of these physical errors can be considered to be a function of the mechanical expertise available and is therefore considered to be a given tolerance.

Thin brass shims were added between the N-type connector and the mounting plate to bring the coupling down to ~ -50dB. *Figure 5.10* and *Figure 5.11* show the result of these changes.

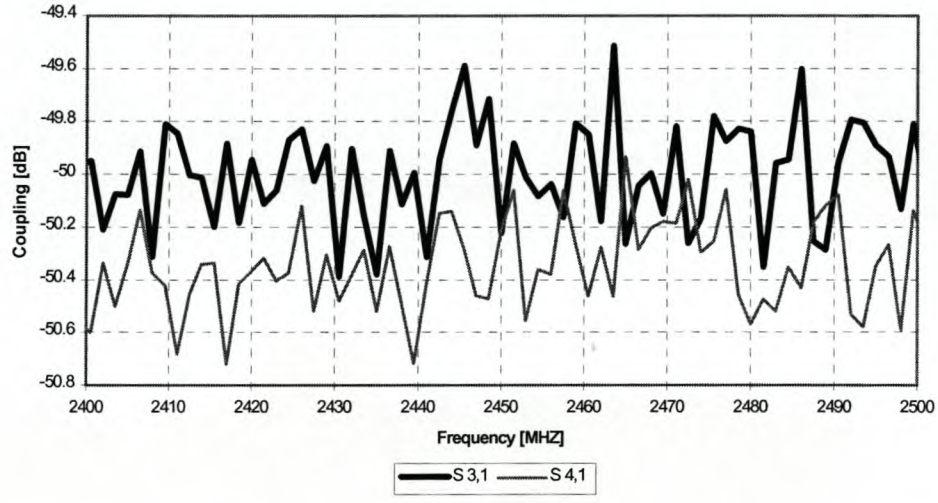

Figure 5.10 Final waveguide coupling : Ports 3 and 4

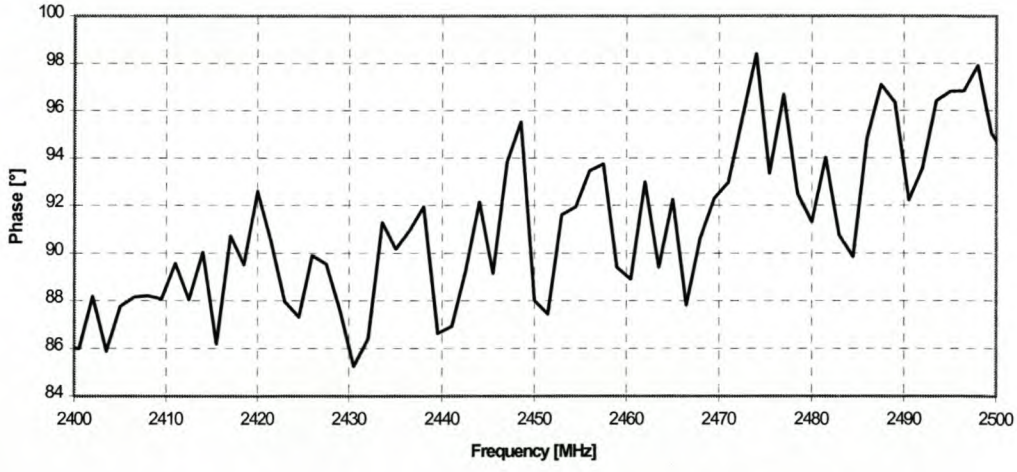

Figure 5.11 Final waveguide phase difference : port 3 to 4

5.2.3 Coaxial section

From *(b)*, the length of the coaxial section is calculated as:

$$\frac{3.\lambda_c}{4} = \frac{3.\lambda}{4\sqrt{\varepsilon_r}} = \frac{3.c/2.45e+9}{4\sqrt{2.1}} = 63.329mm$$

Note that we take three times the quarter wavelength for the 270°.

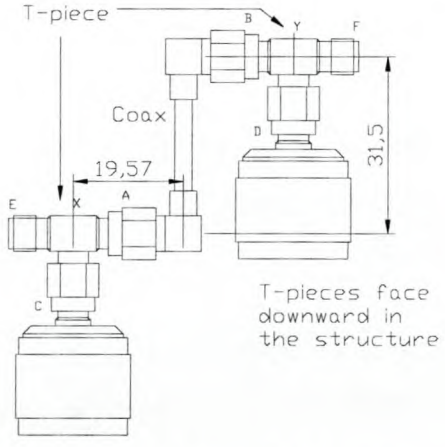

Figure 5.12 Coaxial structure

From *Figure 5.12* we can see that the "coaxial section" is split up into a piece of coax cable, two right-angled coax SMA connectors, two T-pieces and two N to SMA adapters. The adapters do not contribute to the phase difference, as each wave travels through an adapter. Neither does the one leg of the T-piece (distances X-C and Y-D).

Section X-Y should be equal to 270° or 63.3mm – *if* the connectors do not influence the effective dielectric of the structure. Bits of air in the right-angled connector end points or the right angle itself, might require a physically longer coaxial cable.

At first the coax was calculated to be ~24mm long. This is calculated from the 63.3mm, but subtracting the distance between the centres of the T-piece and the right-angled connector – twice. This distance was originally calculated as approximately 20mm. Half a millimetre was added for the "air" effect.

The coaxial cable was assembled and the phase length measured. By connecting one T-piece to the cable and terminating the "male" side of the connector to 50Ω, one can measure the

distance E-X-A-B in degrees (refer to *Figure 5.12*). This would be equal in distance to X-A-B-Y, as E-X is equal in distance to B-Y. A small portion of the power would be split off into the load, but we are only interested in the phase difference. At 2.45GHz the distance was only 238°. This required another 32°, or 7.4mm, which gives a total coax length of ~31.5mm. A new cable was assembled and the distance is as indicated in *Figure 5.12*, with the phase length as shown in *Figure 5.13*. The phase at 2450MHz is 1.8° more than required, but this was considered to be accurate enough for the design.

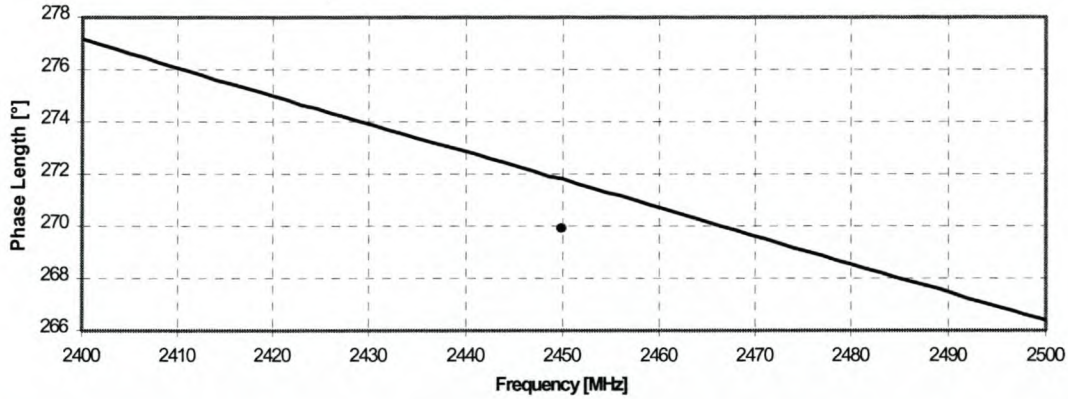

Figure 5.13 Phase length of the coaxial section

5.3 Results

The full structure was assembled and the coupling, directivity and input matching were measured. The input matching of all four ports was also measured, as the matching at the connecting port would influence any device connected to the coupler. This is usually a detector diode or a spectrum analyser for the two coupling ports (3 and 4). For the best results, detector diodes with a 50Ω input match should be used.

(Note that the following graphs are shown over a wider band than the previous simulations and measurements.)

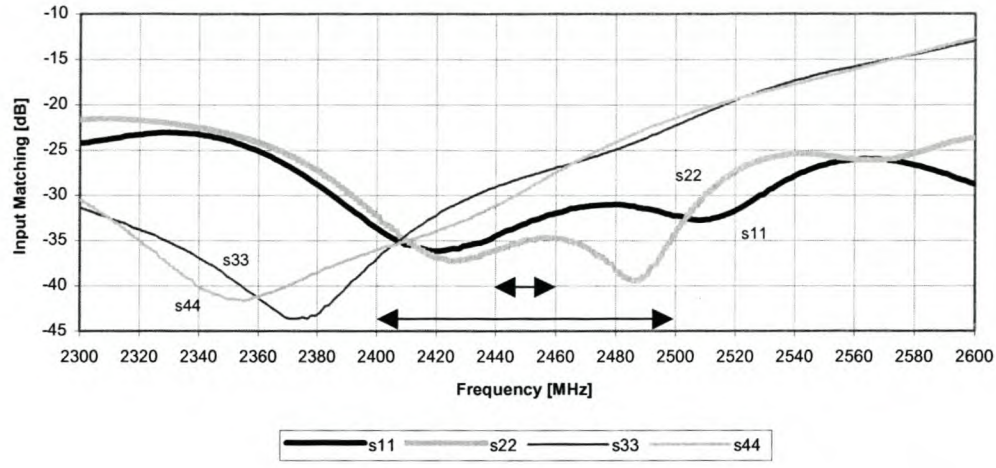

Figure 5.14 Input matching - ports 1 to 4

From *Figure 5.14*, the input matching of any port is equal to or better than -21dB over the 2.4GHz to 2.5GHz band. For a narrower band of 2.45GHz ± 10MHz, the matching is better than –26dB.

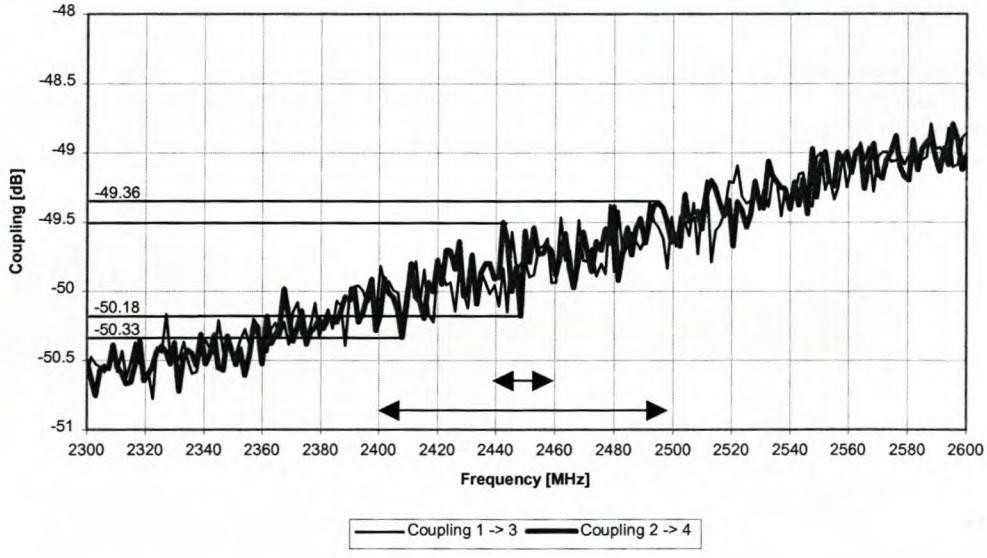

Figure 5.15 Coupling port 1 to port 3 and port 2 to port 4

The coupling was designed at –50dB and for the band of 2.45GHz ± 10MHz; a variation of 0.68dB is measured. From 2.4GHz to 2.5GHz the variation is 0.97dB. These values could be much lower if the measurement ripple was removed. The test equipment (network analyser and waveguide to coaxial transitions) is only accurate down to a certain signal level – and these measurements are reaching those limits. An alternative would be to use a signal generator (a stronger signal) and a spectrum analyser (higher sensitivity) to re-measure the coupling (and directivity). Note that the termination of the spectrum analyser has to be 50Ω for the unit to function correctly.

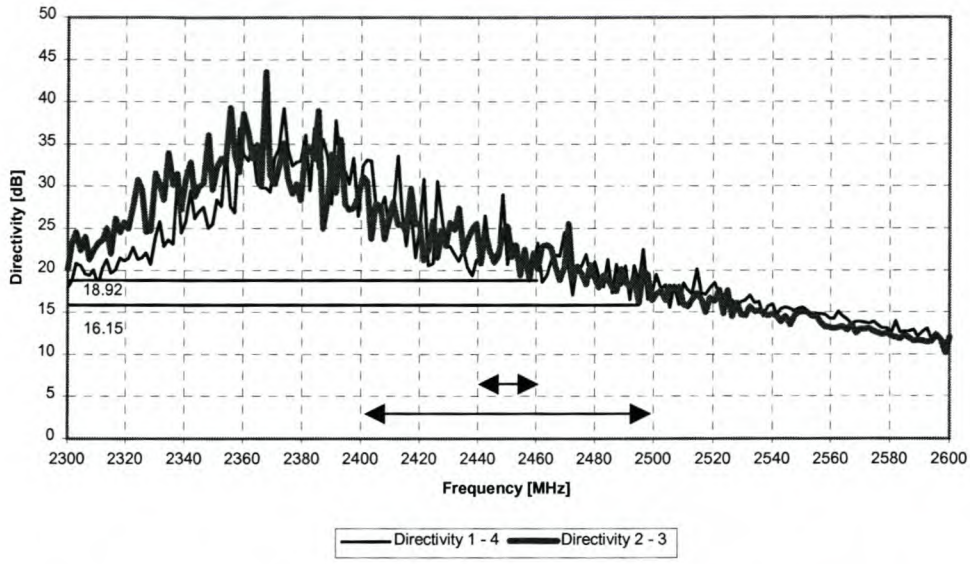

Figure 5.16 Directivity of the Dual Directional Coupler

The directivity is better than 18.9dB over the narrower band and better than 16.15dB over the 2.4GHz to 2.5GHz band. Once again there might be a slight improvement if the measurement ripple could be removed.

Table 5-1 Directional Coupler Comparative Results

Manufacturer	Bandwidth [MHz]	Coupling [dB]	Directivity [dB]
Muegge	20	60 ± 0.3	20
National	100	60 ± 0.25	27
Hybrid / in-house	20	50 ±0.4	18.9

Comparing the results to those of commercial units, the in-house hybrid coupler has almost the same specifications as the Muegge coupler. Both commercial units also use some hybrid set-up to save space, but they are a factor 6 (Muegge) to a factor 10 (National) more expensive. From *Figure 5.16*, the directivity at a lower frequency is better than at the designed frequency. With another iteration on the coaxial line, this region could be moved to the required centre frequency. Combined with some fine-tuning on the coupling factors, the coupler could be improved to the same league as the National coupler, without too much of an increase in the overall costs.

Chapter overview

In this chapter we looked at a few basic waveguide directional coupler topologies. Since most of these use a second waveguide for coupling, a hybrid set-up was proposed to save on the

space requirements. The practicality of such a coupler was investigated and simulated to obtain a physical structure. The coupler was constructed and, after a few iterations, was considered to satisfy the required coupling and directivity. Both the directivity and the coupling are compared to those of commercial units and the performance of the hybrid coupler compares favourable with these.

Chapter 6 System Control

Each of the components we designed (the SMPS, matching unit and coupler), are only tools – building blocks. On their own, they are handy, but their full potential is only reached when used as a system. This chapter looks at how such a system can be put together and the specifics of the system that was used in evaluating the sub-components.

6.1 Control Requirements

Since the user has no wish to be involved with the sub-level control (at least not all the time), a higher-level interface communicates to the user, while an automated software handles the substructure procedures – feedback, data capture, etc. The control can be located in either a micro-controller with a control panel or on a PC as is the case in this thesis. Both would require the necessary analogue and digital interfaces.

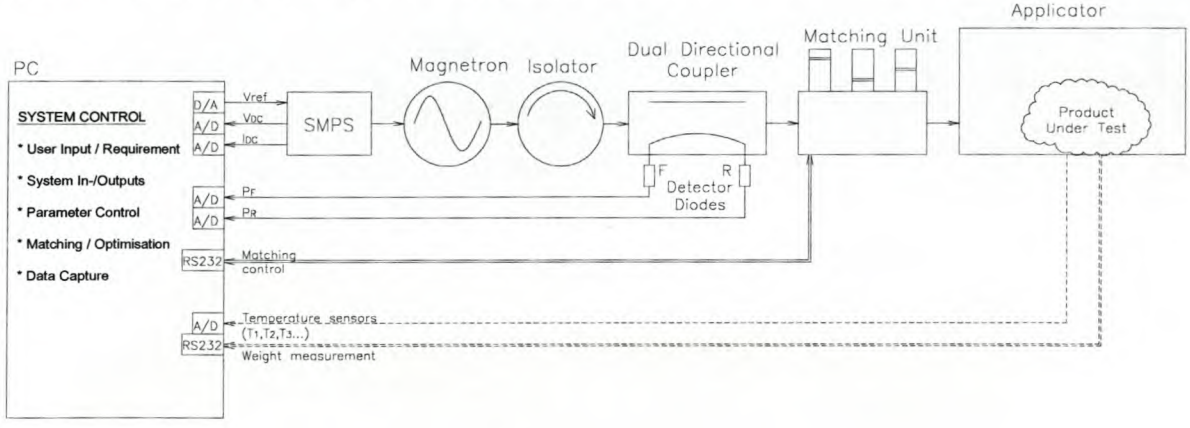

Figure 6.1 System

The control software would include the following (*Figure 6.1*):

- User input. The user expects a certain outcome / result from the system. This can include a constant set output power (RF), a set product temperature or a specified "process" that requires the power / temperature to change with time or according to an external input (weight and rate of drying or moisture level, product colour, etc.).
- System in- and outputs. Analogue to digital (A/D) and digital to analogue (D/A) converters capture and set values / parameters in the system. These values can be part of the control of the system or simply as extra information for further analyses. Digital interfaces can include RS232 communications to peripherals.

- Parameter control. This is the control loop / control algorithm that keeps the output parameter stable at the level set by the user. A standard proportional / integral / derivative (PID) control loop can be used. More advanced control strategies like adaptive control or robust control can also be used. The specific strategy will depend on the use of the system and the level of control required and will include, among other parameters, a model of the product under test and a model of the SMPS. If temperature control is part of the required output, the thermal model of the product would form part of this control loop.
- Load matching / optimisation. Although the matching is external to the main performance requirement from the user (e.g. a constant temperature), matching the load will have an improvement in the efficiency of the system. Matching can also reduce the product processing time in the case of drying wood (as an example). If the matching unit keeps the wood matched to the magnetron, microwave absorption will be optimal and so would the rate of drying. Under normal (unmatched) conditions, the wood would dry slower as the mismatch increases when moisture starts evaporating from the wood.
- Data capture / recording. The data from the system in-/outputs can be stored for further analyses of the process / product under test. A clear view of the accuracy of the measurements should be kept in mind when doing these analyses – i.e. how accurate are measurements? The relative size of measured results to system noise levels is also of importance.

6.2 Control Software

Let's evaluate the system and control software according to the guidelines in paragraph 6.1. (Refer to *Figure 6.1* for the structure of the system and *Figure 6.3* for a block diagram of the control software.)

- The user input is simply a set effective RF output power (P_f-P_r = Constant). As the system and its sub-components are under evaluation and not a specific product, we try to keep "complex" requirements to a minimum. Note: While measuring the load line of the magnetron (*Figure 7.14*), there is no direct input from the user as the control voltage is predetermined.
- From the sub-components, the following inputs are measured and displayed to the user:
    - The anode current (Idc).
    - The cathode voltage (Vdc).
    - The amount of power delivered to the applicator (P_f).

- The amount of power reflected from the applicator (P_r).
- An RS232 interface communicates to the microprocessor in the impedance matching unit and the displacement of the offset shorts can be calculated from these communications.

The software also has one analogue output:

- The reference voltage as a function of the required output power (V_{ref}).

RMS converters and sample averaging are used to minimise the effect of noise on the input lines. Optional inputs can include product temperature from thermal couples or a weight reading from a scale. These were not included in this system.

The measured voltages require some post processing to convert the measured values to the actual values. For the output current and voltage, a simple scaling factor is used. For the forward and reflected power levels, a more complex algorithm is needed. *Figure 6.2* shows the voltage versus power measurements of one of the power detector diodes. The curve is approximated by a polynomial expression (also shown) and the equivalent power for a detected voltage is calculated. The power is then scaled according to the coupling factor of the directional coupler.

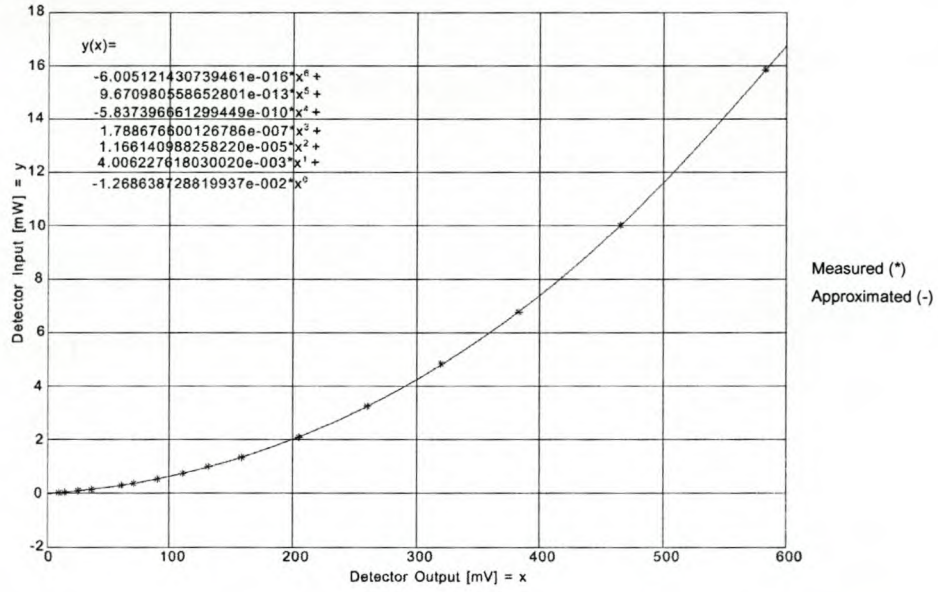

Figure 6.2 Voltage Curve of a Detector Diode

- Since a fixed output was the only requirement, a simple weighed correcting factor determined the manner in which the control voltage adapted to different output levels. A 1W dead band limited any unnecessary changes in the output power from small

mismatches between the set and measured power levels. At start-up, the supply is set to a certain "minimum" output power. This allows the matching unit to do an initial match at low power. After a few seconds, parameter control is implemented and the required output power is delivered.

- An output match is triggered every time the reflected power increases by more than 1W from its previous minimum. Even if the reflected power stayed the same, a better match might be possible. After a previous matching sequence, the matching could be at a local minimum. As the product's characteristics change, it can move away from the minimum and an improvement in the matching might once again be possible. By triggering a matching sequence every 30s, the system looks for these possible improvements. Extra forced sequences are also added during the initial, low power operation of the magnetron. For information on the matching algorithm, refer to paragraph 6.3.
- Data capturing. Since the control program is already running on a PC, the measured in- / outputs are simply stored to disk on a regular basis.

6.3 Load Matching

Finding an optimum match can be quite an exercise. The characteristics of the load can change with frequency and also with temperature as it heats up. The characteristics referring to the absorption of microwave power are the dielectric constant (ε_r) and the loss tangent ($\tan\delta_e$). The higher these values are, the better the absorption of microwave energy.

One way of determining the optimum match is by using a conjugate gradient algorithm [22]. In simplified terms, this technique evaluates the gradient of the matching curve that is currently being followed - like walking on the contour of a hill - and then moves according to the "downhill" gradient. This technique works well with the Magic T matching unit used in the specific article. For the matching unit in the system, we stuck to the basics and simply minimised the amount of reflected power (P_r) thereby improving the input match. The offset shorts were moved one after the other, from the unit nearest to the load to the furthest.

Some of the concerns that were addressed during the matching routine are:

- The shorts should not "drift" to the extremities. By first moving the short closer to the waveguide during matching, the unit will try to find a match with the shorts closer rather than further away from the waveguide.

- No excessive movement of the shorts. Since the matching entails mechanical movement, which implies component wear and tear, improvements to the matching had to be "substantial" (more than 0.2W) for further movement on the specific short.
- The directivity of the directional coupler could also be used to limit the offset short activity: If 1000W of power was transmitted in the forward direction, the finite directivity of the coupler (18dB) would result in 15W being measured on the reflective port. Any measurements trying to improve the match below this value (18dB below the forward power), cannot rely on accurate measurements and the exercise would be futile.

Figure 6.3 shows a block diagram of the system control software.

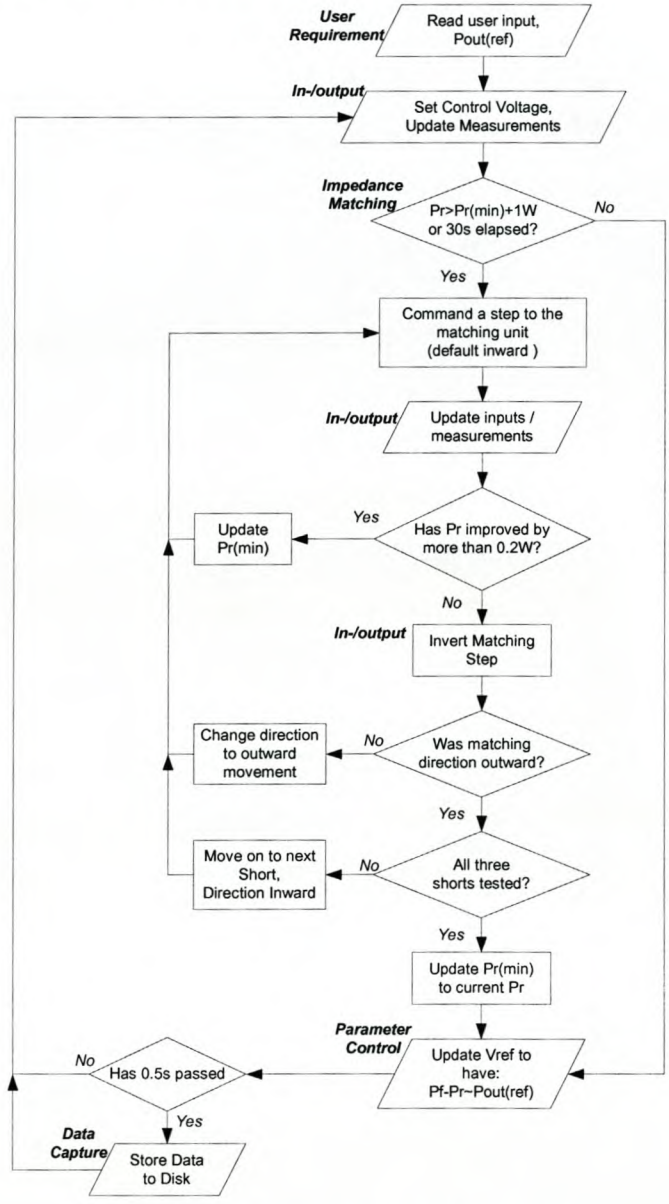

Figure 6.3 Software Block Diagram

Chapter Overview

This chapter gave a simplified overview of the software and control used to steer the magnetron supply system. The subject of matching the impedance was also visited briefly. In the next chapter, we will evaluate the software and the system as a functional unit.

Chapter 7 System Results

To put the system to test, a few different scenarios are put forward. These scenarios seek to display some of the tests that can be required in a laboratory. We will evaluate:

- A standard microwave absorbent load.
- The effect of the FA-TX.
- The output frequency spectrum of the magnetron.
- Some matching problems.
- Measuring the load line of a magnetron.

7.1 Constant RF Output Power and Matching

The full system is running as was described in the previous chapters. The user sets a fixed output power (300W) and the output is logged - *Figure 7.1*. To illustrate the effect of the matching unit, matching is first delayed for 30s. The initial low power region (0-10s) could be used to do a preliminary match on the system before a higher power level is applied at 10s.

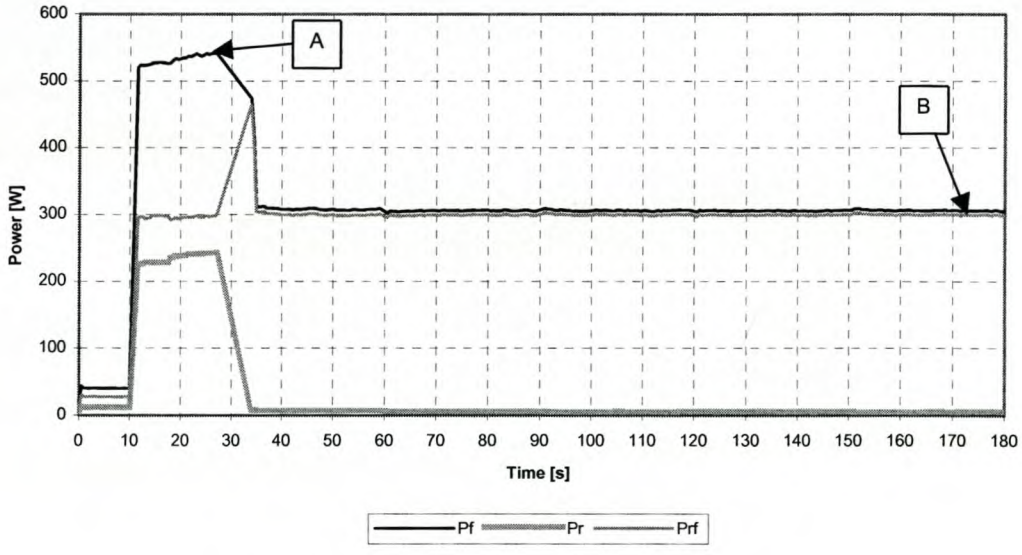

Figure 7.1 Water Load 1 – Pref=300W

The efficiency of the *system* can be calculated by dividing the output power by the sum of the losses in the system and the output power. This incorporates the efficiency of the magnetron, the SMPS and the matching. From measurements, the magnetron is ~52% efficient at point A and the SMPS 89%.

$$\eta = \frac{P_{rf}}{P_{loss,magnetron} + P_{loss,SMPS} + P_r + P_{rf}} = \frac{300W}{503W + 130W + 241W + 300W} = 25\% \text{ at point A}$$

After system matching is allowed, the efficiency improves to:

$$\eta = \frac{300W}{372W + 84W + 7W + 300W} = 39\% \text{ at point B} - \text{a 14\% improvement in overall system efficiency or a 56\% improvement in system yield!}$$

The measured system efficiency seems to be very low. In a best-case scenario, the efficiency of the magnetron is 70% and that of the SMPS is 89%. The best system efficiency would then be: 62.3% at maximum RF output power and zero reflected power – i.e. a perfect match. At lower power levels, as is the case with these measurements, the efficiency of the magnetron can be as low as 45% resulting in a system efficiency of ~40%. The results are therefore at expected levels.

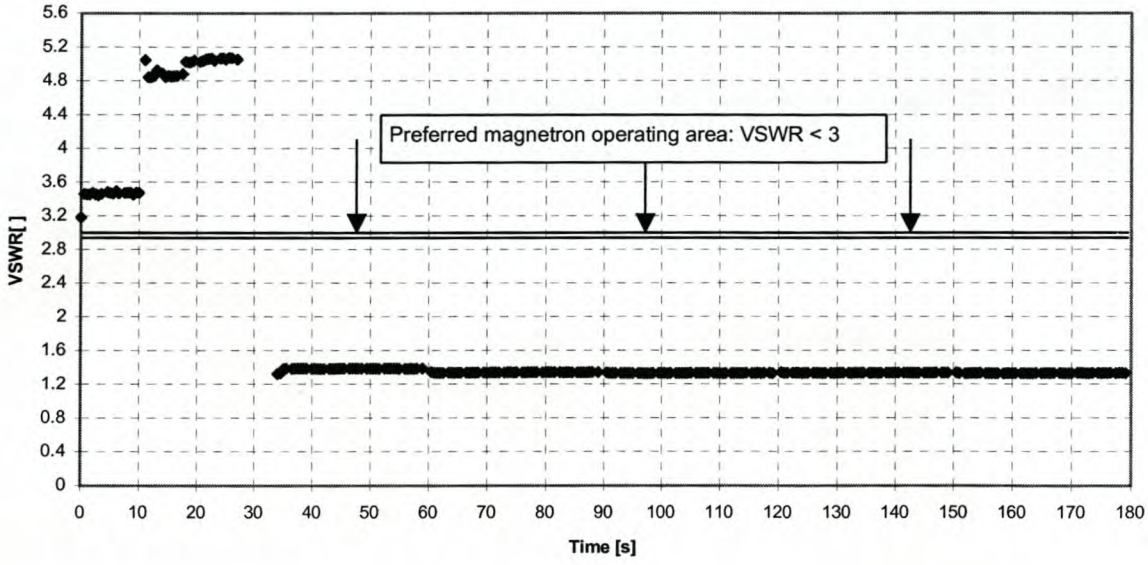

Figure 7.2 Water Load 1 – VSWR Improvement

Figure 7.2 shows the improvement in the VSWR of the load. Note the gap in measurements at 34s, 60s 90s, 120s 150s and 180s. Since the matching sequence can take more than 0.5s, data points might be skipped during matching sequences. The control voltage is also only updated after a complete matching sequence, which explains the jump in and subsequent recovery of P_{rf} at 34s, *Figure 7.1*.

We evaluate the overall success of the system in how well it achieved the user requirement of a fixed 300W output. Excluding the initial low power region and the 7s overshoot during the

first matching sequence, the output only varied between 292W and 305W. This is a variation of less than 3% from the user requirement.

7.2 The effect of the FA-TX

As was noted in paragraph 3.3, the output of the SMPS is affected by switching the FA-TX on/off during operation. This example shows some of the further effects the FA-TX has, be that directly or indirectly. The system is once again set-up to provide 300W to a water load. After the initial matching, the FA-TX is switched off.

After switch-off, the DC voltage increases by ~150V to maintain the same output power - *Figure 7.3*. As described in 2.1, back-bombardment needs to increase to maintain the cathode temperature. This increase in voltage does just that.

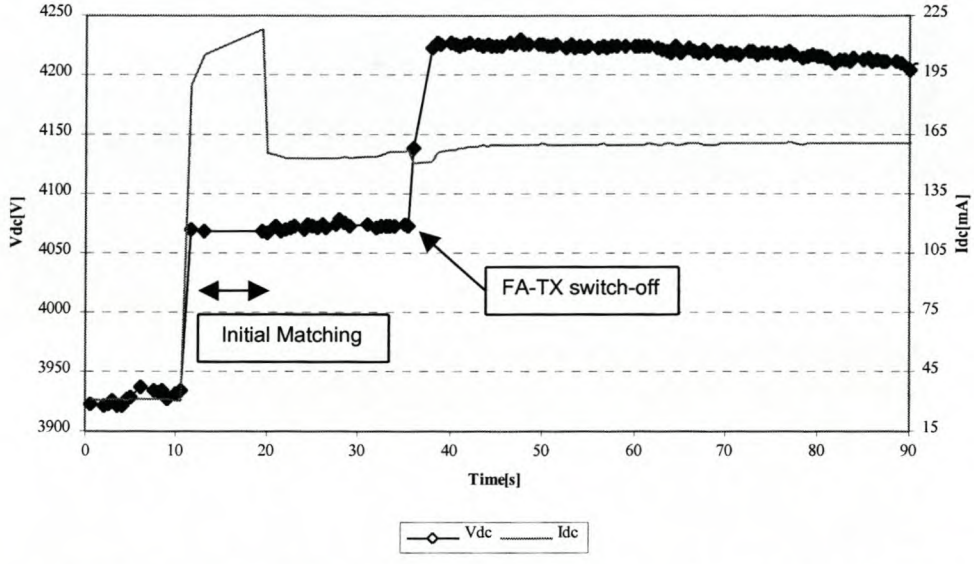

Figure 7.3 Water Load 2 – DC input change as FA-TX is switched off

Secondly, P_r drops to almost zero - *Figure 7.4*. Why would the amount of reflected power drop when the FA-TX is switched off? For an explanation, we can look at the output spectrum of the magnetron, with the FA-TX on and off – *Figure 7.5*.

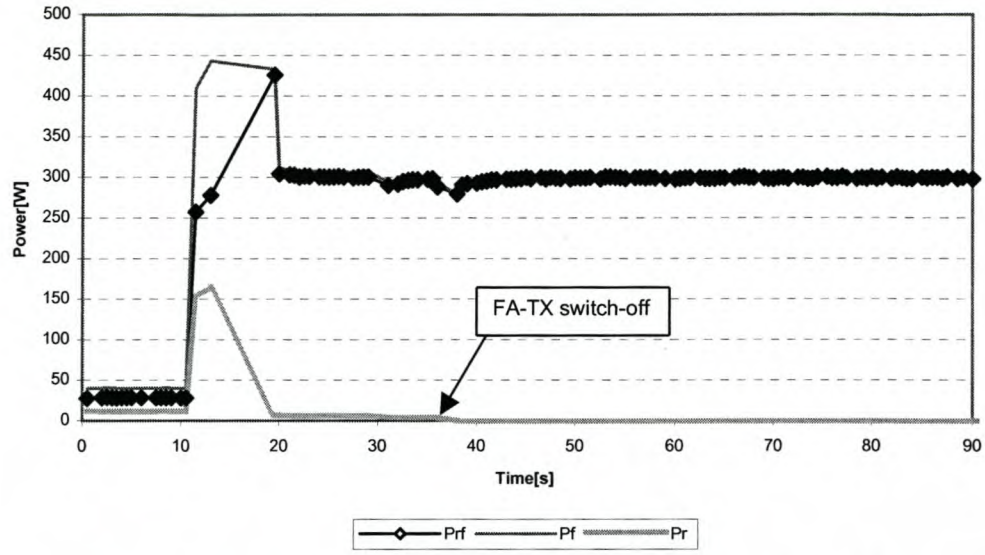

Figure 7.4 Water Load 2 – RF output as FA-TX is switched off

When the FA-TX is switched on, the matching unit has to match a 22MHz band of power. With the transformer off, this band reduces to only 2.5MHz and a better match is possible therefore P_r drops dramatically. The wider band / spreading is a result of "modulation" – the unwanted ripple – on the anode current, *Figure 3.12*.

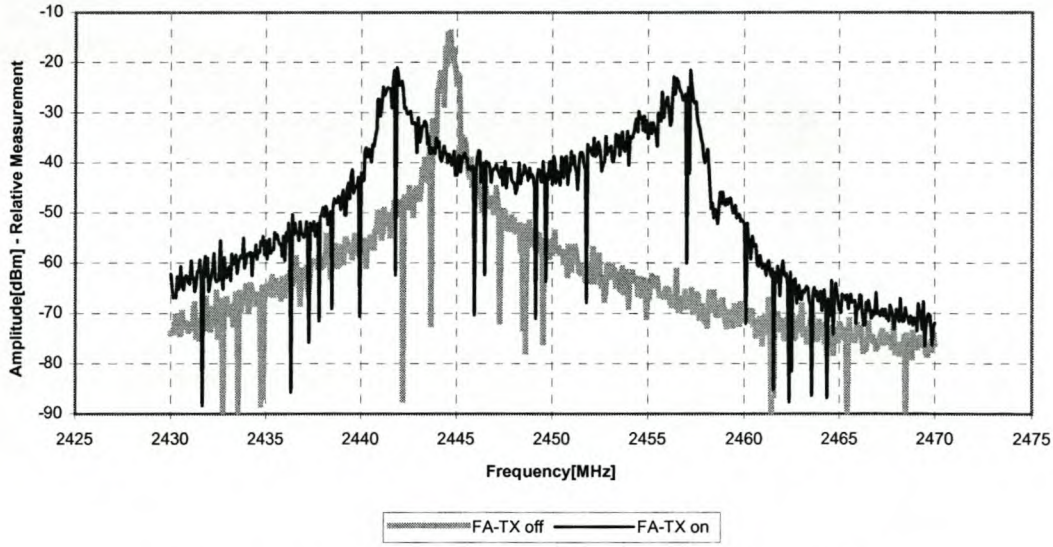

Figure 7.5 Output Spectrum - Filament On and Off

7.3 Output Spectrum

When using a voltage doubler supply (2.3.2), the DC current to the magnetron changes from zero to maximum current every 20ms. This results in a very wide output frequency spectrum,

approximately 37MHz - *Figure 7.6*. The output spectrum from this system is a maximum of 22MHz and can be as low as 2.5MHz with the FA-TX off – *Figure 7.5*.

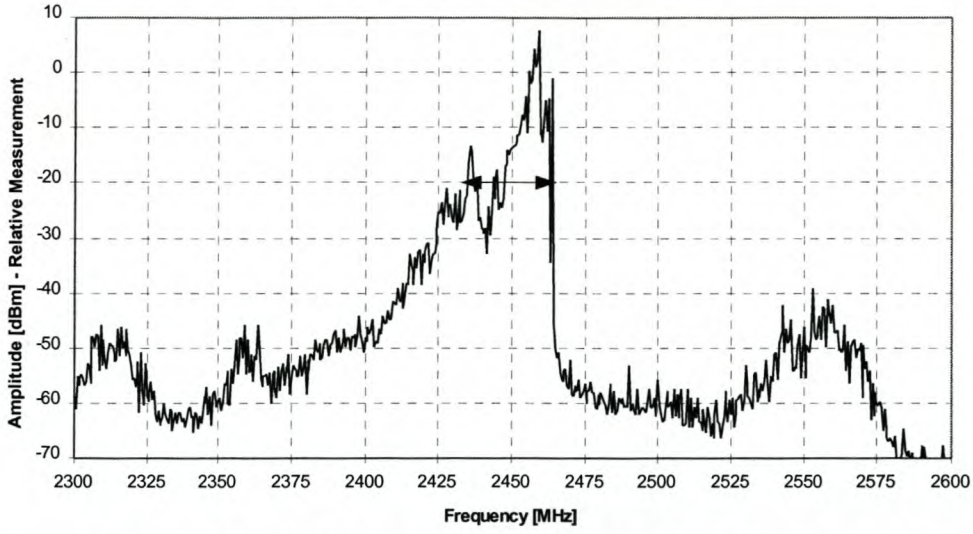

Figure 7.6 Voltage Doubler Magnetron Output Spectrum

By changing the reference output power, a change in the output frequency can also be measured. *Figure 7.7* shows the output for $400W_{rf}$ (196mA) and $450W_{rf}$ (222mA). The change in the DC current results in a 4.5MHz shift in the output spectrum. This puts a limit to the successfulness of load matching at low power levels, since the output spectrum will shift when higher power levels are applied.

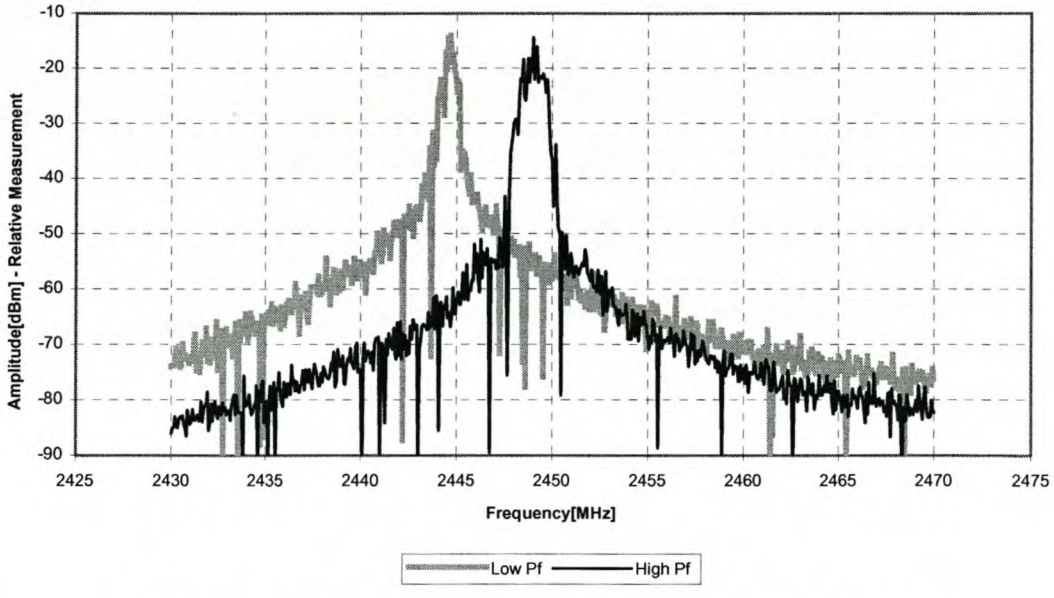

Figure 7.7 Frequency change with a change in P_{out} (Idc)

7.4 Impedance Matching

So far, we have only matched a "passive" load – water. To put the matching unit through its paces, more dynamic loads are tested.

7.4.1 Abrupt Load Changes

A block of wood is placed inside the oven and then moved during operation. As the block is moved, the amount of absorbed power will change as it moves between nulls and peaks on the energy grid inside the oven. The load will also tend to "pull" the microwave energy, altering the fields inside the oven. This changes the matching seen by the magnetron.

With the user power level set at $200W_{rf}$, *Figure 7.8* shows the output of the system. The block is moved at 45s and 99s. If we include the measurements at the time the load is moved, the output deviates by up to 37% from the set value. If a few seconds is allowed for matching (approx. 5s), this variation drops to only 5% as the system adapts to the load change.

Figure 7.9 shows the VSWR of the load. After moving the load, the VSWR increases sharply. Within 10s, the VSWR is improved from 3.4 to 1.4 and then down to 1.2. After the second displacement, the improvement is only down to 1.7, but this is still a very good match. Evaluating the improvement in the VSWR and the recovery of the output power, the system is able to handle this "obstacle" quite well. *Figure 7.10* displays the movement of the offset shorts.

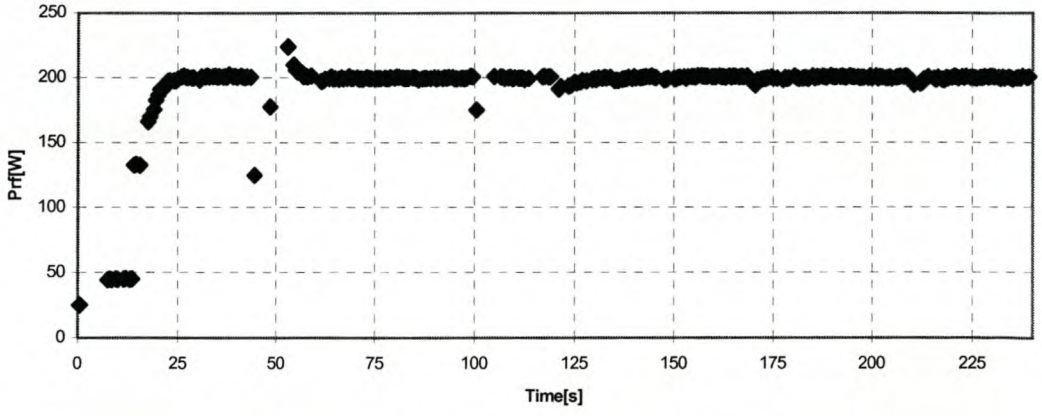

Figure 7.8 Load Movement – Prf, 200W

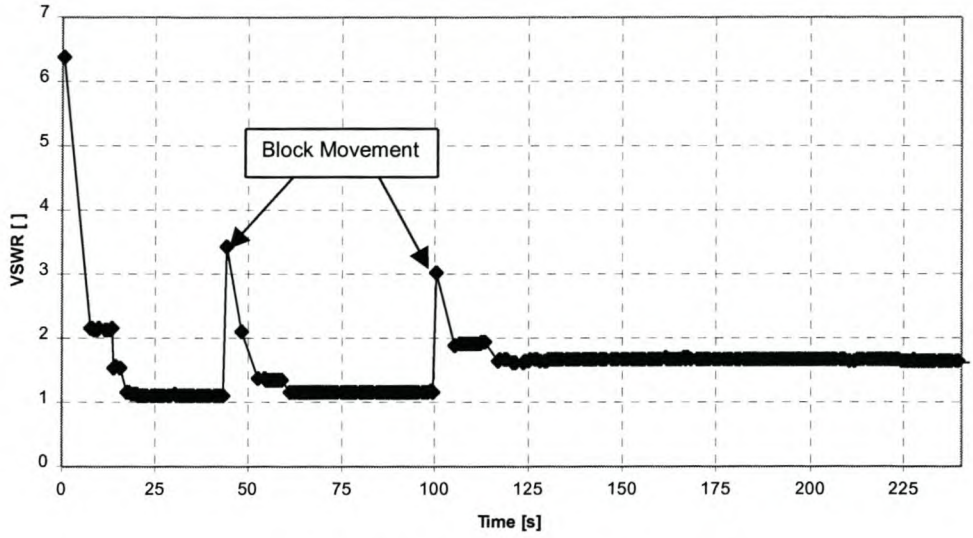

Figure 7.9 Load Movement – VSWR

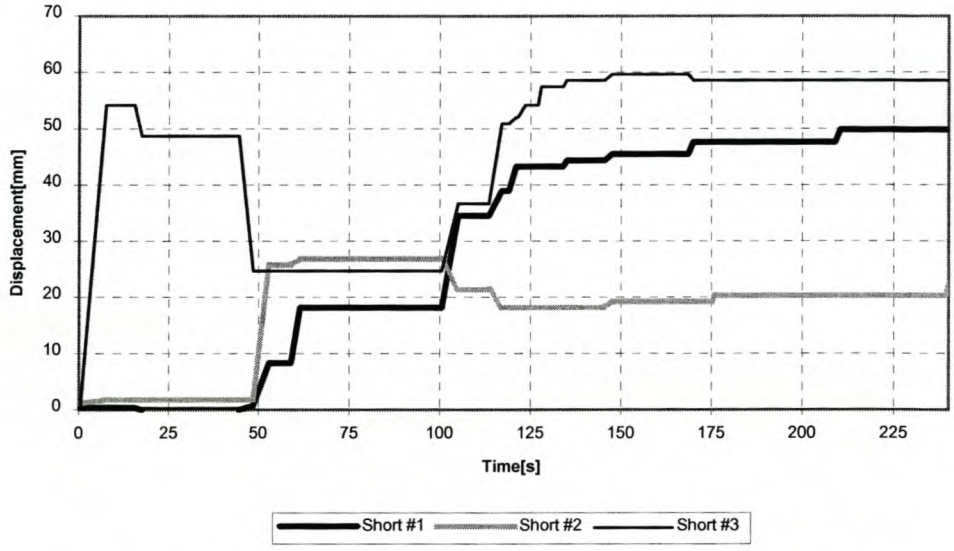

Figure 7.10 Load Movement – Offset Short Displacement

The matching unit is able to do an initial match for the system within 18s. After a load change, it adapts within 19s to the new impedance. To put the matching time into perspective, we compare this to test results gained when consulting on brick drying. The initial match of the system during thís consultation could only be matched down to a VSWR of 1.9 using a stub-matching unit. After about 170min, the VSWR only increased to 2.1. As the bricks started losing their last bit of moisture, the VSWR increased from 2.1 to 2.7 in 9min. The matching unit is therefore able to match a load change that happens a lot faster and do so within a fraction of the time it would take a "natural" load change to occur.

7.4.2 Continuous Load Change

As a second test, a wet sponge is placed inside the cavity while the matching is observed. This cannot be considered a standard load and would fall in the "extreme test" category. *Figure 7.11* shows the VSWR and P_{rf} during the test.

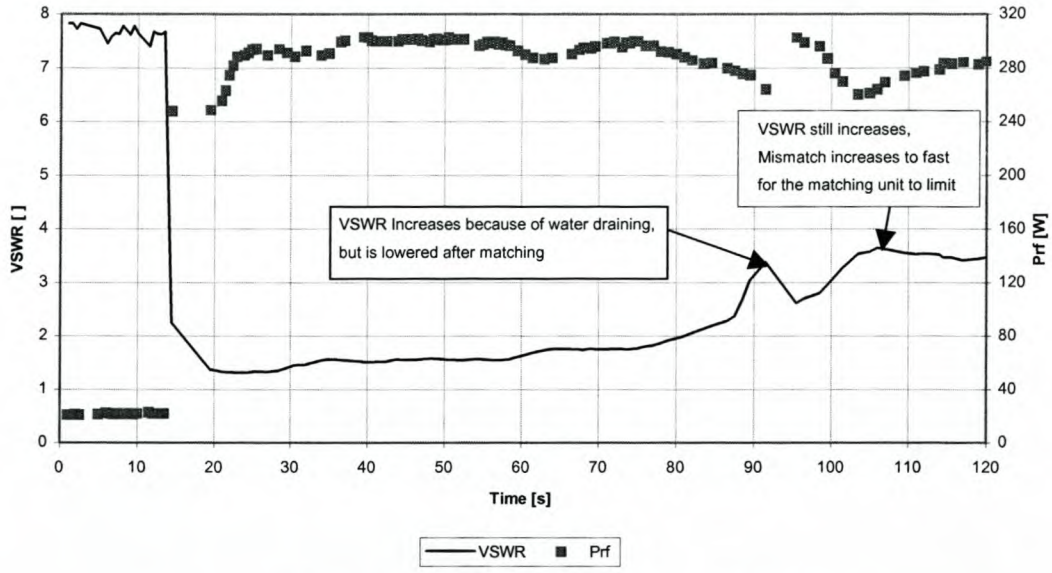

Figure 7.11 Sponge Drying – VSWR and P_{rf}, 300W_{rf}

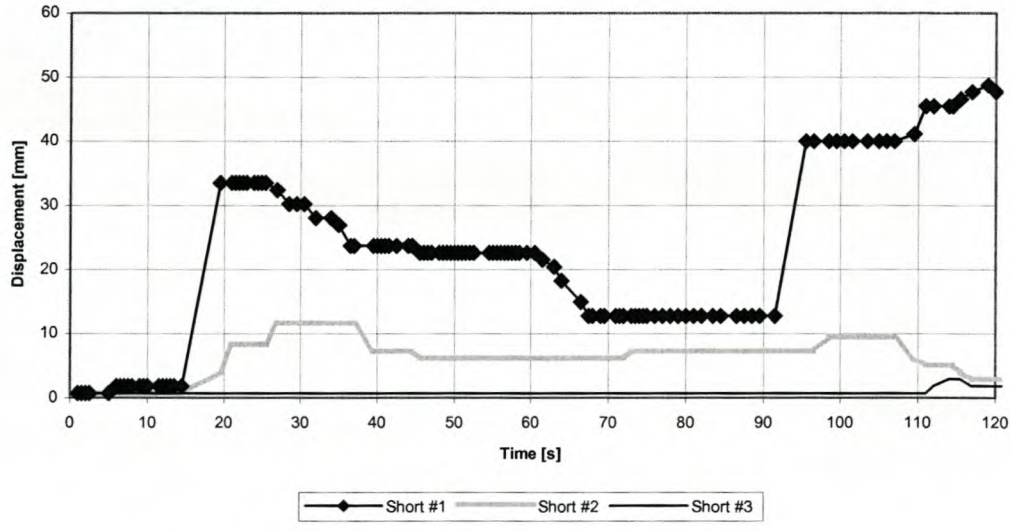

Figure 7.12 Sponge Drying – Offset Short Displacement

During the first part of the test, the matching unit keeps the VSWR below 2 – a good match. As time passes, the wet sponge starts to heat up and the water inside the sponge drains to the bottom of the cavity. This is a continued load displacement / movement. At 80s, the VSWR starts to increase, but the matching unit gives a brief relieve. After 120s, the system seems to be unable to keep up with the changes in the load. The matching is maintained at a VSWR of approx. 3.6 – far better than the unmatched VSWR of 7.8, but greater than the recommended

3. *Figure 7.12* shows the displacements of the shorts, indicating that the matching unit is actively trying to keep up with the matching. Even with this "extreme" experiment, the unit gives a positive contribution to the load matching. P_{rf} also stays within 14% of the set value.

7.4.3 Matching with a Different Supply

The matching unit can also be used with a standard voltage doubling magnetron supply. A bucket of water is once again used as a load. *Figure 7.13* shows the VSWR and P_{rf} during the test. Since this is a fixed supply, the output power cannot be set. The matching unit has no difficulty in lowering the VSWR of the load and thereby increases the system output by 26% ($400W_{rf}$ to $506W_{rf}$).

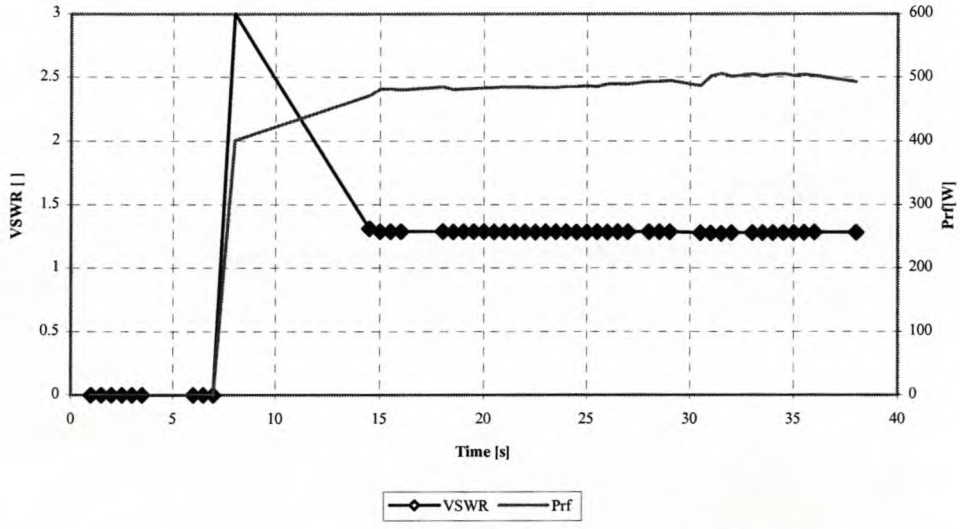

Figure 7.13 Voltage Doubler Supply Matching – VSWR and P_{rf}, $500W_{rf}$

7.5 Magnetron Load Line and Efficiency

By connecting the magnetron to an isolator and sweeping the DC current from minimum to maximum, one should be able to measure the load line (V_{DC} vs. I_{DC}) of the magnetron.

The control program was altered to step V_{ref} from a value where the magnetron is operating, down to a level where the output current / voltage is too low to maintain RF power. The voltage is then increased in steps up to the maximum current level for the magnetron – 330mA according to datasheets. *Figure 7.14* shows the load line for the specific magnetron. The "scattered" measurements below 20mA are from the uncertainty of operation below the π-mode voltage, which is approximately 3900V for this magnetron.

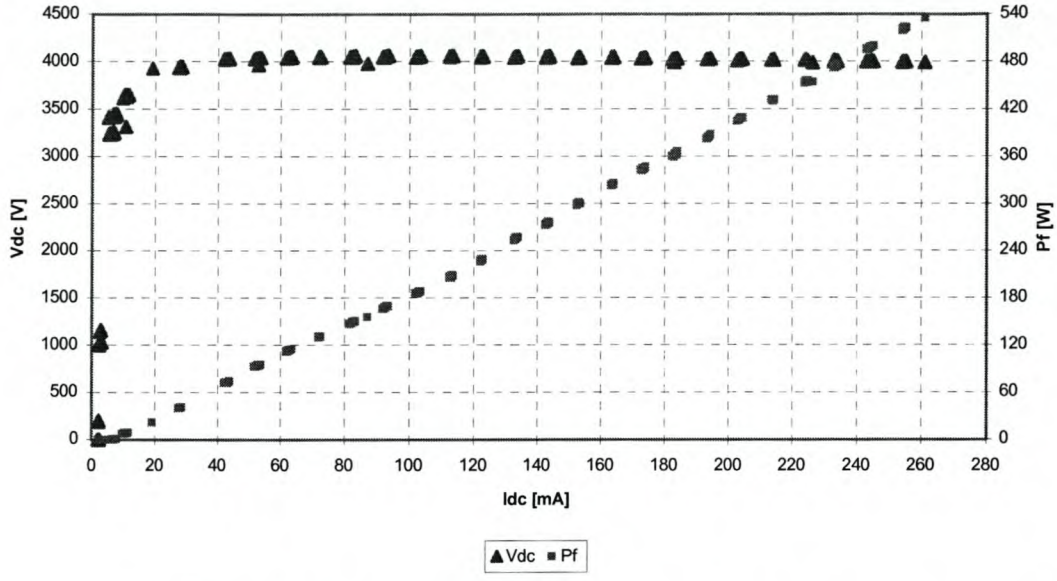

Figure 7.14 Magnetron Load Line – V_{DC} and P_f vs. I_{DC}

The test also determines the accuracy of the assumption that I_{DC} is linear to P_f - *Figure 7.15*. Except for a slight offset - no output power for I_{DC}<10mA – I_{DC} is linear towards P_f. In the case of V_{ref} versus I_{DC}, the relationship is also linear with an offset of 0.3V.

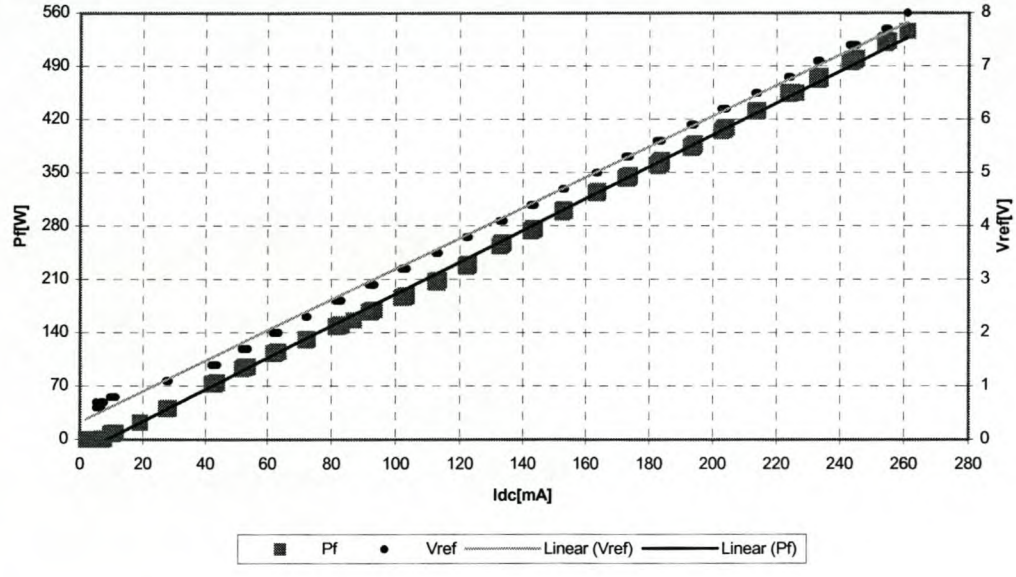

Figure 7.15 Linearity – P_f and Vref vs. I_{DC}

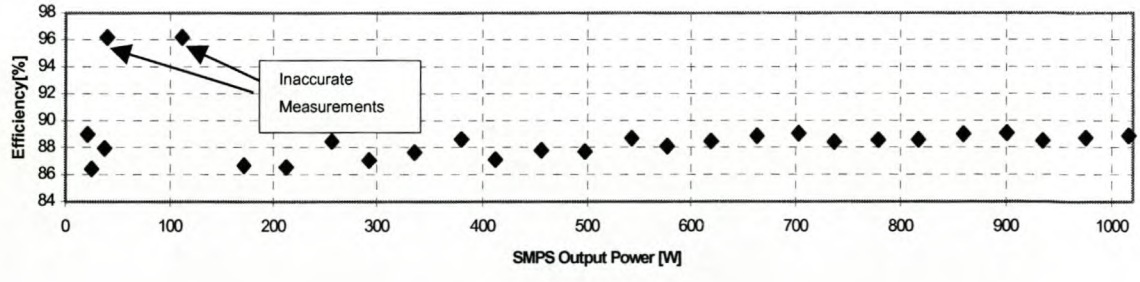

Figure 7.16 SMPS Efficiency

Figure 7.16 shows the efficiency of the SMPS for different output power levels. The efficiency varies between 86.5% and 89% (excluding the two suspect values).

As a matter of interest, the efficiency of the magnetron can also be captured – *Figure 7.17*. The efficiency is much lower than the expected 70%. The 70% is associated with industrial size magnetrons (~6kW). Commercial units usually have some compromise in lowering production costs - efficiency might one. The average commercial user would not be aware of the lower efficiency because of the typical oven usage profile.

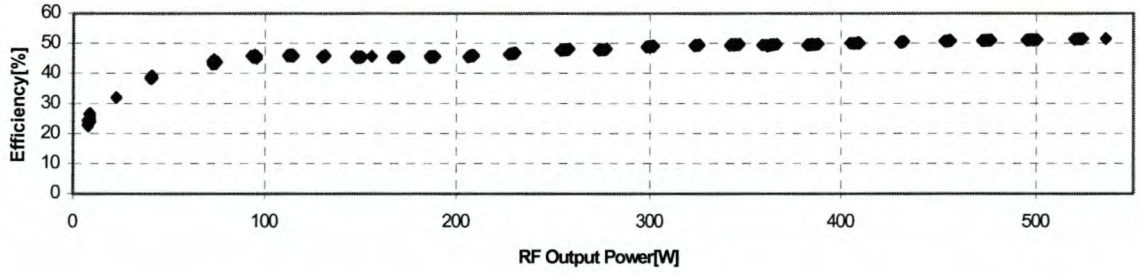

Figure 7.17 Magnetron Efficiency

Summary of System Results

From the measurements, we can conclude the following:

- The assumption of a linear P_f to I_{DC} (except for the slight offset) was accurate and can be used in further control strategies.
- The output frequency is dependent on I_{DC}. This implies that an impedance matching at low power levels will not be as accurate as one would have liked it to be. A step-wise increase in power will encourage matching which will be better than an abrupt high power mismatch.
- Continuous matching is accomplished with varying success, depending on the load type.
- The efficiency of the SMPS is slightly lower than the expected 90%, but is still good at 86-89%.
- Although the power control deteriorated with more extreme loads, control was still adequate as the deviations were only for short periods.

Chapter 8 Conclusion and Recommendations

8.1 Conclusion

Extra laboratory equipment was required for consultation on microwave heating / assisted heating. The specific requirements - a variable RF output power, RF feedback and an optimum system - were satisfied by designing a HV SMPS, a dual directional coupler and waveguide impedance matching unit.

The SMPS was measured as capable of delivering 1.1kW at 4100V to a magnetron. A response time of only 4ms for a 100% change in output current ensures fast response time to user requirements.

The dual directional coupler employed a hybrid waveguide-coaxial mechanism to obtain a directivity of 18.9dB across the frequency band of the magnetron. This ensures accurate measurement of the system output and load matching.

The third component, an electro-mechanical impedance matching unit, added WR340 waveguide matching capabilities. Excellent Smith chart coverage was obtained as well as a good response time in matching the microwave load.

These components gave good to excellent results as individual blocks, but also when combined as a complete system. As a *system*, it is a fixed microwave output power source. This "source" was tested with different loads as indicated in Table 8-1.

Table 8-1 System Performance Summary

	Load change	Maximum deviation from set power (excluding incident of forced load change)	Initial VSWR	Final VSWR	Improvement in system efficiency (from matching)
$H_20 - 300W_{rf}$	None	2.7%	5	1.3	56%
$H_20 - 100W_{rf}$	None	2.9%	2.4	1.8	18%
Block of wood	Abrupt Displacement	5%	6.4	1.7	134%
Wet sponge	Continuous Displacement	14%	7.7	3.4	170%

With a standard water load, the system only deviated from the set output by 3%. The efficiency improvement through load matching yielded a good response with improvements

of up to 56% at higher power levels. When testing more "abnormal" loads, the power deviation is higher, up to 14%. The improvement in the efficiency easily makes up for this shortfall at 170%.

By stepping the output of the SMPS from minimum to maximum, the functionality of the system is further extended to include the load line measurement of a magnetron. A very wide range of magnetrons can also be supported by simply adjusting the maximum current levels of the SMPS.

8.2 Recommendations

There are a few improvements that can be made to the system:

- The SMPS design can be improved by selecting a more suitable transformer core.
- The SMPS is also susceptible to grounding problems. This can be improved by confirming that all points of noise and ground loops are sufficiently isolated.
- The current control loop does not utilise the full potential of the SMPS resulting in sub-optimal response times and output power stability. The control can be extended to include the model of the supply, which should provide the optimum solution.

Further investigation into the effects of the filament and FA-TX on the system and the subsequent secondary effects on the SMPS, will be advantageous in improving the system. A better understanding of magnetron moding and the detection / prevention thereof, can also improve system stability and lifecycle.

On the whole, a low cost, flexible system was designed that can deliver microwave power according to user specifications – and can do so at an optimal system performance through impedance matching.

Chapter 9 References

[1] H. Püschner, *"Heating with microwaves"*, Philips Technical Library, 1966

[2] A.F. Harvey, *"Microwave Engineering"*, Academic Press, London and New York, 1963

[3] Ernest C. Okress, *"Microwave Power Engineering"*, Academic Press, London and New York, 1968

[4] Roger Meredith, *"Engineers' Handbook of Industrial Microwave Heating"*, The Institution of Electrical Engineers, London, 1998

[5] Roger Meredith, *"Trends in High Power Generators for Industrial Microwave"*, Microwave and High Frequency Heating, 1995

[6] *"Tube Specifications: 2M137"*, Matsushita Electronics Corporation, 1985

[7] N. Mohan, T. Undeland, W. Robbins, *"Power Electronics – Converters, Applications and Design"*, John Wiley & Sons, 1995

[8] Robert E. Collin, *"Foundation for Microwave Engineering - Second Edition"*, McGraw-Hill, 1992

[9] Max W. Medley, Jr., *"Microwave and RF Circuits: Analysis, Synthesis and Design"*, Artech House, 1992

[10] A. Frickey, *"Conversions Between S, Z, Y, h, ABCD and T Parameters which are valid for Complex Source and Load Impedances"*, IEEE Transactions on Microwave Theory and Techniques, Vol. 42, no. 2, February 1994

[11] W.B.W. Alison, *"A Handbook for the Mechanical Tolerancing of Waveguide Components"*, Artech House, 1987

[12] Douglas W. Jones, *"Control of Stepping Motors, a tutorial"*, , 1998

[13] A.C. Metaxas, *"Foundations of Electroheat – a unified approach"*, John Wiley & Sons, 1996

[14] Keith Billings, *"Switchmode Power Supply Handbook – 2nd edition"*, McGraw-Hill, 1999

[15] Abraham I. Pressman, *"Switching Power Supply Design – 2nd edition"*, McGraw-Hill, 1998

[16] A.C. Metaxas & R.J. Meredith, *"Industrial Microwave Heating"*, Peter Peregrinus Ltd., 1983

[17] Hubert Aigner, *"Improving the Full-bridge Phase-shift ZVT Converter for Failure-free Operation Under Extreme Conditions in Welding and Similar Applications"*, 1998 IEEE Industry Applications Conference, 1998

[18] Bill Andreycak, *"Phase Shifted, Zero Voltage Transition Design Considerations and the UC3875 PWM Controller"*, Unitrode Application Note, 1992

[19] George C. Chryssis, *"High-frequency Switching Power Supplies – Theory and Design – 2nd edition "*, McGraw-Hill, 1989

[20] Harris semiconductor datasheet, *"HGTG20N60B3D 40A, 600V IGBT"*, file name: fn3739.pdf, 1997

[21] P. C. Sen, *"Principles of Electric Machines and Power Electronics"*, John Wiley & Sons, 1989

[22] J.J. Mallorquí, A. Aguasca, A. Cardama, R. Pagès, J. Mª Haro, *"Automatic self-matching network for industrial microwave heating based on conjugate gradient algorithm"*, IEE Electronics Letters, Vol. 35, no. 4, 1999

Appendix A Power Supply Stored Energy

Energy is stored in a few components in a magnetron supply, in this case specifically inductors and capacitors. Some are "parasitic" in origin such as the magnetic energy stored in the core and the leakage flux of the HV transformer, but most are from filtering components. These could be filtering of the high-voltage output (smoothing choke, capacitor / pi-network filter) or smoothing the DC into a SMPS (bus capacitor). Since filtering at high frequencies requires smaller component values, less energy is stored compared to low frequency filtering components. The amount of energy stored is a function of the capacitance / inductance of the specific component.

This energy is usually nothing to be concerned about and actually helps the supply to function properly. A problem arises under short circuit or fault conditions. Although the line supply would be disconnected in the event of a fault, these "reservoirs" would still supply energy to the magnetron until they are depleted. The magnetron might sustain severe damage in this time, though it lasts only a few milliseconds.

But how much energy is in fact stored? The following available supplies are compared:

(a) A domestic voltage doubler supply rated at 850W RF – i.e. a 1200 W supply – with little smoothing / DC filtering.

(b) A 2kW lab supply with a lot of smoothing for a very stable output frequency. A pi filter (2x HV capacitor and smoothing inductor) is used on this supply.

(c) The SMPS built during this thesis – a 2kW supply with a good deal of smoothing.

(a) Energy stored in the leakage inductance of the HV transformer secondary:

$$E = \tfrac{1}{2}LI^2 = \tfrac{1}{2}.100mH.0.3^2 = 0.0045Joule$$

energy in the output capacitor:

$$E = \tfrac{1}{2}CV^2 = \tfrac{1}{2}.1.13uF.2050^2 = 2.374Joule$$ - note that the capacitor charges to only half the output voltage or ½ x 4100V.

=> Total energy = 2.37 Joule

(b) Energy in the pi-filter network: capacitor – inductor – capacitor,

$$E = 2.\tfrac{1}{2}CV^2 + \tfrac{1}{2}LI^2 = 2.\tfrac{1}{2}.10uF.4100^2 + \tfrac{1}{2}.10H.0.3^2 = 168.55Joule$$

(c) Energy in the leakage inductance (17uH) and output filter capacitors (27nF):

$$E = \tfrac{1}{2}CV^2 + \tfrac{1}{2}LI^2 = \tfrac{1}{2}.27nF.4100^2 + \tfrac{1}{2}.17uH.0.3^2 = 0.227Joule \Rightarrow {}^{1}/_{743} \text{ of (b)}$$

Of course the SMPS first rectifies the line voltage and uses a bus capacitor. The energy stored in the bus capacitor is:

$$E = \tfrac{1}{2}CV^2 = \tfrac{1}{2}.4.7mF.310^2 = 225.8Joule$$

Even more than the big pi-filter! This energy cannot reach the magnetron during an output-fault, since the IGBT's isolate the supply during any detected fault conditions.

There are a few different SMPS topologies that can be used and each will store more or less energy, depending on the design and smoothing requirements.

Meredith [4] also considers the line supply. Since the AC line voltage is connected continuously, it is an "infinite" supply and the amount of energy available is a function of the time it takes to isolate the line from the power supply and is proportional to the kVA rating of the magnetron supply.

For a basic supply with no electronic protection, the time would be the time it takes to switch the mechanical overload protection, typically 30ms. On a thyristor-controlled supply, it would be a maximum of 10ms until the next zero crossing of the current. For a SMPS, the fault circuitry could be slower than the switching frequency for high-frequency supplies. On the supply built, the over-current fault circuitry will switch the supply off in 100us if it cannot limit the fault current to within the set operating specification of the magnetron.

If we compare available line energy, the thyristor supply has 100 times more line energy available than the SMPS and the basic supply 300 times more.

Note that these calculations were done for relatively small supplies of only 1-2kW, compared to the 6kW of an industrial 2.45GHz supply and 60kW for an industrial 900MHz supply. The energy stored in these supplies would be a lot more – and far more destructive.

How much energy is 1 Joule? It takes 167 J to heat a kilogram of solder by one degree Celsius, calculated from the typical specific heat of solder. Therefore a solder joint (say 4g) would be raised by 251°C above ambient if the power stored in the pi-filter was discharged into it. At this temperature, low temperature solders would have melted and high temperature solders would be on the verge of melting with possible damage to the supply.

Appendix B Matching unit design

This appendix details the software interface and the schematic of the matching unit controller.

B.1 Software Interface

Start-up initialisation determines whether control is from the "Manual" switches or via the serial port. The appropriate dip switch is set on the front of the unit and the change in control is implemented as soon as the unit is switched on.

At switch-on, all the offsets are moved to the "home" / minimum limit position.

Serial / remote control:

The serial port receives one byte (8 bits, 9600 baud) that is encoded as follows:

Bits 1-5 The number of steps to be taken. "00000" implicates a movement to "home"
Bit 6 The direction of movement: 0 = inward, 1 = outward
Bits 7, 8 The number of the motor / offset to move: 01 / 10 / 11 => #1 / #2 / #3

If the number of steps has been completed, a byte is send back from the unit with the following encoding.

0000 0000 No error / command successfully completed.

001 xxxxx Minimum limit reached during the execution of the command, a number of xxxxx steps from the command were not taken.

010 xxxxx Maximum limit reached during the execution of the command, a number of xxxxx steps from the command were not taken.

011 xxxxx Data error:
- 00000 – program still busy with previous command.
- 00001 – a downward movement was requested, but the previous command already gave a "minimum limit reached" result.
- 00010 – an upward movement was requested, but the previous command already gave a "maximum limit reached" result.

Note that only one motor / offset can be moved at any single time. The limit indicator LED's will also only light up during the movement of an offset and will not stay lit.

Manual / local control:

Up / down buttons Move one step (~0.3mm) in the indicated direction. Holding down the button will result in repeated steps until a limit switch is triggered or the button is released.

"Home" command A home command can be executed by pressing and releasing the up and down buttons of the specific offset simultaneously.

Example: Command byte ="246" or "11-1-10110"$_2$,
That is, move offset number 3 / "11"$_2$ outward, 22 / "10110"$_2$ steps.
If after 10 steps the offset reaches the maximum limit, the reply would be:
"76" or "010-01100"$_2$
Which implies: "010" maximum limit reached during the command, 12 / "01100"$_2$ of the original number of steps were not taken (22-10 steps).

B.2 Schematic

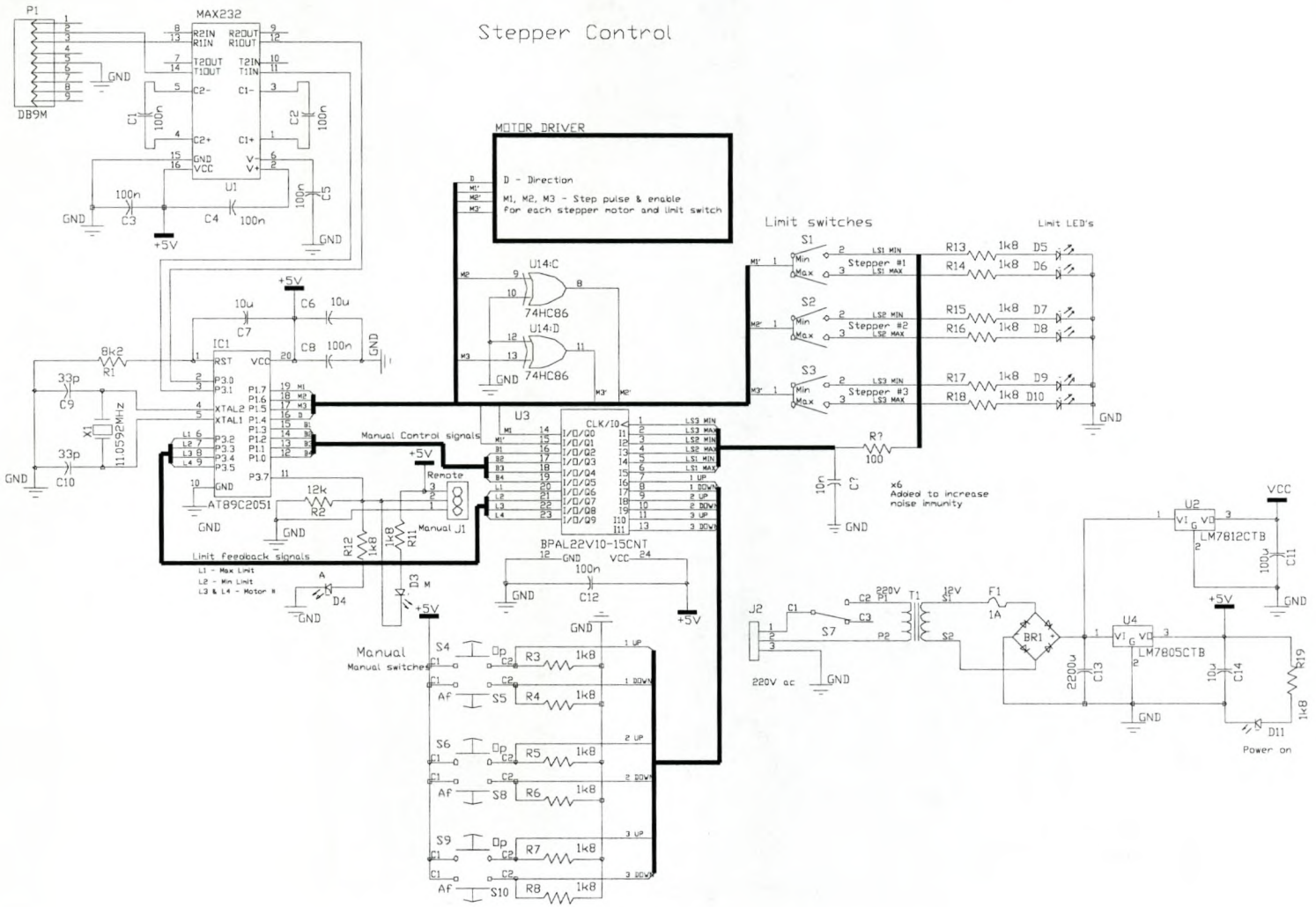

Figure B.1 Stepper Controller Schematic - (page 1)

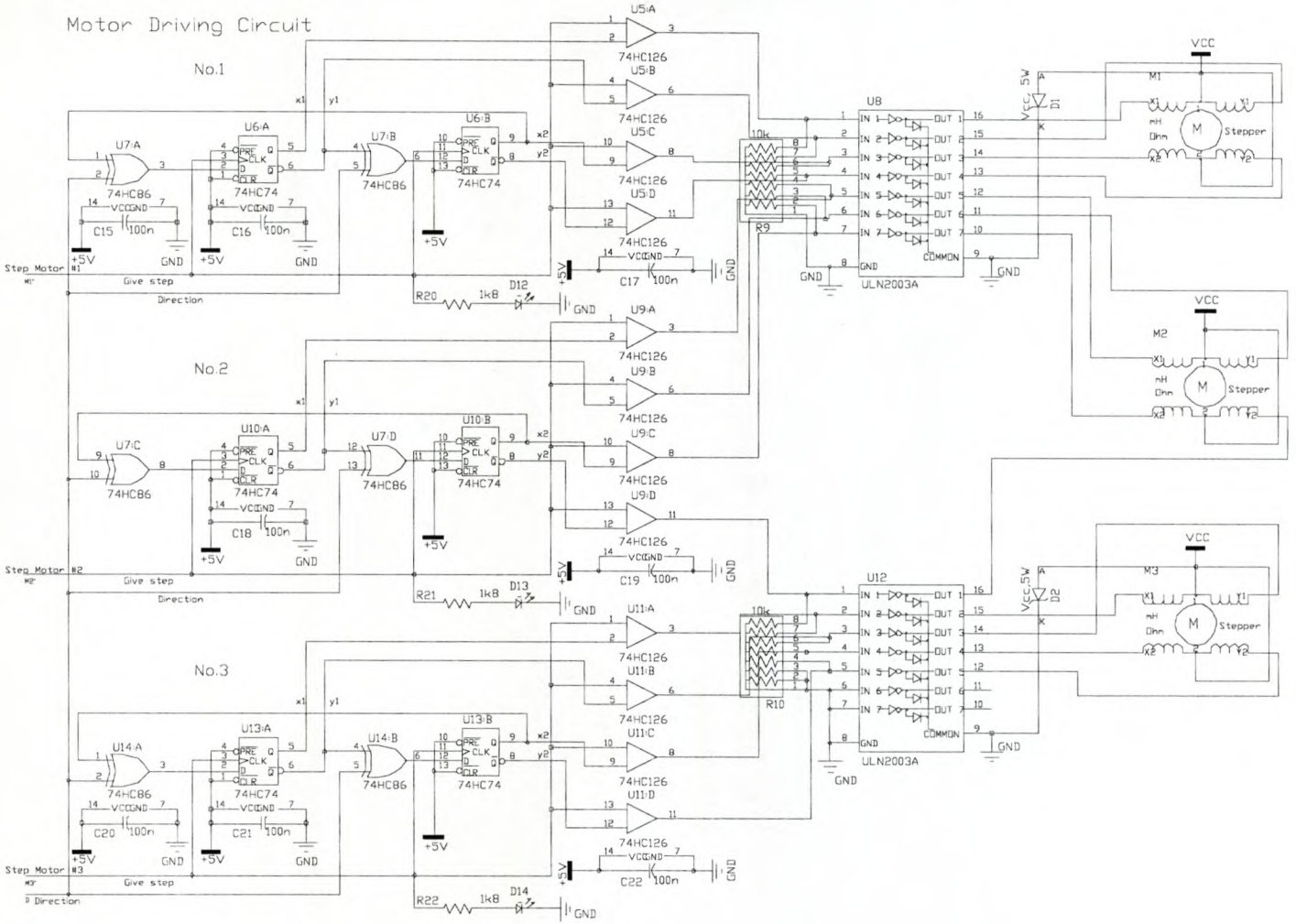

Figure B.2 Stepper Controller Schematic - (page 2)

B.3 Control / Front Panel

Figure B.3 Stepper motor control panel

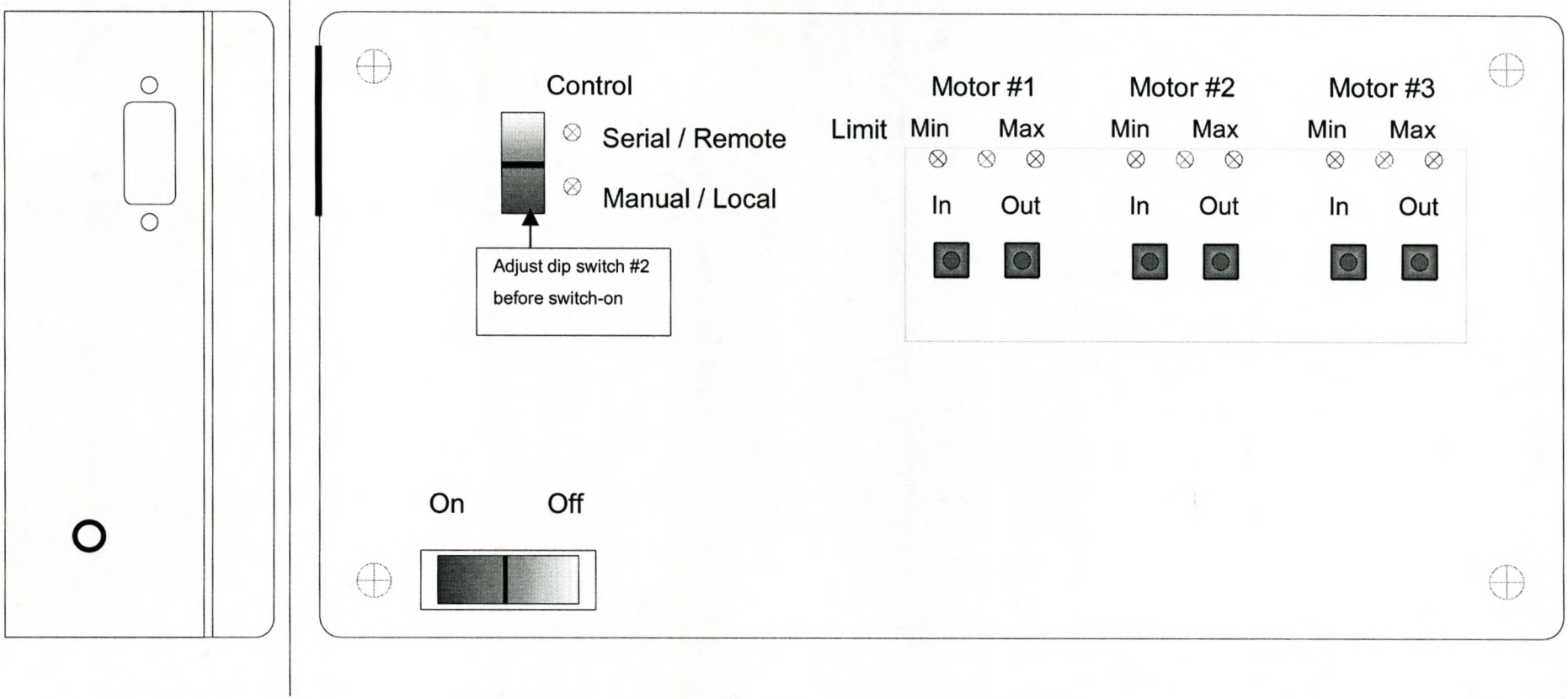

Appendix C System Photographs

This appendix contains pictures of the different components that were designed, as well as one of the full system as it was set up for measurements.

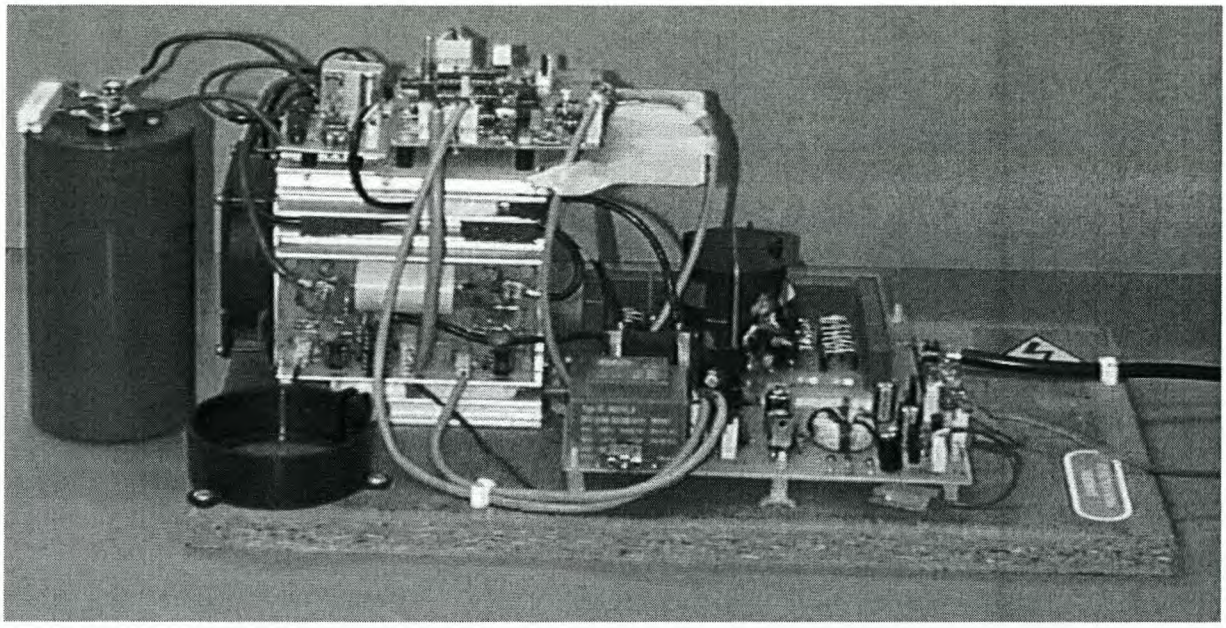

Figure C.1 2kVA, 5kV Switch-mode power supply

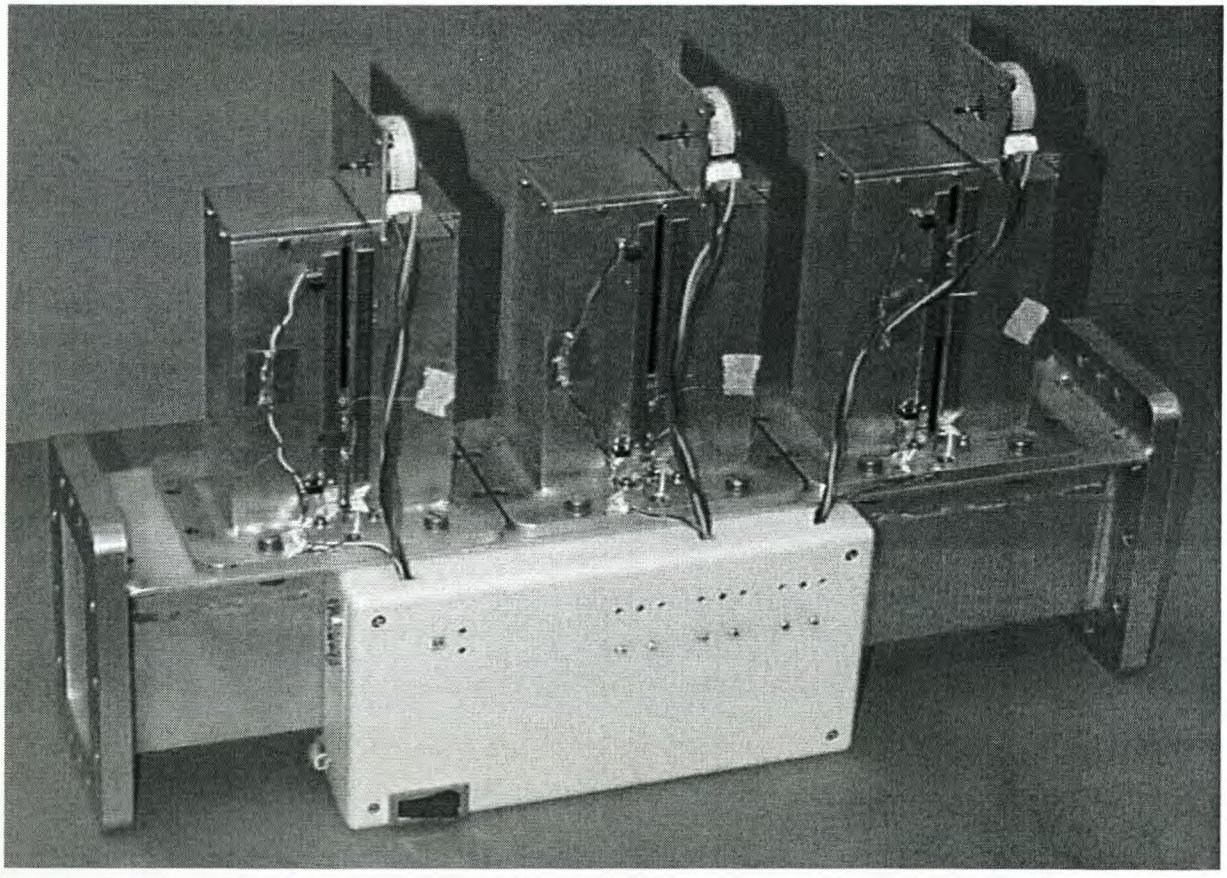

Figure C.2 Offset short matching unit

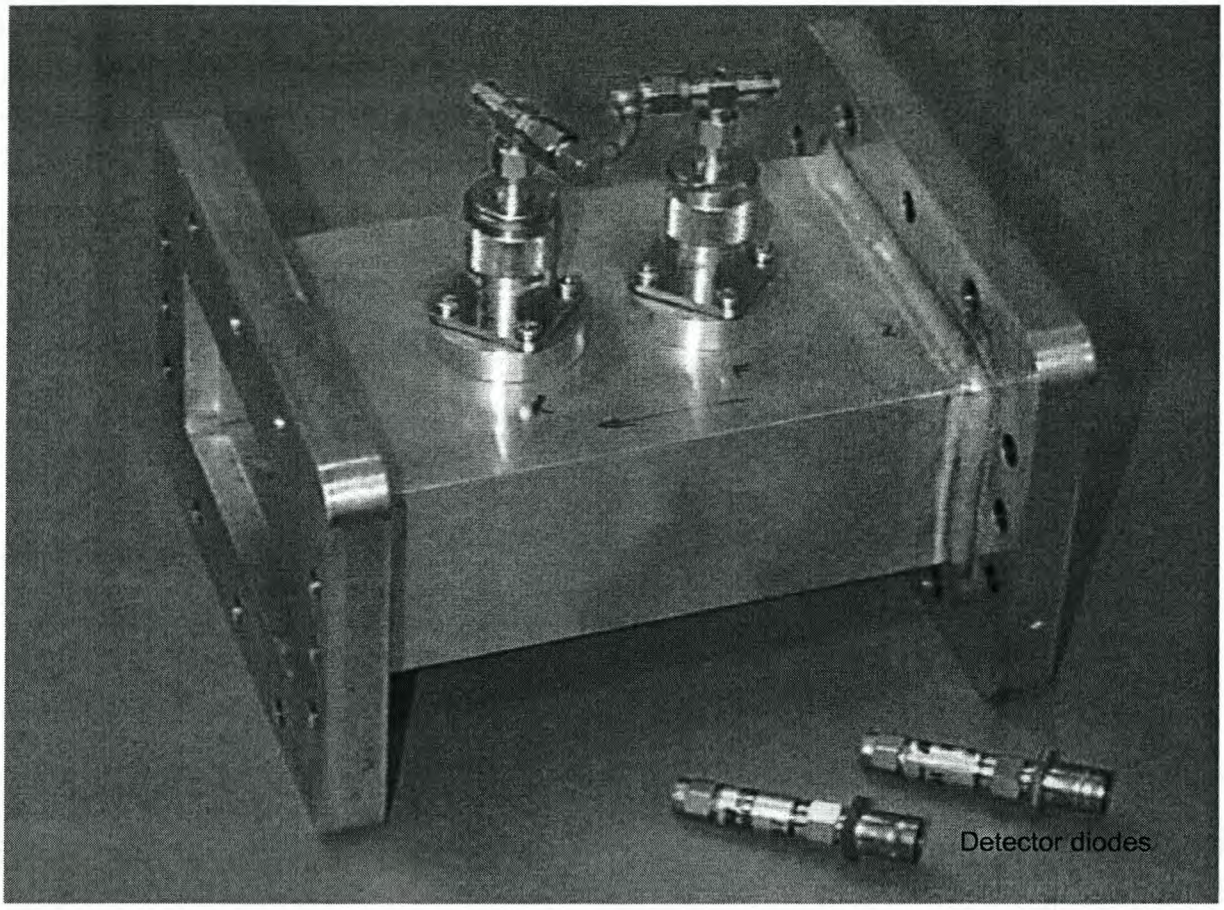

Figure C.3 Dual directional coupler

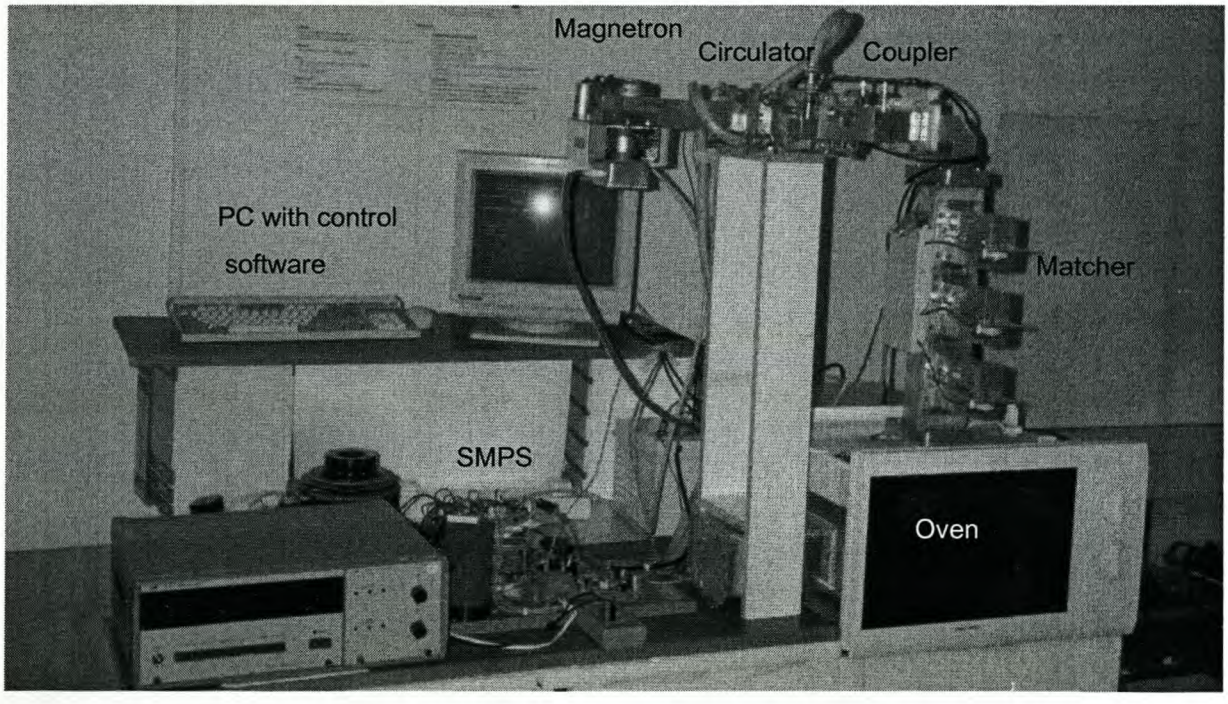

Figure C.4 Constant power, microwave system